STADIUS
Center for Dynamical Systems, Signal Processing and Data Analytics

Citation/Reference	M. Lavanga *et al.*, "The effect of early procedural pain in preterm infants on the maturation of EEG and heart rate variability," *Submitt. to PAIN*, pp. 1–11, 2020.
Archived version	Author manuscript: the content is identical to the content of the published paper, but without the final typesetting by the publisher
Published version	Submitted
Journal homepage	https://journals.lww.com/pain/pages/default.aspx
Author contact	your email mlavanga@esat.kuleuven.be your phone number +32 16 37 38 28
Abstract	Preterm infants show a higher incidence of cognitive, social and behavioral problems, even in the absence of major medical complications during their stay in the neonatal intensive care unit (NICU). Several authors suggest that early life experience of stress and procedural pain could play a role in the altered development of cognition, behavior or motor patterns. Early life experience of pain has been shown to impact cerebral development and maturation resulting in an altered development of cognition, behavior or motor patterns in later life. However, it remains very difficult to assess this impact of procedural pain on physiological development. This study describes the maturation of EEG signals and heart rate variability in a prospective cohort of 92 preterm infants (< 34 weeks GA) during their NICU stay. We took into account the number of painful, i.e. skin-breaking, procedures they were subjected to early in life. Using physiological signal modelling, this study shows that a high exposure to early procedural pain, measured as skin-breaking procedures (SBPs), increased the level of discontinuity in both EEG and heart rate variability in preterm infants. These findings have also been confirmed in a subset of the most vulnerable preterm infants with a gestational age lower than 29 weeks. We conclude that a high level of early pain exposure in the NICU increases the level of functional dysmaturity, which can ultimately impact preterm infants' future developmental outcome.

IR

(article begins on next page)

PAIN

The effect of early procedural pain in preterm infants on the maturation of EEG and heart rate variability

--Manuscript Draft--

Manuscript Number:	PAIN-D-20-00619R1
Full Title:	The effect of early procedural pain in preterm infants on the maturation of EEG and heart rate variability
Article Type:	Research Paper
Keywords:	Pain, stress, skin breaking procedure, EEG, HRV, development, premature infants
Corresponding Author:	Mario Lavanga, Biomedical Engineering Katholieke Universiteit Leuven Leuven, Vlaams Brabant BELGIUM
Corresponding Author Secondary Information:	
Corresponding Author's Institution:	Katholieke Universiteit Leuven
Corresponding Author's Secondary Institution:	
First Author:	Mario Lavanga, Biomedical Engineering
First Author Secondary Information:	
Order of Authors:	Mario Lavanga, Biomedical Engineering
	Bieke Bollen, Psychology
	Alexander Caicedo, Electrical Engineering
	Anneleen Dereymaeker, Medicine
	Katrien Jansen, Medicince
	Els Ortibus, Medicine
	Sabine Van Huffel, Electrical Engineering
	Gunnar Naulaers, Medicine
Additional Information:	
Question	**Response**
Have you posted this manuscript on a preprint server (e.g., arXiv.org, BioXriv, PeerJ Preprints)?	No

Powered by Editorial Manager® and ProduXion Manager® from Aries Systems Corporation

Dear editor-in-chief

I am writing to you to submit the manuscript entitled “The effect of early procedural pain in preterm infants on the maturation of EEG and heart rate variability” as a potential research paper. The current article is the result of an extensive investigation of the effect of early-procedural pain on the functional maturation of premature infants. The development has been investigated by means of EEG and the heart-rate variability (HRV). The latter is a well-known probe of the autonomic nervous system, while the former is normally used to investigate the cortical activity and its reactivity to pain and stress. This study focused on the extraction of different physiological biomarkers to describe the level of development of patients and its relationship with the early-life pain. Specifically, the association between those features on one side and pain and the age on the other was investigated by means of linear mixed-effect regression. The aim was to assess the impact of cumulated procedural pain throughout the maturation in the neonatal intensive care unit (NICU). This research involved 92 patients with gestational age below 34 weeks with different recordings during their stay at the hospital (normally, within 5 days from birth, at 34 weeks post-menstrual age and at discharge). The procedural pain or perinatal stress was quantified by means of the skin breaking procedure.

Our findings suggests three novel aspects. First, the accumulation of early pain seems to induce a more dysmature EEG, which means a more discontinuous and slow-wave neonatal EEG. Second, the heart-rate variability seems to present higher oscillatory activity under accumulation of early pain or stress. Lastly, this association is not only significant after age-correction, but those trends persist even if a subset of patient with gestational age below 29 weeks is considered. A possible reason why EEG results dysmature and HRV more variable is the pain sensitization. This process might lead to a greater neuronal burst activity and alteration of stress response system, which ultimately impact the physiological signals involved in this study. The presence of a dysmature EEG further highlights how crucial the pain monitoring in the NICU can be to preserve the future development outcome of the infant. Up to our knowledge, this is the first study that tries to monitor the effect of the skin breaking procedure by means of functional monitoring, instead of the structural imaging.

The current fits a potential publication in Pain. The current articles investigates the relationship between the pain and stress and functional monitoring, showing that the procedural pain can induce a dysmature EEG and a more variable HRV. The paper aims to help clinicians to optimize the analgesia strategy directly at the cot-side and preserve the neurodevelopment outcome of the patient.

Sincerely

Mario Lavanga

Department of Electrical Engineering (ESAT), STADIUS Center for Dynamical Systems, Signal Processing and Data Analytics, KU Leuven, Kasteelpark Arenberg 10, box 2446, 3001, Leuven, Belgium

Reviewer #1: This paper addresses an important question, namely how pain and/or stress impacts brain function in early life. The authors conclude that more discontinuous EEG and larger HRV is associated with infants that are exposed to high levels of early procedural pain. The number of infants included in the study is high and careful decisions about missing data or other subtle analytical choices have been well dealt with. The authors should be commended on collecting this large data set in this challenging patient group. They have built of methods developed in previous literature and have identified new associations between the number of skin breaking procedures and patterns of EEG activity and HRV.

We would like to thank the reviewer for the constructive feedback. We focused on the clarity of the text by adding an explicit statement of our primary hypothesis. The comments of greater interest for the reviewer are in blue. In this perspective, we would like to start from the third comment of the reviewer.

1. *It is also difficult to work out what the primary hypotheses were and what constituted secondary analysis. For example, did the authors hypothesize that there would be a 'decreasing' rate of EEG discontinuity with increased pain exposure? I think the data in this study is really important, and if it was well-framed then it would add to our understanding of how early life experience impacts the development of brain function. Nevertheless, I believe it needs substantial editing so that the hypothesis is clearly explained, the results presented in a way that directly address the original questions and then secondary analysis presented to support these findings.*

We acknowledge the absence of a clear-cut sentence of the main hypothesis of this study. We investigated if pain-related stress could induce dysmaturity in both EEG and HRV and therefore impact brain and heart rhythmicity. The text was modified in the Introduction, Methods, Results and Discussion to follow the testing of this hypothesis. Refer to question 2 and 3 for changes in the last two sections of the article.

We modified the text in the Introduction as follows:

We hypothesized that pain-related stress increases electrophysiological dysmaturity, i.e. a higher EEG discontinuity due to a higher number of dispersed neuronal bursts and a higher HRV of long-term oscillations. A quantitative analysis of EEG and HRV was used to monitor decreasing rate of EEG discontinuity and increasing HRV respectively (De Wel et al., 2017; Hoyer et al., 2013; M. Lavanga et al., 2017; Mario Lavanga et al., 2018; O'Toole, Pavlidis, Korotchikova, Boylan, & Stevenson, 2019). Specifically, functional maturation charts were obtained to understand whether a high level of SBPs can induce dysmature patterns in EEG and HRV suggesting an impact on the developmental outcome of the patient.

We modified the text in Methods – Functional measurement as follows:

Different features were computed to track the functional maturation of neonates during their NICU stay and assess the level of dysmaturity in the electrophysiological signals, based on previous studies (De Wel et al., 2017; Hoyer et al., 2013; O'Toole et al., 2019). Dysmaturity in EEG signals was defined as a discontinuity and persistence of delta waves (Valenza et al., 2017), while dysmaturity of HRV was defined as a higher amplitude of the slow-wave oscillations (Javorka et al., 2017). The computational steps to derive EEG and HRV dysmature patterns are reported in the paragraph below.

2. *Nevertheless, I think the paper would benefit from extensive editing, in terms of both English language and the presentation of the Results and Discussion. At the moment the Results describe the graphs in detail but do not explain the context of the results clearly enough. At times the Results read a little more like a figure legend, rather than a description of the study findings.*

We rewrote the entire Results section to address cohesion, scientific rigor and a greater clarity as justly asked by Reviewer 1. We also referred to the primary hypothesis as discussed in section 1. We highlighted in blue the part of greater interest to address the primary hypothesis and avoid a text structure similar to a figure legend.

We rewrote the Results – Patients Demographics as follows:

Infants demographics and clinical characteristics are summarized in Table 2 for the entire dataset and in Table 3 for the early-GA dataset. As expected, patients with a higher number of cumulated SBPs at 5 days also had a lower gestational age, a lower PMA at the moment of the recording, higher CRIB score and higher number of days of mechanical ventilation and of CPAP (Table 2). Caffeine treatment (yes/no) at 5 days and APGAR score did not significantly differ between SBP groups, while the number of patients receiving caffeine was different at 34 weeks between SBP groups. In the subset of early-GA infants (<29 weeks), only birth weight differed significantly between infants of the low and high SBP group (Table 3). Only one patient from the high SBP group received medication that could exert a CNS depressant effect at the 34 weeks recording. However, the patient was kept in the overall analysis because the medication was only provided during one recording of the patient and because we did not observe significant changes in the regression models when this recording was omitted.

Skin breaking procedures

Figure 2 clearly shows that there is a peak in the number of SBPs in the first days of life, followed by an exponential decay. In particular, there is already a significant drop in SBPs after 5 postnatal days.

We rewrote the text in Results - Relationship between EEG and HRV functional variables and early skin breaking procedures as follows:

The relationship between the electrophysiological maturational trends and the early SBPs was examined for the entire dataset and reported in Table 4 and Table 5. After FDR correction, early SBPs were negatively associated with the EEG complexity index, during QS as well as nQS (e.g., $CI(F_{P2})$ has $B_{SBP} = -1.585$ with $p \leq 0.05$ in nQS and $CI(C_3)$ has $B_{SBP} = -2.23$ with $p \leq 0.05$ in QS). Early SBPs were also associated to an increase in range EEG asymmetry in QS (e.g., $asym(\theta)$ with $B_{SBP} = 0.051$ with $p \leq 0.01$). For HRV, the power in the HF band was positively associated with SBPs in both QS and nQS (P(HF) has $B_{SBP} = 0.003$ with $p \leq 0.05$ and has $B_{SBP} = 0.003$ with $p \leq 0.01$ in QS). These results imply that a high level of SBPs is associated with a discontinuous EEG trace and with a higher vagal tone after PMA and GA correction.

3. *In addition, while the Discussion also outlines details from the figures and included references and quotes from other literature, it doesn't directly bring these ideas together to build upon existing understanding and showcase the important findings in this paper.*

Since we added a sentence for the primary hypothesis, we highlighted how pain-related stress is associated to a dysmature EEG and, in general, with changes of brain rhythmicity. Together with the

comments of reviewer 2, we also highlighted the possible effect of cumulated pain on nociceptive and central circuitry and how pain can affect the resting EEG of neonate.

We modified the text in Discussions as follows:

In this study, we confirmed our hypothesis that a high number of early skin breaking procedures in premature infants is associated with a dysmature EEG. We also found that a high amount of SBPs is associated with a higher heart rate variability.

Data were collected in a neonatal unit where a lot of attention is given to monitoring and minimizing pain and discomfort, and where individualized developmental care and family integrated care principles are fundamental to the unit's care philosophy. Nevertheless, this study confirms that preterm infants experience a high amount of skin breaking procedures during their NICU stay.

(…)

To our knowledge, this is the first study that shows the effect of pain-related stress on the functional maturation of the brain and the autonomic nervous system in premature infants. Our results show that a high number of early skin breaking procedures is significantly associated to an EEG with lower EEG complexity and higher rEEG asymmetry, which can imply a dysmature EEG [32,34,43,58], and a higher HRV. Although the level of SBPs is strongly correlated with GA and PMA (see Table 2 and Table 3) as expected, the association between EEG and HRV variables and SBPs was not only confirmed after controlling for age at birth and age at recording, but was also supported by the decrease in prediction error when procedural pain was entered in the model. Simple main effect analyses show at which recording time the functional variables statistically differ between high and low SBPs groups. Post hoc analyses confirm that EEG shows dysmature traits in the first weeks of life, while the vagal tone is higher at PSG in the infants that experience a high amount of SBPs. Similar results were obtained in the early-GA group in terms of an association between high SBPs, dysmature EEG and greater HRV. Interestingly, the results tend to be similar in the QS state (Table 5 and Table 6), while no significant differences were found in nQS for the early-GA group compared to the entire dataset .

References

De Wel, O., Lavanga, M., Dorado, A., Jansen, K., Dereymaeker, A., Naulaers, G., & Van Huffel, S. (2017). Complexity Analysis of Neonatal EEG Using Multiscale Entropy: Applications in Brain Maturation and Sleep Stage Classification. *Entropy*, *19*(10), 516. https://doi.org/10.3390/e19100516

Hoyer, D., Tetschke, F., Jaekel, S., Nowack, S., Witte, O. W., Schleußner, E., & Schneider, U. (2013). Fetal Functional Brain Age Assessed from Universal Developmental Indices Obtained from Neuro-Vegetative Activity Patterns. *PLoS ONE*, *8*(9), 1–8. https://doi.org/10.1371/journal.pone.0074431

Javorka, K., Lehotska, Z., Kozar, M., Uhrikova, Z., Kolarovszki, B., Javorka, M., & Zibolen, M. (2017). Heart Rate Variability in Newborns. *Physiol. Res*, *66*, 203–214. https://doi.org/10.33549/physiolres.933676

Lavanga, M., De Wel, O., Caicedo, A., Heremans, E., Jansen, K., Dereymaeker, A., … Van Huffel, S. (2017). Automatic quiet sleep detection based on multifractality in preterm neonates: Effects of maturation. *Proceedings of the 39th Annual International Conference of the IEEE Engineering in Medicine and Biology Society (EMBC)*, 2010–2013. https://doi.org/10.1109/EMBC.2017.8037246

Lavanga, M, Wel, O. De, Caicedo, A., Jansen, K., Dereymaeker, A., Naulaers, G., & Huffel, S. Van. (2018). A brain-age model for preterm infants based on functional connectivity. *Physiological*

Measurement, *39*(4), 044006. https://doi.org/10.1088/1361-6579/AABAC4

Lavanga, Mario, De Wel, O., Caicedo, A., Jansen, K., Dereymaeker, A., Naulaers, G., & Van Huffel, S. (2018). A brain-age model for preterm infants based on functional connectivity. *Physiological Measurement*, *39*(4), 044006. https://doi.org/10.1088/1361-6579/aabac4

O'Toole, J. M., Pavlidis, E., Korotchikova, I., Boylan, G. B., & Stevenson, N. J. (2019). Temporal evolution of quantitative EEG within 3 days of birth in early preterm infants. *Scientific Reports*, *9*(1). https://doi.org/10.1038/s41598-019-41227-9

Valenza, G., Citi, L., Lanata, A., Gentili, C., Barbieri, R., & Scilingo, E. P. (2017). Applications of Heartbeat Complexity Analysis to Depression and Bipolar Disorder. In *Complexity and Nonlinearity in Cardiovascular Signals* (pp. 345–374). https://doi.org/10.1007/978-3-319-58709-7_13

Reviewer #2: In this paper the authors assess the correlation between early noxious experience (within the first 5 days of life) and measures of EEG dysmaturity (Entropy and Asymmetry) and Heart Rate Variability in preterm born infants. This is to evaluate the impact of noxious experience on the development of brain function and autonomic nervous system.

This is an interesting study, but needs more precision, references and clarifications. Most of the issues and confusions are related to the use of a large plethora of indices which are not justified, explained or used. Also to the report of results which have not been formally tested.

We would like to thank the reviewer for the very interesting comments and constructive feedback. We performed a new analysis, added new figures and improved the scientific methodology of our research. We modified the text accordingly in order to improve the manuscript and reported the changes in red. We also used a different reference style in the reply to avoid confusion with the original manuscript. We hope that the text satisfies the reviewer's criteria.

Clarification in the methods

Subjects characterization:

What about at the characteristic of the sample at time of recording? Were any of the infants receiving neuroactive medication? Did they all have an ultrasound or MRI scan at the time of consent? What was their neurological assessment at time of study? Also you need to be precise, which other variable were collected?

Also, it would be helpful to have a sort of Gantt chart with a summary of subject numbers for each time point. Making clear how many had all 3 time points measured and have the full SBP information, etc.

In Table 2 and 3, we provided medical characteristics of infants in the low and high SBP group in terms of GA, PMA, CRIB score, APGAR score, days of mechanical ventilation and CPAP during their hospital stay, the number of infants receiving caffeine treatment and the results of the brain ultrasound scans for both the full dataset and the early GA dataset (GA $\leq$ 29 weeks). We also took into account data on other neuroactive medications (such as dopram, fentanyl, luminal, chloral hydrate, dormicum, contramal, catapressan) on the day of the recordings. . Only one infant received this type of medication at the 34 weeks recording. We have reanalyzed the data without the recordings of this patient. Since the effects we found did not change statistically, we preferred to preserve the dataset without excluding any patient from the analysis.

As suggested by the reviewer, we also provided a Gantt-chart-like overview of all patients' SBP data in Figure 1 and Figure R1. The three colors represent the recording at 5 days (Blue), the recording at 34 weeks (Red) and the recording at PSG (Yellow). The length of the bar represent the cumulative number of SBP at the moment of the recording. For the second and third recordings, the total count has to consider the previous bar to get the number of SBPs at that time point. The black line represents the 50 SBPs threshold used in this study. The figure shows that most of the pain is cumulated up to the first recording (blue bars). Furthermore, it frequently happens that patients have only the first and third recording (blue and yellow bars), while some of them have only the second and third measurement or the first and the second one. This is a consequence of the following recording distribution: 83 recordings at 5days, 62 recordings at 34w and 83 recordings at PSG, for a total of 228 (the total number has been corrected in text).

We modified the text in the subsection Data Acquisition as follows:

Medical and nursing electronic charts were reviewed from birth till discharge home by a physician and by two GCP qualified neonatal research nurses. Variables that were obtained included gestational age (GA) at birth, birth weight (BW), illness severity at birth (e.g. CRIB score (The International Neonatal Network, 1993)) and the number of skin-breaking procedures per day. Also, data on neuroactive medications (caffeïne, dopram, fentanyl, luminal, chloral hydrate, dormicum, contramal, catapressan) administered on the day of the recording were obtained. Caffeïne was routinely administered at a dose of 5 mg/kg.

We modified the text in the subsection Electrophysiological data collection as follows:

In total, 92 patients with 228 recordings and information about the number of SBPs were analyzed. The Gantt chart in Figure 1 summarizes the number of recordings and cumulated SBPs at the different timestamps.

We would also like to refer to subsection Results – Patient Demographics, which was also rewritten to reply to the other reviewer's questions:

Infants demographics and clinical characteristics are summarized in Table 2 for the entire dataset and in Table 3 for the early-GA dataset. As expected, patients with a higher number of cumulated SBPs at 5 days also had a lower gestational age, a lower PMA at the moment of the recording, higher CRIB score and higher number of days of mechanical ventilation and of CPAP (Table 2). Caffeine treatment (yes/no) at 5 days and APGAR score did not significantly differ between SBP groups, while the number of patients receiving caffeine was different at 34 weeks between SPB groups. In the subset of early-GA infants (<29 weeks), only birth weight differed significantly infants of the low and high SBP group (Table 3). Only one patient from the high SBP group received medication that could exert a CNS depressant effect at the 34 weeks recording. However, the patient was kept in the overall analysis because the medication was only provided during one recording of the patient and because we did not observe significant changes in the regression models when this recording was omitted.

2. Recording and Analysis:

1. *What was the reference for EEG and ECG recordings? Also, the filtering band is very narrow considering that Vanhatalo has shown that neonatal EEG has very large SATs and also that the spindle on the delta brushes can go above 20 Hz.*

We thank the reviewer for this valuable comment, which requires a detailed reply. Vanhatalo et al. has clearly shown that spindles can spread up to 30 Hz (even 40 Hz), but they mainly concentrate up to 20 Hz (see time-frequency distribution in (Vanhatalo & Kaila, 2006). In general, most of the power is concentrated in the low-frequency bands (up to 5 Hz), which explains the "definition" of a dysmature EEG by (Pavlidis, Lloyd, Mathieson, & Boylan, 2017b) with following traits: discontinuity (variation in power due to SATs), persistence of slow-waves (most of the energy in delta band) and asynchrony.

Interestingly, De Wel et al. (De Wel et al., 2017) and Räsänen et al. (Räsänen, Metsäranta, & Vanhatalo, 2013) (in collaboration with Vanhatalo) used respectively the [1-20] Hz band and [1-25] Hz band for quantitative EEG analysis in preterm infants. For the same type of patients, O'Toole et al. (O'Toole, Pavlidis, Korotchikova, Boylan, & Stevenson, 2019) and Zhang et al. (Zhang et al., 2009) used 0.5-30 Hz

band, but O'Toole et al. focused on 1-20 Hz for the simulated amplitude integrated EEG (range EEG). There are various computational reasons for this frequency band compression:

1. It simplifies the reduction of the discontinuity of EEG as the disappearance of slow-wave bursts. We do not doubt that this approach is considered an oversimplification to some, but this approximation is easier to test mathematically.
2. This simplification also reduces the computational costs of the MSE and the range EEG.
3. The mathematics behind MSE and rEEG normally compresses the information of the EEG. The range EEG is computed between 1-20 Hz and MSE behaves as low-pass filtering procedure to coarse the signal (De Wel et al., 2017).

However, we clearly acknowledge the limits to simplify the discontinuity of EEG by delta-burst oscillations. There are more complex cross-frequency and cross-amplitude coupling mechanisms to consider (Pavlidis et al., 2017b), which add more complex information to the signal and require more refined methods. In future studies, we aim to expand our analysis in order to preserve the highest-frequency bands.

We modified the text in Methods – Electrophysiological data collections as follows:

Before any functional analysis, both EEG and HRV signals were preprocessed to remove artefacts and define sleep states. In order to remove movement-related and non-cortical information, EEG signals were band-pass-filtered between 0.5 and 20 Hz and independent component analysis to filter EOG was then applied. The narrow filtering band is based on the quantitative analysis of discontinuous EEGs by De Wel et al. (De Wel et al., 2017) and of amplitude integrated EEGs by O'Toole et al. (J. M. O'Toole, Boylan, Vanhatalo, & Stevenson, 2016).

2. *How long and how was the window for artefact detection moved? Sliding, non-overlapping,…what is the correspondence with the window to calculate the various indices?*

We apologize for the lack of clarity. Thresholding criteria were applied in each feature extraction window as digital filter. For example, before the computation of MSE, the signal was split in windows of 150 secs and the listed statistical parameters, standard deviation, maximal amplitude and the maximal absolute sample to sample difference, were computed in each window. If all the indices were below the defined threshold, the MSE was computed. Otherwise, the processing of data was skipped and replaced with NaN (Not-A-Number) value.

We reorganized the text to provide clarity on the preprocessing pipeline. Methods – Electrophysiological data collections now states:

EEG data were then used to define two processing epochs of 20 minutes each related to quiet sleep state and a combination of awake and active sleep, which is called *nonQuiet sleep* (nQS). The behavioral analysis was performed with the algorithms described in (Ansari et al., 2018; Dereymaeker et al., 2017), the probabilistic output of which was summed to look for the two 20 minute epochs. QS was derived as a window around the maximum of a quiet-sleep probability profile, while nQS as a window around the minimum.

Before the extraction of any functional feature, the last step of the preprocessing for both sleep epochs was a segmentation in non-overlapping sliding windows and a threshold filtering according to the following criteria: standard deviation above 50 μV, absolute difference sample-to-sample above 50 μV

and absolute amplitude above 200 μV (Isler, Stark, Grieve, Welch, & Myers, 2018). The size of each window was different for each extracted variable and is specified in following subparagraphs. It is important to highlight that the window was excluded from the processing if more than 4 channels exceeds one of the criteria thresholds.

3. *What is the meaning of the relative power indices of HRV? Why have you used them? I would remove them to slim the analysis down.*

We followed the advice of the reviewer and removed the HRV relative indices from the analysis.

4. *HRV is expressed as continuous wavelet transform, which is really cool, and calculated over 20 mins in QS and nQS and then? It is not clear what is averaged.*

The continuous wavelet transform (CWT) derives a time-frequency distribution of HRV (as it is shown for the fetal heart rate in (David, Hirsch, Karin, Toledo, & Akselrod, 2007) and for EEG in (Vanhatalo & Kaila, 2006)). In layman terms, the CWT computes an instantaneous spectrum of the signal. Therefore, it is possible to compute the power in a certain frequency band for each time sample. Consequently, a time-series is obtained for LF, HF and VLF power. In order to obtain one single value per recording, we consider the average of those times series.

We modified the text in the HRV power feature section as follows:

The CWT computes an instantaneous power spectrum of the signal and the band-power can then be computed for each time sample. Consequently, power time-series are obtained for the LF, HF and VLF power. The CWT was estimated in both QS and nQS using the entire 20 minutes and power time-series were averaged over both epochs.

5. *Be consistent in your nomenclature. What is the difference between Multiscale Entropy and Sample Entropy? Also your layman explanation is not really in layman terms and you should properly explain what is measured with SampEn. How does SampEn reflect the traditional EEG characteristics (e.g. discontinuity, bursting, etc.).*

We apologize for the lack of clarity. We tried to improve the text according to the explanations reported in the following bullet points:

A. The sample entropy is precisely the negative natural logarithm of the conditional probability that a dataset of size N, which presents repetition of an m-points pattern with a certain tolerance r, will also present repetition of an m+1 points pattern within the same tolerance (Lake, Richman, Griffin, & Moorman, 2002).
B. The sample entropy also represents the entropy at scale 1, which means the time series does not undergo any processing before the computation of the sample entropy
C. The multiscale entropy is a generalized version of the sample entropy, which underlines computation of this metric at different scales τ. The MSE performs a moving average and a downsample of the signal, before obtaining the SampleEn. The scale τ represents the length of window in which you perform the moving average . For example, scale 2 and 3 represents a moving average of order 2 and a downsampling at half and third of the sample rate.
D. This process will enhance the slower-patterns in the computation of the sample entropy. The MSE represents the SampEn at different scales and hence different frequency bands. The

higher the scale, the slower the enhanced trends. Therefore, MSE at scale 20 can represent the effect of the slower bands (like delta) (Costa, Goldberger, & Peng, 2002; De Wel et al., 2017).

E. In general, SampEn is low in case of discontinuity and early-life EEG and increases with age (Zhang et al., 2009)
F. In case we consider the area under the MSE curve, the complexity index (the area under the curve) is low in case of discontinuity and it increases with age (De Wel et al., 2017). The advantage of MSE in case of the neonatal EEG is twofold. Firstly, the complexity considers all scales and it automatically includes the sample entropy. Secondly, the coarse graining procedure will enhance the discontinuous and slow-wave bursts pattern, which is central in EEG neonatal development (Vanhatalo & Kaila, 2006)

In a nutshell, the SampEn and complexity index are lower in case of discontinuity. We concentrated on the complexity index and MSE for their comprehensive entropy information and focus on slow-wave activity.

We modified the text in the subsection of Multiscale Entropy as follows:

A more refined maturity index of the neonatal EEG is the multiscale entropy (MSE), as described by (Bosl, Tierney, Tager-Flusberg, & Nelson, 2011; Costa et al., 2002; De Wel et al., 2017). It is based on the more common index of the Sample Entropy, which measures the predictability of the signal. Its actual definition is the negative natural logarithm of the conditional probability that a dataset of size N, which presents repetition of an m-points pattern with a certain tolerance r, will also present repetition of an m+1 points pattern within the same tolerance (Lake et al., 2002). The tolerance r is normally defined as 20% of the standard deviation of the signal. The MSE is a generalized version of Sample Entropy at different scales τ, which means the signal is coarsely grained with a moving average and downsample of order τ. The advantage is two-fold: MSE does not only contain the information of the regular Sample Entropy at scale 1, but the coarse-graining process enhances the slower-patterns in the computation of the sample entropy.

In general, the Sample Entropy is low in case of discontinuity and early-life EEG and increases with age (Zhang et al., 2009). Similarly, the area under the MSE curve or the cumulated MSE for all scales, $CI = \sum_{\tau} MSE(\tau)$, is low in case of discontinuity and it increases with age (De Wel et al., 2017). This metric is known as the complexity index (CI) and is a general measure of irregularity across scales. Therefore, the MSE will investigate how the matching probability varies for long-term variations (high scales or low-frequencies) and for short-term-variations (small scales or high-frequencies), combining both the investigation of EEG discontinuity and slow-wave patterns.

6. *What is the added value of amplitude-integrated EEG feature over Sample Entropy? You say that they are both used to quantify EEG dysmaturity.*

The advantage of the range EEG is twofold. Since it estimates the amplitude integrated EEG, the range EEG provides information that the clinician can visually relate to. As discussed in (O'Toole et al., 2019), the asymmetry of the range EEG, the unbalance towards the upper margin of this time series, decreases with age since the lower margin. The increase of the lower margin or decrease in asymmetry is a fundamental sign to indicate a decrease in discontinuity and emergence of sleep-wave cyclicity. The range EEG is more interpretable type of metric. The second advantage is an inherent estimation of the range EEG at different EEG frequency bands. Consequently, it provides a different spectral information compared to MSE.

We reordered the features list in Methods – Functional measurements because we wanted to explain first how clinicians will approach the quantification of dysmaturity and then report more sophisticated engineering features like MSE. We modified the text in subsection Amplitude-integrated EEG feature as follows:

Clinicians normally rely on the amplitude-integrated EEG (aEEG) for the assessment of Brain maturity and the emergence of sleep-wake cycle. The great advantage is the simplicity of interpretation compared to a full-channel EEG (Pavlidis et al., 2017b). Therefore, we decided to quantify the level of EEG dysmaturity with a more interpretable metric. The aEEG was estimated by means of the range EEG and the discontinuity of EEG features was quantified by means of range EEG (rEEG) asymmetry (O'Toole et al., 2019). This variable (…)

(…) Studies show the higher the asymmetry the higher the discontinuity of EEG (O'Toole et al., 2019; John M. O'Toole & Boylan, 2019). (…)

7. *Is rEEG calculated for every channel?*

Yes, the range EEG is computed for all channels. Subsequently, it is averaged to obtain one single time series from the different channels. This process imitates the amplitude integrated EEG (Toole & Boylan, 2017).

We modified the text in subsection Amplitude-integrated EEG feature as follows:

The rEEG is computed for each channel and one signal is obtained by the median of all range EEGs to resemble the approach of aEEG.

8. *Why calculate the indices in short time windows and then grand average over th whole period? Calculate them directly on the whole period. Also why do the windows for SampEn and rEEG have different lengths?*

We would like to thank the reviewer for this valuable suggestion. The reasons to split the signals in multiple windows for the computation of the MSE and the range EEG are multiple. The sample entropy is computationally hungry due to the iterative matching procedure (Manis, Aktaruzzaman, & Sassi, 2018), especially if the time period is large and the sample rate is high. Therefore, the split makes the procedure computationally feasible. Moreover, De Wel et al. showed that the differences in complexity are minimal between 100 sec and 200 sec. Normally, the shorter the window the greater the differences in entropy since it reduces the number of possible matches. Based on the findings by De Wel et al. and Popivanov (De Wel et al., 2017; Popivanov et al., 2006), the length 150 sec is long enough to describe the nonlinear properties of the signal without great computational costs.

The split in multiple windows is also allowed since the features extraction is performed in different sleep states. The EEG background features are not expected to have great variations on a window-by-window basis. Consequently, one can perform a computation on window basis and average the attributes in a time – fashion. However, we also acknowledge the limits of this methodology. The next step should look into the variability (e.g. the standard deviation) of the computed features in non-overlapping windows.

Concerning the differences between range EEG and multiscale entropy, it is important to stress the scopes of those two features. The range EEG mainly mimics short-term variations of aEEG and the split in different frequency bands allows to observe the contribution to the overall discontinuity by each

cortical rhythm. On the contrary, the MSE and the CI mainly concentrate on the slow-wave trends and nonlinear properties of the signal that requires a long enough time span to have an accurate description.

9. *Rather than using 50 SBP, which is quite arbitrary, why not use the median to split HIGH and LOW SBP?*

Defining a threshold for what is considered a low or high level of early SBPs is indeed an important issue.

1. The first reason was to be able to relate our work to earlier studies. We drew on the work of (Brummelte et al., 2012; Duerden et al., 2018), who also defined a threshold of 50 SBPs in their studies on the impact of early SBPs on brain development (MRI) and behavior.
2. It is also important to take into account that the current studies has two SBPs distribution: one for the entire dataset of preterm infants and one for the patients with a low gestational age, as reported in Figure R2/Figure 3. Both panels report the mean, median and the 75% quantile of the SBP distributions. The entire dataset has a non-normal distribution with a fat-tail on the right, while the dataset of the low gestational age infants resembles a normal distribution. This implies that a median split in the first case will combine a variety of very different "high-level" SBPs, while a median split on $GA \leq 29\ weeks$ will create a group of more similar "high-level" SBPs since there is no fat-tail.
3. In case of non-normal distribution, outlier detection normally considers data points "rare" or "high" if they are above the 75% quartile, which is 46 in case of the entire dataset. Therefore, one might consider data points above the common upper limit of the interquartile range to define the HIGH SBPs group.
4. Importantly, using this threshold of 50, the difference in the number of SBPs persists between preterm infants in the low and high SBP group throughout NICU stay.

However, thise can be considered a limit on its own. Future studies will focus on the testing of different thresholds with a combined investigation of the continuous SBP variable.

We modified the text in Methods – Data acquisition as follows:

We calculated the sum of SBPs in the first five days of life. Subsequently, SBP scores were binarized (LOW SBPs versus HIGH SBPs) with a threshold of 50 SBPs in the first five days of life to detect patients who experienced a high number of skin-breaking procedures, and thus a high level of early procedural pain. This threshold was based on earlier findings on the impact of early-life SBPs in preterm infants [8,18] and our analysis of the distribution of the cumulative SBPs (discussed in the results section). This makes it possible to compare the neuroanatomical changes reported by these authors with the neurophysiological changes that we describe. Brummelte et al. [8] and Duerden et al. [18] considered procedural pain as the cumulated SBP up to their first MRI scan (normally around PMA 32 weeks or 21 postnatal days). Our first recording was planned to be as close as possible to postnatal day 5. However, sometimes it had to be carried out a few days earlier or later because of the preterm infant's unstable medical condition, or because of EEG equipment or technician availability.

We modified the text in Results – Patients demographics as follows:

The distribution of cumulated SBPs at 5 days are reported for the entire dataset and for the subset of patients with GA $\leq$ 29 weeks in Figure 3. In the entire dataset, the median number of cumulated SBPs at 5 days is 34.5 and the distribution has a fat-tail on the right. It implies that a median threshold would give rise to more heterogeneous levels of SBPs in the high SBP group. The early-GA distribution has a

median of 50 without a fat-tail, therefore it contains more similar high-level SBPs. Importantly, Figure 2 shows that, using this threshold, the difference in the number of SBPs persists throughout NICU stay between preterm infants in the low and high SBP group.

10. *The multiple comparisons are only for the SampEn, right? Can you please clarify in the text?*

The false discovery rate (FDR) can be applied to correct for the number of channels/brain region location (Duerden et al., 2018; Ranger et al., 2013), but it can also be used to correct for the total number of extracted features (Ghosh, Chen, & Raghunathan, 2006; Kim, Chen, Park, Ziegler, & Jones, 2008). The FDR was here applied to correct for the features pool size. Additionally, the FDR was also used to rank features, which explain their order of appearance in the different tables.

We modified the text in Methods – Statistical analysis as follows:

The false discovery rate (FDR) can be applied to correct for the number of brain region locations in case of channel-dependent features (Duerden et al., 2018; Ranger et al., 2013), but it can also be used to correct for the total number of extracted features (Ghosh et al., 2006; Kim et al., 2008). FDR was applied in our study to correct for the number of features in the analysis and rank the features from the one with most significant association with SBP to the least significant one.

11. *It is likely that the high concentration of noxious procedures in the first days of life is true for the most preterm neonates (which is also the group with HIGH SBP), but I am not sure that this would be the case for the older group (i.e. LOW SBP). Can you split Figure 1 in HIGH and LOW SBP?*

We provided the requested charts in Figure R3 and in Figure 2. The figure shows that, using this threshold of 50, the difference in the number of SBPs persists throughout NICU stay between preterm infants in the low and high SBP group.

3.Clarification in the results

1. *Table 1 and 2 show that the 3 variables (GA, PMA and SBP) are highly correlated (as expected). Results in Table 3 and 4 show the correlation between the EEG and HRV measures and the three variables independently. But what we need to know is how much extra variance SBP explain on top of that already explained by GA and PMA. I understand that the results of the log-likelihood ratio say that adding SBP significantly reduces the residual variance, but of how much?*

We modified the four tables with new variables to further explain the log-likelihood ratio test. Tables 4,5 and 6 now show the full coefficient of determination (R^2) of the model including SBP group as well as the coefficient of determination of the reduced model, with only GA and PMA (R^2_{Red}). The decrease in error (%) when the SBP variable is added to the model is also shown together with the associated log-likelihood statistics F, which is ultimately a log transform of the error variances ratio.

We modified the text in Methods – Statistical analysis as follows:

The full coefficient of determination (R^2) of the model including SBP group as well as the coefficient of determination of the reduced model, with only GA and PMA (R^2_{Red}) were also computed. The decrease in error (%) when the SBP variable is added to the model was also obtained together with the associated log-likelihood statistics F, which is ultimately a log transform of the error variances ratio.

We modified the text in Results as follows:

The central role of SBPs is confirmed by the log-likelihood ratio test and the decrease in error variance reported in Table 4 and Table 5. In nQS, the decrease in error variance ranges from 3.07% to 4.49 % with an associated improvement of R^2 from R^2_{Red}, while the decrease oscillates between 2.95% up to 10% in the QS epoch. All the reported variables had significant improvement in the regression performance as indicated by the associated p-values.

2. *The results in this sentence have not actually been tested "The complexity plane results tilted for both the PMA axis and the SBP axis. This means that the highest complexity (in yellow) is obtained for low SBPs and high PMA, while the lowest complexity is obtained for low PMA and high SBPs."*

It was indeed confusing to use SBP as a continuous variable in this Figure, while it was used as a binary variable in the analyses. Therefore, we decided to remove the plane and rephrase sentences that were not scientifically rigorous. A complete reply with new charts is reported in 3.4.

3. *Why have you selected theta asymmetry and HF HRV in particular for Figure 3?*

As anticipated in 2.10 and the modified method sections, the features are ranked according to FDR. Therefore, Figure 5 and 6 reports the theta asymmetry as first EEG variable and the power in HF of HRV as the first HRV variable to appear in Table 5. Figure 7 replaces the theta asymmetry with the alpha asymmetry according to Table 7. According to the same logic, we replaced the CI of channel T4 with channel Fp2 in Figure 4.

4. *This sentence is incorrect: "Therefore, Figure 4 shows that the asymmetry of the theta band and the power in the HF band stay higher in case of a high number of SBPs throughout the development" We do not know that. Overall HF band is higher in case of HIGH SBPs vs LOW, however it could be that the two developmental trajectories are not always significantly different. To have this kind of conclusions the significance of the difference between the two regressions has to be tested at every time point (day of PMA). With the current analysis you cannot draw any conclusion about the developmental trajectory and the figures should be substituted with bar charts (LOW vs HIGH SBP at any age). Also we should look at the results after the variance associated with GA has been removed.*

We thank Reviewer 2 for pointing out this inconsistency. As the Reviewer states, the reported conclusion could only be confirmed with a test at each day of PMA, which is not feasible since there are not enough data points for each day. Results of the likelihood ratio tests tell at least that the two trajectories reported in Figure 4,5,6,7,8 are different.

To address the question at which measuring point differences between the high and low SBP group are present and/or change over time in our variables of interest, we performed a two-way ANOVA with SBP group (high/low) and measuring point (5 days, 34 weeks, PSG). The results of these analyses are summarized in the boxplots in Figures 4, 5, 6, 7 and 8. The complete overview of the two-away ANOVA test for each feature is in the supplementary tables 4B, 5B and 6B.

The results for the entire dataset show a significantly lower the complexity index at the5 days recording in the SBP group compared to the low SBP group (Figure 4). Also, a significantly higher range EEG asymmetry was found in the High SBP compared to the low SBP group in the 5 days and 34 weeks

recording (Figure 5). For the vagal tone significant differences were only found for PSG recording, with a higher P(HF) in infants in the high SBP group

This type of testing does not enable to test at each PMA, but it supports a more dysmature EEG (lower complexity and higher asymmetry) soon after birth and a higher parasympathetic activity at PSG in the high SBP group.

Another aspect to take into account is the effect of gestational age. Although we did not remove the effect of GA on the variance of the feature in the ANOVA analyses, analyzing the reduced dataset with GA <=29 weeks can partially address this question. The two ways ANOVA tests do not show significant differences during nQS in both asymmetry in alpha band and P(HF) (Figure 7 and Figure 8) or any other feature (Table 6). In quiet sleep, however, we found a significant difference between the high and low SBP group in EEG asymmetry at 34 w (p= 0.02). Moreover, we found a significant difference between the SBP groups in P(HF) at PSG (p = 0.04).

In conclusion, we agree with the reviewer that the current methods cannot prove that the trajectory of of children in the high SBP group is characterized by a consistent dysmaturity throughout the development, especially because we can not fully filter the effect of GA. Nevertheless, the additional analysis support that preterm infants in the high SBP group have lower EEG complexity and higher asymmetry in the first recordings. This difference in asymmetry persists in the early GA dataset. Furthermore, a significantly higher vagal power is present at PSG in the high SBP group.

These two-ways ANOVA's have been carried out for each feature.

We modified the text in Results as follows:

The differences in maturational trends reported by Table 4 and Table 5 are investigated at each recording time by the two ways ANOVA test. Based on the FDR ranking in Table 4 and Table 5, we reported $CI(F_{P2})$ in nQS, $asym(\theta)$ in QS and $P(HF)$ in QS in Figure 4, 5 and 6.

In non-quiet sleep, we found a statistically significant interaction effect between measuring point and SBP group on EEG complexity index ($F(2,178) = 6.62, p \leq 0.01$). Figure 4 shows that the complexity index increases over time (main effect of measuring point: $F(2,178) = 42.17, p \leq 0.01$). Simple main effects analysis showed that preterm infants in the high SBP group have a lower complexity index than children in the low SBP group at the 5 days recording ($p \leq 0.01$). This difference is not statistically significant for the 34 weeks ($p = 0.59$) or PSG ($p = 1$) recording.

In quiet sleep, we found a statistically significant measuring point-by-SBP group interaction effect for $asym(\theta)$ ($F(2,208) = 8.52, p \leq 0.01$, Figure 5). As expected, rEEG asymmetry decreased over time (main effect of measuring point $F(2,208) = 101.71, p \leq 0.01$). Simple main effects analysis showed a higher rEEG asymmetry in preterm infants in the high SBP group compared to the low SBP group at the first measuring point at 5 days ($p \leq 0.01$). This difference was still marginally significant at the 34 weeks recording ($p = 0.05$). For the last recording (PSG), rEEG asymmetry did not statistically differ between the low and high SBP group ($p = 0.72$). Figure 6 shows that the HF oscillations increases over time (main effect of measuring point: $F(2,191) = 5.97, p \leq 0.01$), but statistically significant interaction effect between measuring point and SBP group is found ($F(2,191) = 4.56, p \leq 0.01$). The simple main effect analysis shows a higher $P(HF)$ in the high SBP group at the PSG recording time ($p \leq 0.01$), but there is no difference for the 5 days ($p = 0.43$) or 34w ($p = 1$) recording time.

The results for the patients with a GA below 29 weeks are reported in Table 6 only for QS. The variables in nQS did not pass the FDR test. Similarly to the entire dataset, the HF power and the asymmetry in the alpha and theta band in QS have a positive association with the SBP variable ($P(HF)$ has $B_{SBP} = 0.005$ with p<0.01 and asym(alpha) has $B_{SBP} = 0.064$ with $p \leq 0.05$). Unlike the entire dataset, the sympathetic tone P(LF) is also significantly associated with the SBP variable (P(LF) has B_{SBP}= 0.009 with p<0.05). The LLR test and F-statistics support the significant decrease in error variance and improvement in R^2. The change in error ranges from 6.38% to 13.2%.

Based on FDR ranking, we reported the $asym(\alpha)$ in QS and $P(HF)$ in QS in Figure 7 and 8 and we showed the results of simple main effect analysis based on the ANOVA test. In a subset analysis of infants with <29 weeks GA, we found a significant SBP-by-measuring point interaction on rEEG asymmetry in quiet sleep ($F(2,71) = 3.86, p = 0.03$). Asymmetry decreased over time (main effect of measuring point: : $F(2,71) = 61.61, p \leq 0.01$). At the 34 weeks recording, infants in the high SBP group showed a significantly higher rEEG asymmetry than the infants in the low SBP group (p =0.02). At the recording at 5 days and the PSG recording, this difference did not reach significance ((p =0.91 and p =0.98, respectively). A significant SBP-by-measuring point interaction on P(HF) is found in quiet sleep ($F(2,67) = 3.49, p = 0.04$). HF oscillations also increase over time (main effect of measuring point: $F(2,67) = 6.49, p \leq 0.01$). Post-hoc analysis showed this difference in HF oscillations between the high and low SBP group is only significantly different at the last, PSG, recording (p =0.04).

5. *In Figure 2 and 5 you should remove the 3D plane figure as you have not used SBP as a continuous variable, but split in two groups. Also why do we have two colors for each group?*

As suggested by the reviewer, we removed the plane and replaced with the boxplots trend as reported in 3.4 and replaced with the boxplot figures with results of the two-ways ANOVA.

6. *Rearrange Table 4, 5, 6 and 7 with subsections according to the measures, i.e. EEG Multiscale Entropy; range EEG asymmetry and Heart Rate Variability.*

As discussed in 2.10, the tables reported the different features according to the FDR ranking. We also reported the overview of all features split by type of attribute in the supplementary materials.

4.Discussions

1. "Our results showed that a high number of early skin breaking procedures are significantly associated to a dysmature EEG and more variable heart rate.". In order for us to understand this sentence, we need to have an introduction about the changes and normative values of EEG and HRV across different PMA.

Pavlidis et al. and Wallois et al. gave a full overview of the EEG development in preterm neonates. The three main features that characterize early-life EEG or dysmature EEG (discontinuity, slow-wave persistence and asynchrony) are all expected to significantly decrease with development (Pavlidis et al., 2017b; Wallois, 2010). The discontinuity and slow-wave persistence normally lowers the EEG complexity (see 2.1), while it increases the asymmetry of the range EEG (see 2.6). As thoroughly discussed in (De Wel et al., 2017; O'Toole et al., 2019), the EEG complexity is expected to increase with the development, while the asymmetry is expected to decrease.

A full overview of HRV development in preterm neonates is reported by Clairambault et al., Curzi-Dascalova et al. and Javorka et al. (Clairambault, Curzi-dascalovab, Kauffmann, & Mkdiguea, 1992; Curzi-

Dascalova, 1994; M. Javorka et al., 2017). The overall variability is expected to increase with increasing age, as well as the absolute power in both HF and LF.

We modified the text in Discussion as follows:

Developmental studies show that both EEG and HRV are expected to change with infant's development. If electrophysiological patterns in these signals keeps the traits and grapho-elements which are typical of early gestational age, they are labelled as dysmature. The two main features of dysmature EEG, which are discontinuity and slow-wave persistence, are all expected to significantly decrease with development (Pavlidis et al., 2017b; Wallois, 2010). As demonstrated by (De Wel et al., 2017; O'Toole et al., 2019), EEG complexity increases with increasing PMA, while range EEG asymmetry is higher in the first week of life and has a downward trend with development. For HRV, the band-power of the main HRV tones (VLF,LF and HF) are all expected to increase with infants' development (Clairambault et al., 1992; Curzi-Dascalova, 1994; K. Javorka et al., 2017).

2. In the discussion you suggest that early noxious experience may affect spinal cord and thalamocortical connections development, which is true, but in this paper you are looking at resting EEG activity, which does not involve the spinal cord and not sure about how thalamocortical connections play a role. You need to explore the literature which suggest that early noxious experience may alter resting activity as well as nociceptive activity.

We thank the reviewer to have raised this point, which is a complex problem with intertwined relationship between spinal, thalamo-cortical and cortico-cortical connections. The following bullet points list can be helpful:

1. Vinall et al. suggested that premature infants are exposed to multiple pain procedures, which can be considered as painful stimulation able to increase the sensitization to pain (Vinall et al., 2014), which can ultimately impact the thalamus and the thalamo-cortical connections (Duerden et al., 2018).
2. Kostovic et al. and Pavlidis et al. discussed the specific role of subcortical areas, the brain subplate, thalamo-cortical connections and delayed cortico-cortical connections in generation of EEG bursts (Kostović & Judaš, 2010; Pavlidis, Lloyd, Mathieson, & Boylan, 2017a).
3. According to Verriotis et al., the development of pain circuitry clearly shows an increase of delta and diffused delta brushes in case of pain stimulation (Verriotis, Chang, Fitzgerald, & Fabrizi, 2016).
4. Both adults and infants employ the thalamo-cortical connections for the transmission of pain information to the higher cortex level (Verriotis et al., 2016). However, the underdeveloped cortico-cortical connections and the missed activation of specific cortical and subcortical regions show a diffused activity in fMRI studies.
5. Although specific literature about stress and neonatal EEG bursts was not found, the literature seems to clearly show the relationship between pain and delta bursts. Additionally, Doesburg et al. (Doesburg et al., 2013) also found that a different brain rhythmicity was associated with cumulated pain, which ultimately entailed a lower visual-perceptual ability.
6. In a nutshell, the pain processing might induce a transmission of information towards the cortex, which ultimately increased diffused delta bursts and therefore the discontinuity of EEG. See (Vinall et al., 2014)(Verriotis et al., 2016)(Fabrizi et al., 2011; Ruth Eckstein Grunau, 2013)

We modified the text in discussion as follows:

Early pain might act on the infant's development through different mechanisms, mainly sensitization to pain of the central nervous system and lowering sensory threshold (Fitzgerald, 2005). Early pain and injuries might developmentally regulate nociceptive pathways, such as hyperinnervation of the periphery and increasing receptive fields of the dorsal horn of neurons (Reynolds & Fitzgerald, 1995; Torsney & Fitzgerald, 2003). This peripheral sensitization might lead to the central sensitization, which can affect the central nociceptive pathways and thalamus. Consequently, the thalamocortical projections will be abnormally distributed since their topography and structural organization is activity-dependent (Duerden et al., 2018). In premature infants, any impact on the thalamus development and thalamo-cortical connections will have a direct impact on the cortical activity, since the high-amplitude delta bursts type of activity is a result of the predominance of the subcortical centers (Kostovic & Judas, 2010; Pavlidis et al., 2017a). During the development of thalamocortical projections, the axons of the thalamus will contend the activity on the cortex. If early pain disrupts the thalamo-cortical connections, the activity on the cortex will also be different (Duerden et al., 2018).

Previous research showed that pain stimulation might induce higher delta activity and delta brushes, which are diffused over the entire cortex due to underdeveloped cortico-cortical connections, as also supported by fMRI studies (Verriotis et al., 2016). This widespread diffused delta activity is present up to 35 weeks of GA, before it is replaced by a mature cortical response at full-term age (Slater et al., 2010). We therefore speculated that neonatal pain might induce a different brain rhythmicity, especially in terms of δ band, and might lead to a greater discontinuous tracing on the cortex, as also shown in Figure 4, 5 and 6. Since pain-related stress and cumulated pain might ultimately induce a diffused delta-burst activity (Fabrizi et al., 2011; Jones et al., 2017; Slater et al., 2010), pain can ultimately increase the discontinuity of the EEG and contribute to a more dysmature pattern. Therefore, the greater rEEG asymmetry and the lower EEG complexity are the result of a more dysmature tracing.

Clearly, other subtle factors or causes of this persistence EEG dysmaturity cannot be excluded. However, Doesburg et al. (Doesburg et al., 2013) also found that a different brain rhythmicity was associated with cumulated pain, which was associated to reduced visual-perceptual abilities, and Grunau et al. showed that pain-related stress is associated with a lower cognitive outcome (Ruth E. Grunau et al., 2009). In parallel, several authors have shown that a dysmature EEG in premature infants is associated with worse cognitive outcome (Kong et al., 2018; Le Bihannic, Beauvais, Busnel, de Barace, & Furby, 2012; Watanabe, Hayakawa, & Okumura, 1999). Furthermore, early-life pain and the resulting disruption of thalamocortical pathways are also associated with a lower cognitive outcome (Duerden et al., 2018). Therefore, our results might provide the functional link which can discriminate infants at risk for developmental delay: a higher SBP load might induce a more dysmature EEG which is related to and induce a lower development outcome. Currently, follow-up developmental testing is taking place in our patient sample so we will be able to link the current results with developmental outcome measures in the future.

3.You have not shown "increased neuronal burst activity" or relationship (or discussed existing evidence) between your indices of EEG dysmaturity, EEG discontinuity and delta brush occurrence.

We apologize for the lack of clarity, the sentence should now be more clear in light of answers to 4.1, 2.6 and 2.1. The discontinuity of EEG is increased in case of high SBPs. Therefore, a more dysmature EEG is potentially characterized by a higher burst load. The relationship between rEEG asymmetry, burst

activity and evolution of EEG was specifically discussed by (O'Toole et al., 2019). A burst is normally delta-wave overlapped with higher frequency activity, known as delta brush.

We modified the text in Discussion as reported in 4.3.

4.You have not proved the second half of this sentence in the Conclusions: "We found a more discontinuous EEG and a larger HRV in infants that were exposed to high levels of early procedural pain. The larger burst activity might be due to a higher cortical response due to more frequent pain stimulation."

We apologize for the lack of scientific soundness and we removed the sentence.

5.Wording:

1. Use the word pain carefully. Procedural pain is not accurate as we do not know the experience of the subject. Procedural skin-breaking procedures is more accurate.

Brummelte et al., Grunau et al., Duerden et al. and Manon et al. refereed to SBPs as procedural pain (Brummelte et al., 2012; Duerden et al., 2018; Ruth Eckstein Grunau, 2013; Ranger et al., 2013). We decided to keep this term for sake of comparison.

2. Clinicians do not rely on pain scale because pain and stress cannot be easily discriminated, but because the infant cannot report their experience.

We removed the sentence:

It is important to highlight that stress and pain have a tight relationship, but they cannot be easily discriminated (Ruth Eckstein Grunau, 2013; Ranger, Johnston, & Anand, 2007). Consequently, clinicians rely mainly on pain scales (Vinall & Grunau, 2014).

3.The DISAPPEARANCE (not the APPEARANCE) of delta brushes is considered a sign of somatosensory cortex development.

We removed any reference to appearance of delta brushes.

4.The first time you use acronyms you need to write them in full (MSE, ANS, etc.)

We modified the text accordingly.

5.Always use Heart Rate Variability and not variations of the heart-rate, etc. also HRV already stands for Heart Rate Variability, so do not write HRV variations

We modified the text accordingly.

6.I think in this sentence "short and long-term variations of the HRV" you mean "short and long-term variations of the heart rate"

We modified the text in short and long-term HRV according to 5.5

7.Make <= notation consistent in Tables 2 and 3.

We modified the captions of the tables in a consistent way.

References

Ansari, A. H., De Wel, O., Lavanga, M., Caicedo, A., Dereymaeker, A., Jansen, K., … Van Huffel, S. (2018). Quiet sleep detection in preterm infants using deep convolutional neural networks. *Journal of Neural Engineering*, *15*(6), 066006. https://doi.org/10.1088/1741-2552/aadc1f

Bosl, W., Tierney, A., Tager-Flusberg, H., & Nelson, C. (2011). EEG complexity as a biomarker for autism spectrum disorder risk. *BMC Medicine*, *9*(1), 18. https://doi.org/10.1186/1741-7015-9-18

Brummelte, S., Grunau, R. E., Chau, V., Poskitt, K. J., Brant, R., Vinall, J., … Miller, S. P. (2012). Procedural pain and brain development in premature newborns. *Annals of Neurology*, *71*(3), 385–396. https://doi.org/10.1002/ana.22267

Clairambault, J., Curzi-dascalovab, L., Kauffmann, F., & Mkdiguea, C. (1992). Heart Rate Variability in Normal Sleeping and Preterm Neonates Full-Term. *Early Human Development*, *28*, 169–183.

Costa, M., Goldberger, A. L., & Peng, C.-K. K. (2002). Multiscale Entropy Analysis of Complex Physiologic Time Series. *Physical Review Letters*, *89*(068102). https://doi.org/10.1103/PhysRevLett.89.068102

Curzi-Dascalova, L. (1994). Development of sleep and autonomic nervous system contorl in premature and full-term newborns. *Archives de Pediatrie*, *2*(I 995), 255–262. https://doi.org/10.1016/0929-693X(96)81138-9

David, M., Hirsch, M., Karin, J., Toledo, E., & Akselrod, S. (2007). An estimate of fetal autonomic state by time-frequency analysis of fetal heart rate variability. *Journal of Applied Physiology*, *102*(3). Retrieved from http://jap.physiology.org/content/102/3/1057.long

De Wel, O., Lavanga, M., Dorado, A., Jansen, K., Dereymaeker, A., Naulaers, G., & Van Huffel, S. (2017). Complexity Analysis of Neonatal EEG Using Multiscale Entropy: Applications in Brain Maturation and Sleep Stage Classification. *Entropy*, *19*(10), 516. https://doi.org/10.3390/e19100516

Dereymaeker, A., Pillay, K., Vervisch, J., Van Huffel, S., Naulaers, G., Jansen, K., & De Vos, M. (2017). An Automated Quiet Sleep Detection Approach in Preterm Infants as a Gateway to Assess Brain Maturation. *International Journal of Neural Systems*, 1750023. https://doi.org/10.1142/S012906571750023X

Doesburg, S. M., Chau, C. M., Cheung, T. P. L., Moiseev, A., Ribary, U., Herdman, A. T., … Grunau, R. E. (2013). Neonatal pain-related stress, functional cortical activity and visual-perceptual abilities in

school-age children born at extremely low gestational age. *Pain*, *154*(10), 1946–1952. https://doi.org/10.1016/j.pain.2013.04.009

Duerden, E. G., Grunau, R. E., Guo, T., Foong, J., Pearson, A., Au-Young, S., … Miller, S. P. (2018). Early procedural pain is associated with regionally-specific alterations in thalamic development in preterm neonates. *Journal of Neuroscience*, *38*(4), 878–886. https://doi.org/10.1523/JNEUROSCI.0867-17.2017

Fabrizi, L., Slater, R., Worley, A., Meek, J., Boyd, S., Olhede, S., & Fitzgerald, M. (2011). A shift in sensory processing that enables the developing human brain to discriminate touch from pain. *Current Biology*, *21*(18), 1552–1558. https://doi.org/10.1016/j.cub.2011.08.010

Fitzgerald, M. (2005, July). The development of nociceptive circuits. *Nature Reviews Neuroscience*, Vol. 6, pp. 507–520. https://doi.org/10.1038/nrn1701

Ghosh, D., Chen, W., & Raghunathan, T. (2006). The false discovery rate: a variable selection perspective. *Journal of Statistical Planning and Inference*, *136*(8), 2668–2684. https://doi.org/10.1016/j.jspi.2004.10.024

Grunau, Ruth E., Whitfield, M. F., Petrie-Thomas, J., Synnes, A. R., Cepeda, I. L., Keidar, A., … Johannesen, D. (2009). Neonatal pain, parenting stress and interaction, in relation to cognitive and motor development at 8 and 18 months in preterm infants. *Pain*, *143*(1–2), 138–146. https://doi.org/10.1016/j.pain.2009.02.014

Grunau, Ruth Eckstein. (2013). Neonatal pain in very preterm infants: long-term effects on brain, neurodevelopment and pain reactivity. *Rambam Maimonides Medical Journal*, *4*(4), e0025. https://doi.org/10.5041/RMMJ.10132

Isler, J. R., Stark, R. I., Grieve, P. G., Welch, M. G., & Myers, M. M. (2018). Integrated information in the EEG of preterm infants increases with family nurture intervention, age, and conscious state. *PLOS ONE*, *13*(10), e0206237. https://doi.org/10.1371/journal.pone.0206237

Javorka, K., Lehotska, Z., Kozar, M., Uhrikova, Z., Kolarovszki, B., Javorka, M., & Zibolen, M. (2017). Heart Rate Variability in Newborns. *Physiol. Res*, *66*, 203–214. https://doi.org/10.33549/physiolres.933676

Javorka, M., Krohova, J., Czippelova, B., Turianikova, Z., Lazarova, Z., Javorka, K., & Faes, L. (2017). Basic cardiovascular variability signals: mutual directed interactions explored in the information domain. *Physiological Measurement*, *38*(5), 877–894. https://doi.org/10.1088/1361-6579/aa5b77

Jones, L., Fabrizi, L., Laudiano-Dray, M., Whitehead, K., Meek, J., Verriotis, M., & Fitzgerald, M. (2017). Nociceptive Cortical Activity Is Dissociated from Nociceptive Behavior in Newborn Human Infants under Stress. *Current Biology*, *27*(24), 3846-3851.e3. https://doi.org/10.1016/J.CUB.2017.10.063

Kim, S. B., Chen, V. C. P., Park, Y., Ziegler, T. R., & Jones, D. P. (2008). Controlling the False Discovery Rate for Feature Selection in High-resolution NMR Spectra. *Statistical Analysis and Data Mining*, *1*(2), 57–66. https://doi.org/10.1002/sam.10005

Kong, A. H. T., Lai, M. M., Finnigan, S., Ware, R. S., Boyd, R. N., & Colditz, P. B. (2018). Background EEG features and prediction of cognitive outcomes in very preterm infants: A systematic review. *Early Human Development*, *127*, 74–84. https://doi.org/10.1016/J.EARLHUMDEV.2018.09.015

Kostovic, I., & Judas, M. (2010). The development of the subplate and thalamocortical connections in the

human foetal brain. *Acta Paediatrica, International Journal of Paediatrics*, *99*(8), 1119–1127. https://doi.org/10.1111/j.1651-2227.2010.01811.x

Kostović, I., & Judaš, M. (2010). The development of the subplate and thalamocortical connections in the human foetal brain. *Acta Paediatrica, International Journal of Paediatrics*, *99*(8), 1119–1127. https://doi.org/10.1111/j.1651-2227.2010.01811.x

Lake, D. E., Richman, J. S., Griffin, M. P., & Moorman, J. R. (2002). Sample entropy analysis of neonatal heart rate variability. *American Journal of Physiology-Regulatory, Integrative and Comparative Physiology*, *283*(3), R789–R797. https://doi.org/10.1152/ajpregu.00069.2002

Le Bihannic, A., Beauvais, K., Busnel, A., de Barace, C., & Furby, A. (2012). Prognostic value of EEG in very premature newborns. *Archives of Disease in Childhood. Fetal and Neonatal Edition*, *97*(2), F106-9. https://doi.org/10.1136/adc.2010.204735

Manis, G., Aktaruzzaman, M., & Sassi, R. (2018). Low Computational Cost for Sample Entropy. *Entropy*, *20*(1), 61. https://doi.org/10.3390/e20010061

O'Toole, J. M., Boylan, G. B., Vanhatalo, S., & Stevenson, N. J. (2016). Estimating functional brain maturity in very and extremely preterm neonates using automated analysis of the electroencephalogram. *Clinical Neurophysiology*, *127*(8), 2910–2918. https://doi.org/10.1016/j.clinph.2016.02.024

O'Toole, J. M., Pavlidis, E., Korotchikova, I., Boylan, G. B., & Stevenson, N. J. (2019). Temporal evolution of quantitative EEG within 3 days of birth in early preterm infants. *Scientific Reports*, *9*(1). https://doi.org/10.1038/s41598-019-41227-9

O'Toole, John M., & Boylan, G. B. (2019). Quantitative Preterm EEG Analysis: The Need for Caution in Using Modern Data Science Techniques. *Frontiers in Pediatrics*, *7*(MAY), 174. https://doi.org/10.3389/fped.2019.00174

Pavlidis, E., Lloyd, R. O., Mathieson, S., & Boylan, G. B. (2017a). A review of important electroencephalogram features for the assessment of brain maturation in premature infants. *Acta Paediatrica*, *106*(9), 1394–1408. https://doi.org/10.1111/apa.13956

Pavlidis, E., Lloyd, R. O., Mathieson, S., & Boylan, G. B. (2017b, September 1). A review of important electroencephalogram features for the assessment of brain maturation in premature infants. *Acta Paediatrica, International Journal of Paediatrics*, Vol. 106, pp. 1394–1408. https://doi.org/10.1111/apa.13956

Popivanov, D., Stomonyakov, V., Minchev, Z., Jivkova, S., Dojnov, P., Jivkov, S., … Kosev, S. (2006). Multifractality of decomposed EEG during imaginary and real visual-motor tracking. *Biological Cybernetics*, *94*(2), 149–156. https://doi.org/10.1007/s00422-005-0037-5

Ranger, M., Chau, C. M. Y., Garg, A., Woodward, T. S., Beg, M. F., Bjornson, B., … Grunau, R. E. (2013). Neonatal Pain-Related Stress Predicts Cortical Thickness at Age 7 Years in Children Born Very Preterm. *PLoS ONE*, *8*(10), e76702. https://doi.org/10.1371/journal.pone.0076702

Ranger, M., Johnston, C. C., & Anand, K. J. S. (2007, October). Current Controversies Regarding Pain Assessment in Neonates. *Seminars in Perinatology*, Vol. 31, pp. 283–288. https://doi.org/10.1053/j.semperi.2007.07.003

Räsänen, O., Metsäranta, M., & Vanhatalo, S. (2013). Development of a novel robust measure for

interhemispheric synchrony in the neonatal EEG: Activation Synchrony Index (ASI). *NeuroImage*, *69*, 256–266. https://doi.org/10.1016/j.neuroimage.2012.12.017

Reynolds, M. L., & Fitzgerald, M. (1995). Long-term sensory hyperinnervation following neonatal skin wounds. *The Journal of Comparative Neurology*, *358*(4), 487–498. https://doi.org/10.1002/cne.903580403

Slater, R., Fabrizi, L., Worley, A., Meek, J., Boyd, S., & Fitzgerald, M. (2010). Premature infants display increased noxious-evoked neuronal activity in the brain compared to healthy age-matched term-born infants. *NeuroImage*, *52*(2), 583–589. https://doi.org/10.1016/j.neuroimage.2010.04.253

The International Neonatal Network. (1993). The CRIB (clinical risk index for babies) score: a tool for assessing initial neonatal risk and comparing performance of neonatal intensive care units. *The Lancet*, *342*(8865), 193–198. https://doi.org/10.1016/0140-6736(93)92296-6

Toole, J. M. O., & Boylan, G. B. (2017). *NEURAL: quantitative features for newborn EEG using Matlab*. Retrieved from http://arxiv.org/abs/1704.05694

Torsney, C., & Fitzgerald, M. (2003). Spinal Dorsal Horn Cell Receptive Field Size is Increased in Adult Rats Following Neonatal Hindpaw Skin Injury. *The Journal of Physiology*, *550*(1), 255–261. https://doi.org/10.1113/jphysiol.2003.043661

Vanhatalo, S., & Kaila, K. (2006). Development of neonatal EEG activity: From phenomenology to physiology. *Seminars in Fetal and Neonatal Medicine*, *11*(6), 471–478. https://doi.org/10.1016/j.siny.2006.07.008

Verriotis, M., Chang, P., Fitzgerald, M., & Fabrizi, L. (2016). The development of the nociceptive brain. *Neuroscience*, *338*, 207–219. https://doi.org/10.1016/J.NEUROSCIENCE.2016.07.026

Vinall, J., & Grunau, R. E. (2014, February 5). Impact of repeated procedural pain-related stress in infants born very preterm. *Pediatric Research*, Vol. 75, pp. 584–587. https://doi.org/10.1038/pr.2014.16

Vinall, J., Miller, S. P., Bjornson, B. H., Fitzpatrick, K. P. V., Poskitt, K. J., Brant, R., … Grunau, R. E. (2014). Invasive procedures in preterm children: Brain and cognitive development at school age. *Pediatrics*, *133*(3), 412–421. https://doi.org/10.1542/peds.2013-1863

Wallois, F. (2010). Synopsis de la maturation des activités cérébrales chez le nouveau-né prématuré. *Neurophysiologie Clinique*, *40*(2), 125–126. https://doi.org/10.1016/j.neucli.2010.02.001

Watanabe, K., Hayakawa, F., & Okumura, A. (1999, September 1). Neonatal EEG: A powerful tool in the assessment of brain damage in preterm infants. *Brain and Development*, Vol. 21, pp. 361–372. https://doi.org/10.1016/S0387-7604(99)00034-0

Zhang, D., Ding, H. H., Liu, Y., Zhou, C., Ding, H. H., & Ye, D. (2009). Neurodevelopment in newborns: A sample entropy analysis of electroencephalogram. *Physiological Measurement*, *30*(5), 491–504. https://doi.org/10.1088/0967-3334/30/5/006

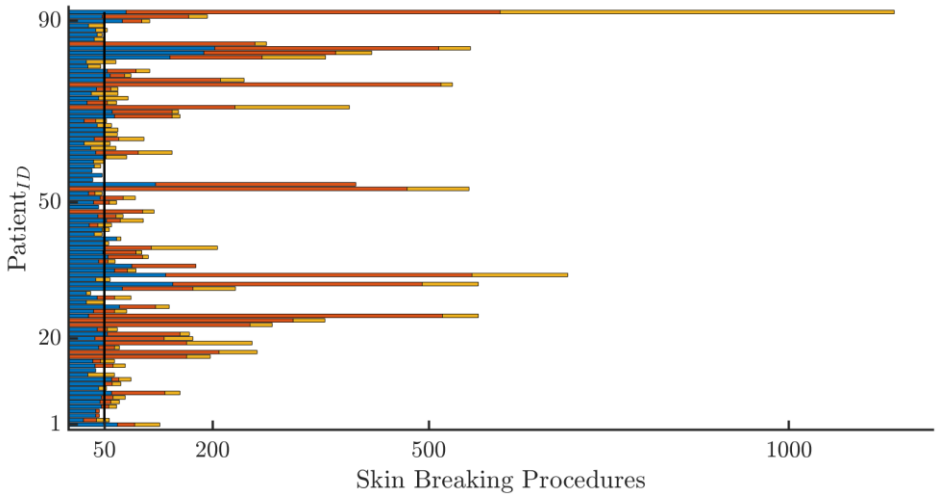


Figure R1/1. **The Gantt-Chart-like overview of all recordings for the different patients.** The number of stacked bars represents the number of recordings and the color is associated for the recording time: blue for the first recording, red for the second recording at 34 w and the yellow is the recording at discharge (PSG). The length represents the cumulative amount of SBPs. In particular, the blue bar is the cumulated SBPs up to first recording, while the red and the yellow bars have the incremental values of cumulated SBPs with respect to the first recording.

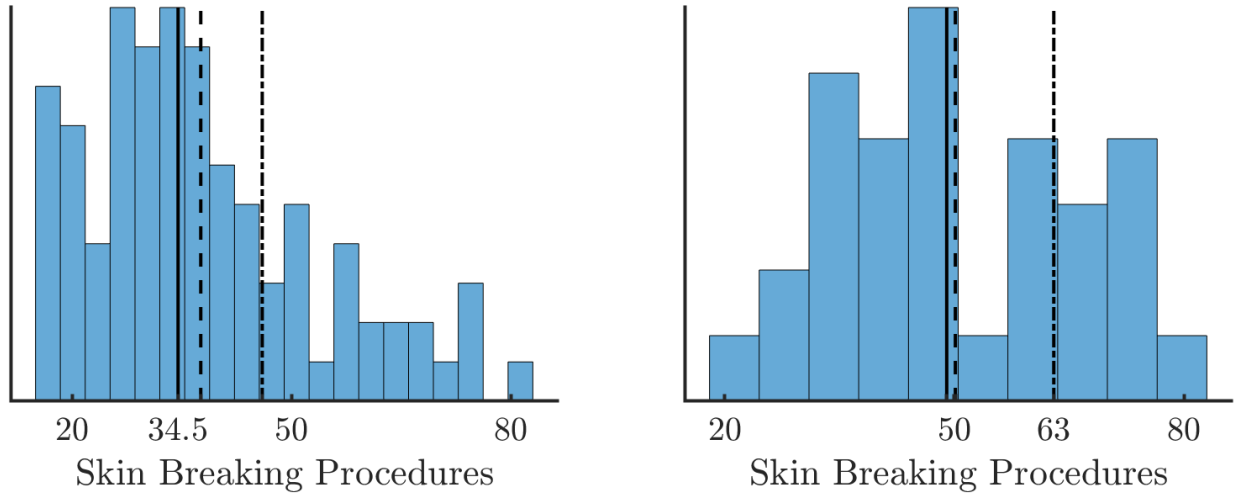


Figure R2/3. **The histogram distributions for the cumulative amount of SBPs at 5 days from birth.** The right panel shows the distribution for the entire dataset, while the second one depicts the distribution for the low gestational age dataset (GA <= 29 weeks). The black continuous line represents the median value of the distribution, the dashed line represents the mean and the dotted dashed line is 75% quantile of the investigated distribution.

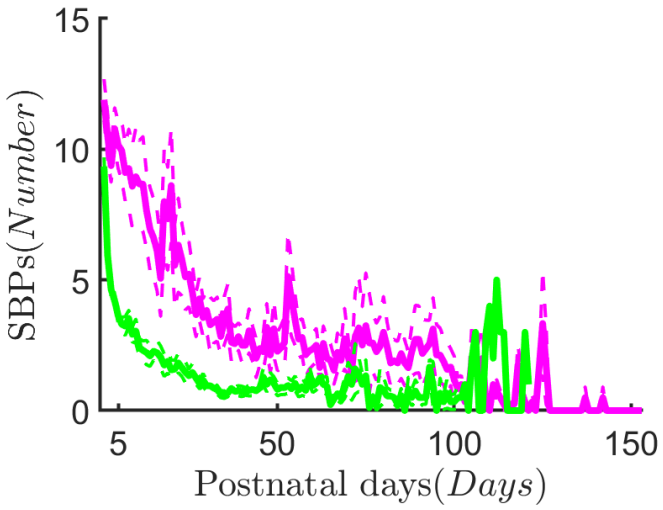


Figure R3. **The average skin breaking procedure charts during their NICU stay.** The SBPs charts are here reported for HIGH SBPs (SBPs>= 50, magenta curve) and for LOW SBPs (SBPSs < 50, green curve).

Table 4B. **Results of the two ways ANOVA test for NQS sleep in the ENTIRE dataset.** For each variable, the F-statistics and the associated p-values are reported for the SBP main effect, for the recording point effect and the interaction effect.

$\boldsymbol{Feature}$	$\boldsymbol{F_{SBP}}$	$\boldsymbol{p_{SBP}}$	$\boldsymbol{F_{REC}}$	$\boldsymbol{p_{REC}}$	$\boldsymbol{F_{INT}}$	$\boldsymbol{p_{INT}}$
$CI(Fp2)$	$F(1,178) = 17.6$	$p \leq 0.01$	$F(2,178) = 42.17$	$p \leq 0.01$	$F(2,178) = 6.62$	$p \leq 0.01$
$P(HF)$	$F(1,193) = 10.01$	$p \leq 0.01$	$F(2,193) = 13.66$	$p \leq 0.01$	$F(2,193) = 7.5$	$p \leq 0.01$
$CI(T4)$	$F(1,178) = 18.79$	$p \leq 0.01$	$F(2,178) = 33.04$	$p \leq 0.01$	$F(2,178) = 4.48$	$p \leq 0.01$
$CI(O2)$	$F(1,178) = 13.38$	$p \leq 0.01$	$F(2,178) = 44.28$	$p \leq 0.01$	$F(2,178) = 4.51$	$p \leq 0.01$

Table 5B. **Results of the two ways ANOVA test for QUIET sleep in the ENTIRE dataset.** For each variable, the F-statistics and the associated p-values are reported for the SBP main effect, for the recording point effect and the interaction effect.

$\boldsymbol{Feature}$	$\boldsymbol{F_{SBP}}$	$\boldsymbol{p_{SBP}}$	$\boldsymbol{F_{REC}}$	$\boldsymbol{p_{REC}}$	$\boldsymbol{F_{INT}}$	$\boldsymbol{p_{INT}}$
$Asym(\theta)$	$F(1,208) = 11.02$	$p \leq 0.01$	$F(2,208) = 101.71$	$p \leq 0.01$	$F(2,208) = 8.52$	$p \leq 0.01$
$CI(C3)$	$F(1,179) = 4.16$	$p = 0.04$	$F(2,179) = 78.76$	$p \leq 0.01$	$F(2,179) = 7$	$p \leq 0.01$
$P(HF)$	$F(1,191) = 14.85$	$p \leq 0.01$	$F(2,191) = 5.97$	$p \leq 0.01$	$F(2,191) = 4.56$	$p \leq 0.01$
$Asym(\delta)$	$F(1,208) = 4.91$	$p = 0.03$	$F(2,208) = 93.87$	$p \leq 0.01$	$F(2,208) = 9.46$	$p \leq 0.01$
$Asym(\alpha)$	$F(1,208) = 3.91$	$p = 0.05$	$F(2,208) = 75.05$	$p \leq 0.01$	$F(2,208) = 4.86$	$p \leq 0.01$
$CI(Fp2)$	$F(1,179) = 2.03$	$p = 0.16$	$F(2,179) = 95.45$	$p \leq 0.01$	$F(2,179) = 9.7$	$p \leq 0.01$
$CI(O1)$	$F(1,179) = 4.15$	$p = 0.04$	$F(2,179) = 94.66$	$p \leq 0.01$	$F(2,179) = 9.83$	$p \leq 0.01$
$CI(O2)$	$F(1,179) = 3.15$	$p = 0.08$	$F(2,179) = 92.16$	$p \leq 0.01$	$F(2,179) = 8.27$	$p \leq 0.01$
$CI(Fp1)$	$F(1,179) = 0.91$	$p = 0.34$	$F(2,179) = 88.25$	$p \leq 0.01$	$F(2,179) = 9.2$	$p \leq 0.01$
$CI(T3)$	$F(1,179) = 3.82$	$p = 0.05$	$F(2,179) = 86.79$	$p \leq 0.01$	$F(2,179) = 8.01$	$p \leq 0.01$
$Asym(\beta)$	$F(1,208) = 2.22$	$p = 0.14$	$F(2,208) = 61.27$	$p \leq 0.01$	$F(2,208) = 4.38$	$p \leq 0.01$
$CI(T4)$	$F(1,179) = 1.95$	$p = 0.16$	$F(2,179) = 83.01$	$p \leq 0.01$	$F(2,179) = 8.23$	$p \leq 0.01$

Table 6B. **Results of the two ways ANOVA test for QUIET sleep in the patients with a GA below 29 weeks**. For each variable, the F-statistics and the associated p-values are reported for the SBP main effect, for the recording point effect and the interaction effect.

$\boldsymbol{Feature}$	$\boldsymbol{F_{SBP}}$	$\boldsymbol{p_{SBP}}$	$\boldsymbol{F_{REC}}$	$\boldsymbol{p_{REC}}$	$\boldsymbol{F_{INT}}$	$\boldsymbol{p_{INT}}$
$P(HF)$	$F(1,67) = 2.36$	$p = 0.13$	$F(2,67) = 6.49$	$p \leq 0.01$	$F(2,67) = 3.49$	$p = 0.04$
$Asym(\alpha)$	$F(1,71) = 3.87$	$p = 0.05$	$F(2,71) = 61.61$	$p \leq 0.01$	$F(2,71) = 3.86$	$p = 0.03$
$P(LF)$	$F(1,67) = 3.56$	$p = 0.06$	$F(2,67) = 7.24$	$p \leq 0.01$	$F(2,67) = 2.5$	$p = 0.09$
$Asym(\theta)$	$F(1,71) = 2.52$	$p = 0.12$	$F(2,71) = 95.23$	$p \leq 0.01$	$F(2,71) = 3.15$	$p = 0.05$

Title	**The effect of early procedural pain in preterm infants on the maturation of EEG and heart rate variability**
Authors	1. Mario Lavanga 2. Bieke Bollen 3. Alexander Caicedo 4. Anneleen Dereymaeker 5. Katrien Jansen 6. Els Ortibus 7. Sabine Van Huffel 8. Gunnar Naulaers
Corresponding author	Mario Lavanga mlavanga@esat.kuleuven.be
Abstract	Preterm infants show a higher incidence of cognitive, social and behavioral problems, even in the absence of major medical complications during their stay in the neonatal intensive care unit (NICU). Several authors suggest that early life experience of stress and procedural pain could play a role in the altered development of cognition, behavior or motor patterns. Early life experience of pain has been shown to impact cerebral development and maturation resulting in an altered development of cognition, behavior or motor patterns in later life. However, it remains very difficult to assess this impact of procedural pain on physiological development. This study describes the maturation of EEG signals and heart rate variability in a prospective cohort of 92 preterm infants (< 34 weeks GA) during their NICU stay. We took into account the number of painful, i.e. skin-breaking, procedures they were subjected to early in life. Using physiological signal modelling, this study shows that a high exposure to early procedural pain, measured as skin-breaking procedures (SBPs), increased the level of discontinuity in both EEG and heart rate variability in preterm infants. These findings have also been confirmed in a subset of the most vulnerable preterm infants with a gestational age lower than 29 weeks. We conclude that a high level of early pain exposure in the NICU increases the level of functional dysmaturity, which can ultimately impact preterm infants' future developmental outcome.

Title	**The effect of early procedural pain in preterm infants on the maturation of EEG and heart rate variability**
Authors	1. Mario Lavanga a. mlavanga@esat.kuleuven.be b. Department of Electrical Engineering (ESAT), Division STADIUS, KU Leuven, Leuven, Belgium 2. Bieke Bollen a. bieke.bollen@uzleuven.be b. Department of Development and Regeneration, faculty of Medicine, KU Leuven, Belgium 3. Alexander Caicedo a. alexander.caicedo@urosario.edu.co b. Department of Applied Mathematics and Computer Science, School of Engineering, Science and Technology, Universidad del Rosario, Bogota', Colombia 4. Anneleen Dereymaeker a. anneleen.dereymaeker@uzleuven.be b. Department of Development and Regeneration, faculty of Medicine, KU Leuven, Belgium 5. Katrien Jansen a. katrien.jansen@uzleuven.be b. Department of Development and Regeneration, faculty of Medicine, KU Leuven, Belgium 6. Els Ortibus a. els.ortibus@uzleuven.be b. Department of Development and Regeneration, faculty of Medicine, KU Leuven, Belgium 7. Sabine Van Huffel a. Sabine.VanHuffel@esat.kuleuven.be b. Department of Electrical Engineering (ESAT), Division STADIUS, KU Leuven, Leuven, Belgium 8. Gunnar Naulaers a. gunnar.naulaers@uzleuven.be b. Department of Development and Regeneration, faculty of Medicine, KU Leuven, Belgium
Corresponding author	Mario Lavanga mlavanga@esat.kuleuven.be
Conflict of interest	All authors declared that the current research is original and it has never been considered in another journal. None of the author has a conflict of interest to disclose.

The effect of early procedural pain in preterm infants on the maturation of EEG and heart rate variability

M Lavanga[1], B Bollen[2], A. Caicedo[3], A. Dereymaeker[2], K. Jansen[2], E Ortibus[2], S. Van Huffel[1], G Naulaers[2]

[1] Department of Electrical Engineering (ESAT), Division STADIUS, KU Leuven, Leuven, Belgium

[2] Department of Development and Regeneration, Faculty of Medicine, KU Leuven, Belgium

[3] Applied Mathematics and Computer Science, School of Engineering, Science and Technology, Universidad del Rosario, Bogota', Colombia

Abstract

Preterm infants show a higher incidence of cognitive, social and behavioral problems, even in the absence of major medical complications during their stay in the neonatal intensive care unit (NICU). Several authors suggest that early life experience of stress and procedural pain could play a role in the altered development of cognition, behavior or motor patterns. Early life experience of pain has been shown to impact cerebral development and maturation resulting in an altered development of cognition, behavior or motor patterns in later life. However, it remains very difficult to assess this impact of procedural pain on physiological development. This study describes the maturation of EEG signals and heart rate variability in a prospective cohort of 92 preterm infants (< 34 weeks GA) during their NICU stay. We took into account the number of painful, i.e. skin-breaking, procedures they were subjected to early in life. Using physiological signal modelling, this study shows that a high exposure to early procedural pain, measured as skin-breaking procedures (SBPs), increased the level of discontinuity in both EEG and heart rate variability in preterm infants. These findings have also been confirmed in a subset of the most vulnerable preterm infants with a gestational age lower than 29 weeks. We conclude that a high level of early pain exposure in the NICU increases the level of functional dysmaturity, which can ultimately impact preterm infants' future developmental outcome.

Introduction

The survival rates of preterm infants increased in recent years, but the incidence of cognitive and behavioral deficits remains higher than in full-term infants even in the absence of specific cerebral lesions [36]. Different authors describe that between 30% and 60% of the preterm population show a lower cognitive and/or behavioral outcome compared to their peers [35,37], without necessarily showing any specific complication during their stay in the neonatal intensive care unit (NICU) [5].

Several authors suggest that pain-related stress and repeated procedural pain could play a role in the altered development of cognition, behavior and motor patterns of premature infants [22,51,56]. Early-life painful experiences seem to impact the brain structure and function on the cortical and subcortical level [18,48,51]. Both frontal and parietal cortex volumes and thickness have been found to decrease in case of procedural pain [48,51]. Similarly, white matter connectivity and thalamic volume are reduced in case of high numbers of early skin-breaking procedures (SBPs), which count events like heel lance, intramuscular injection, chest tube insertion and central line insertion [8,18]. Therefore, the accumulation of painful procedures in the NICU might play a role in the lower cognitive and behavioral outcome. For example, Grunau et al. (2009) found lower cognitive outcome scores at 18 months and more internalizing behavior in preterm infants that underwent a high number of SBPs [23].

The impact of early-life pain on brain development can be assessed via Magnetic Resonance Imaging (MRI). This technique, which mainly shows anatomical abnormalities, is not always available for preterm babies [38]. EEG is a complementary technique, which provides insights in functional brain integrity and has the advantage of being less invasive. The sensitization to pain and the lowering pain threshold in premature infants [20,23] can affect the subplate neurons via excitotoxicity and apoptosis [56], resulting in changes in brain volumes. Pain sensitization can be measured in preterm infants by means of cortical reactivity responses to the heel lance. Those evoked potentials normally are dispersed neuronal bursts on the scalp up to 35 weeks gestational age (GA) [19,50] and they are replaced by mature evoked responses contributing to the EEG background progression from a discontinuous to a continuous trace [44]. Therefore, one might also expect alterations of the spontaneous background cortical oscillations due to pain-related stress [16]. Additionally, Jones et al. [27] highlighted the relationship between infants' heart rate variability (HRV) and EEG evoked-potentials to noxious stimuli, while Cong et al. [10] showed specific changes in HRV in response to heel lance in premature infants.

We hypothesized that pain-related stress increases electrophysiological dysmaturity, i.e. a higher EEG discontinuity due to a higher number of dispersed neuronal bursts and a higher HRV of long-term oscillations. A quantitative analysis of EEG and HRV was used to monitor decreasing rate of EEG discontinuity and increasing HRV respectively [24,32,33,43,58]. Specifically, functional maturation charts were obtained to understand whether a high level of SBPs can induce dysmature patterns in EEG and HRV suggesting an impact on the developmental outcome of the patient.

Methods

The research protocol was examined and approved by the Ethical Committee of University Hospitals Leuven (Belgium) as part of the Resilience trial, which was registered at Clinical Trials.gov (NCT02623400). The study was performed in accordance with the Guidelines for Good Clinical Practice (ICH/GCP) and the latest version of the Declaration of Helsinki.

Participants

A prospective cohort of (n = 92) preterm infants was recruited in the Neonatal Intensive Care Unit (NICU) of the University Hospitals Leuven (Belgium) between July 2016 and July 2018, as part of a larger ongoing study on preterm infant and parental Resilience.

Parents of preterm infants born before 34 weeks gestational age (GA) and/or with a birth weight less than 1500 g were approached for informed consent within the first three days after birth. Exclusion criteria were parental age <18 years, medical (somatic or psychiatric) condition in parent(s) that impeded participation, absence or limited knowledge of Dutch or English, major congenital malformation or central nervous system pathology (grade 3 or grade 4 intraventricular hemorrhage or periventricular leukomalacia – brain ultrasounds were carried out on postnatal days 1, 3 and 7, and then repeated weekly) in the preterm infant at the time of consent.

Data acquisition

Medical and nursing electronic charts were reviewed from birth till discharge home by a physician and by two GCP qualified neonatal research nurses. Variables that were obtained included gestational age (GA) at birth, birth weight (BW), illness severity at birth (e.g. CRIB score [52]) and the number of skin-breaking procedures per day. Also, data on neuroactive medications (caffeïne, dopram, fentanyl, luminal, chloral

hydrate, dormicum, contramal, catapressan) administered on the day of the recording were obtained. Caffeïne was routinely administered at a dose of 5 mg/kg.

Neonatal procedural pain exposure was defined as the sum of all skin-breaking procedures (SBPs). To define these SBP's we drew on the work of Brummelte et al. [8] and Grunau et al. [23], as well as the work of Newnham et al. (2009) in the development of the Neonatal Infants Stress Scale (NISS). We included medical procedures that yield a score of 4 and 5 on the NISS such as chest tube insertion, central line insertion, heel lance, intramuscular injection, eye examination, and other added painful procedures such as wound care. An overview of all procedures is reported in Table 1. SBPs were counted for every category separately for each day. If multiple attempts were carried out, each attempt was counted as a single SBP.

We calculated the sum of SBPs in the first five days of life. Subsequently, SBP scores were binarized (LOW SBPs versus HIGH SBPs) with a threshold of 50 SBPs in the first five days of life to detect patients who experienced a high number of skin-breaking procedures, and thus a high level of early procedural pain. This threshold was based on earlier findings on the impact of early-life SBPs in preterm infants [8,18] and our analysis of the distribution of the cumulative SBPs (discussed in the results section). This makes it possible to compare the neuroanatomical changes reported by these authors with the neurophysiological changes that we describe. Brummelte et al. [8] and Duerden et al. [18] considered procedural pain as the cumulated SBP up to their first MRI scan (normally around PMA 32 weeks or 21 postnatal days). Our first recording was planned to be as close as possible to postnatal day 5. However, sometimes it had to be carried out a few days earlier or later because of the preterm infant's unstable medical condition, or because of EEG equipment or technician availability.

Electrophysiological data collection

Physiological data were measured at three different time points in each patient. The recording protocol comprised a first measurement within five days from birth (5days), another session at 34 weeks post-menstrual age (PMA) (34w) and a last measurement before discharge to home. Measurements lasted for at least 3 hours as a rule, infants underwent a 24-hours polysomnography before leaving the NICU, therefore the last session was labeled as PSG. For some patients the recording schedule was adapted. For infants born at 33-34 weeks GA, only one recording (representing the first two coinciding recordings from birth) was performed since their PMA was around 34w when they were 5 days old. Some infants were transferred to level II units in hospitals closer to home. Therefore, not all infants have multiple recordings and, importantly, some SBP measures could not be tracked. However, we strived for the readmission of infants to our hospital for the PSG measurement before they went home. In total, 92 patients with 228 recordings and information about the number of SBPs were analyzed. The Gantt chart in Figure 1 summarizes the number of recordings and cumulated SBPs at the different timestamps. More details are reported in the statistical analysis section.

Physiological data included EEG and ECG measurements. EEG data were collected according to the 10-20 system using nine monopolar electrodes (F_{p1}, F_{p2} , C_3, C_4 , C_z, T_3, T_4, O_1, O_2) and monitored with the OSG system (OSG BVBA, Brussel). Each EEG signal was referenced to C_z, which was then excluded from further analysis, leaving a total amount of 8 channels. ECG was measured as single lead ECG and was used to derive the tachogram or HRV signal as subsequent R-peak to R-peak intervals (RRi). The R-DECO toolbox [39] was used for R-peak detection.

Before any functional analysis, both EEG and HRV signals were preprocessed to remove artefacts and define sleep states. In order to remove movement-related and non-cortical information, EEG signals were band-pass-filtered between 0.5 and 20 Hz and independent component analysis to filter EOG was

then applied. The narrow filtering band is based on the quantitative analysis of discontinuous EEGs by De Wel et al. [58] and of amplitude integrated EEGs by O'Toole et al. [42].

EEG data were then used to define two processing epochs of 20 minutes each related to quiet sleep state and a combination of awake and active sleep, which is called *nonQuiet sleep* (nQS). The behavioral analysis was performed with the algorithms described in [2,14], the probabilistic output of which was summed to look for the two 20 minute epochs. QS was derived as a window around the maximum of a quiet-sleep probability profile, while nQS as a window around the minimum.

Before the extraction of any functional feature, the last step of the preprocessing for both sleep stage epochs was a segmentation in non-overlapping sliding windows and a threshold filtering according to the following criteria: standard deviation above 50 µV, absolute difference sample-to-sample above 50 µV and absolute amplitude above 200 µV [25]. The size of each window was different for each extracted variable and is specified in following subparagraphs. It is important to highlight that a window was excluded from the processing if more than 4 channels exceeded one of the criteria thresholds.

Since the RR intervals of the tachogram can be affected by premature ventricular contractions (PVC), the RR were corrected as discussed in [39] and the modulation signal m(t) was derived via the *integral pulse frequency modulation (IPFM)* model to investigate the autonomic nervous system stimulation [3].

Functional measurements

Different features were computed to track the functional maturation of neonates during their NICU stay and assess the level of dysmaturity in the electrophysiological signals, based on previous studies [24,43,58]. Dysmaturity in EEG signals was defined as a discontinuity and persistence of delta waves [54], while dysmaturity of HRV was defined as a higher amplitude of the slow-wave oscillations [26]. The computational steps to derive EEG and HRV dysmature patterns are reported in the paragraph below.

1. Amplitude-integrated EEG features

Clinicians normally rely on the amplitude-integrated EEG (aEEG) for the assessment of brain maturity and the emergence of sleep-wake cycle. The great advantage is the simplicity of interpretation compared to a full-channel EEG [45]. Therefore, we decided to quantify the level of EEG dysmaturity with a more interpretable metric. The aEEG was estimated by means of the range EEG and the discontinuity of EEG features was quantified by means of range EEG (rEEG) asymmetry [43]. This variable quantifies the level of dysmaturity by the difference in distance from the rEEG median to lower and upper margin of rEEG itself. These two margins represent respectively the 5^{th} and 95^{th} percentiles of the rEEG [40]. Studies show the higher the asymmetry the higher the discontinuity of EEG [41,43]. Following the guidelines in [43], the asymmetry was derived for the most important EEG frequency bands, which are $\delta = (2-4]\ Hz$, $\theta = (4-8]\ Hz$, $\alpha = (8-16]\ Hz$ and $\beta = (16-20]\ Hz$. The rEEG is computed for each channel and one signal is obtained by the median of all range EEGs to resemble the approach of aEEG. The rEEG was derived for 2 s windows without overlap and all indices were then grand-averaged for each sleep state.

2. Multiscale Entropy

A more refined maturity index of the neonatal EEG is the multiscale entropy (MSE), as described by [7,11,58]. It is based on the more common index of the Sample Entropy, which measures the predictability of the signal. Its actual definition is the negative natural logarithm of the conditional probability that a dataset of size N, which presents repetition of an m-points pattern with a certain tolerance r, will also present repetition of an m+1 points pattern within the same tolerance [31]. The tolerance r is normally

defined as 20% of the standard deviation of the signal. The MSE is a generalized version of Sample Entropy at different scales τ, which means the signal is coarsely grained with a moving average and downsample of order τ. The advantage is two-fold: MSE does not only contain the information of the regular Sample Entropy at scale 1, but the coarse-graining process enhances the slower-patterns in the computation of the sample entropy.

In general, the Sample Entropy is low in case of discontinuity and early-life EEG and increases with age [59]. Similarly, the area under the MSE curve or the cumulated MSE for all scales, $CI = \sum_{\tau} MSE(\tau)$, is low in case of discontinuity and it increases with age [58]. This metric is known as the complexity index (CI) and is a general measure of irregularity across scales. Therefore, the MSE will investigate how the matching probability varies for long-term variations (high scales or low-frequencies) and for short-term-variations (small scales or high-frequencies), combining both the investigation of EEG discontinuity and slow-wave patterns.

CI was computed in 150 sec non-overlapping windows and grand-averaged along the time course of each sleep state [15,47,58]. Multiscale entropy was computed for each channel and each of these complexity indices was considered in the final procedural pain analysis.

3. HRV Power features

In order to assess dysmaturity based on the autonomic activity, the absolute power of the HRV in the high-frequency (HF), low-frequency (LF) and very-low frequency (VLF) bands was computed. The band limits were the following ones: $HF = (0.2 - 4]\ Hz$, $LF = (0.08 - 0.2]\ Hz$, $VLF = (0.0033 - 0.08]\ Hz$ [13]. The power spectral density was computed via the continuous wavelet transform (CWT), with analytical Morlet as mother wavelet. The CWT computes an instantaneous power spectrum of the signal and the band-power can then be computed for each time sample. Consequently, power time-series are obtained for the LF, HF and VLF power. The CWT was estimated in both QS and nQS using the entire 20 minutes and power time-series were averaged over both epochs.

Statistical analysis

Statistical analysis was performed with MatLab (Mathworks, Inc). A linear mixed-effect regression (LME) model was performed to evaluate the association between functional measurements (HRV power, EEG complexity and asymmetry) and early SBPs. In order to correct for the effect of gestational age and post-menstrual age, the final regression model did not only include the binary SBP, but also these two age-related variables as fixed effects. The random effect was expressed by the group represented by each patient and was considered for both the slope coefficients and the intercept of the LME model. Additionally, the regression models were computed for both behavorial sleep states (quiet sleep, QS, and non-quiet sleep, nQS).

The significance of the association between early SBPs and functional measurements was tested in two ways. In order to correct for the multiple comparisons (multiple features coming from multiple channels), the p-value of the SBP coefficient was corrected via the false-discovery rate with $\alpha = 0.05$. The false discovery rate (FDR) can be applied to correct for the number of brain region locations in case of channel-dependent features [18,48], but it can also be used to correct for the total number of extracted features [21,28]. FDR was applied in our study to correct for the number of features in the analysis and rank the features from the one with most significant association with SBP to the least significant one. In addition, the significant contribution of SBP in explaining the maturational trajectory of the functional variables was assessed via the log-likelihood ratio (LLR) test [4]. This ratio test specifically assesses whether adding 'early SBPs' in the prediction model reduces the variance of the residuals of a model which contains only the

age variables (PMA and GA). The full coefficient of determination (R^2) of the model including SBP group as well as the coefficient of determination of the reduced model, with only GA and PMA (R^2_{Red}) were also computed. The decrease in error (%) when the SBP variable is added to the model was also obtained together with the associated log-likelihood statistics F, which is ultimately a log transform of the error variances ratio.

Additionally, two-way ANOVA's were performed on our EEG and HRV variables of interest with SBP group (low versus high) and measuring point (5 days, 34 weeks, PSG) as independent variables. To investigate differences between preterm infants in the high and low SBP at each measuring point, Tukey-Kramer multiple comparison tests were subsequently performed.

These models were tested for both the entire set of patients (n=92) and for preterm infants with a GA $\leq$ 29 weeks (n=31). We specifically focus on this more coherent group of extremely preterm babies because they are most vulnerable to require intensive care and are thus subjected to more SBPs.

Results

Patients demographics

Infants demographics and clinical characteristics are summarized in Table 2 for the entire dataset and in Table 3 for the early-GA dataset. As expected, patients with a higher number of cumulated SBPs at 5 days also had a lower gestational age, a lower PMA at the moment of the recording, higher CRIB score and higher number of days of mechanical ventilation and of CPAP (Table 2). Caffeine treatment (yes/no) at 5 days and APGAR score did not significantly differ between SBP groups, while the number of patients receiving caffeine was different at 34 weeks between SPB groups. In the subset of early-GA infants (<29 weeks), only birth weight differed significantly between infants of the low and high SBP group (Table 3). Only one patient from the high SBP group received medication that could exert a CNS depressant effect at the 34 weeks recording. However, the patient was kept in the overall analysis because the medication was only provided during one recording of the patient and because we did not observe significant changes in the regression models when this recording was omitted.

Skin breaking procedures

Figure 2 clearly shows that there is a peak in the number of SBPs in the first days of life, followed by an exponential decay. In particular, there is already a significant drop in SBPs after 5 postnatal days. The distribution of cumulated SBPs at 5 days are reported for the entire dataset and for the subset of patients with GA ≤ 29 weeks in Figure 3. In the entire dataset, the median number of cumulated SBPs at 5 days is 34.5 and the distribution has a fat-tail on the right. It implies that a median threshold would give rise to more heterogeneous levels of SBPs in the high SBP group. The early-GA distribution has a median of 50 without a fat-tail, therefore it contains more similar high-level SBPs. Importantly, Figure 2 shows that, using this threshold, the difference in the number of SBPs persists throughout NICU stay between preterm infants in the low and high SBP group.

Relationship between EEG and HRV functional variables and early skin breaking procedures

The relationship between electrophysiological maturational trends and early SBPs was examined for the entire dataset and reported in Table 4 and Table 5. After FDR correction, early SBPs were negatively associated with the EEG complexity index, during QS as well as nQS (e.g., $CI(F_{P2})$ has $B_{SBP} = -1.585$ with $p \leq 0.05$ in nQS and $CI(C_3)$ has $B_{SBP} = -2.23$ with $p \leq 0.05$ in QS). Early SBPs were also associated to an increase in range EEG asymmetry in QS (e.g., $asym(\theta)$ with $B_{SBP} = 0.051$ with $p \leq 0.01$). For HRV, the power in the HF band was positively associated with SBPs in both QS and nQS (P(HF)

has $B_{SBP} = 0.003$ with $p \leq 0.05$ and has $B_{SBP} = 0.003$ with $p \leq 0.01$ in QS). These results imply that a high level of SBPs is associated with a discontinuous EEG trace and with a higher vagal tone after PMA and GA correction.

The central role of SBPs is confirmed by the log-likelihood ratio test and the decrease in error variance reported in Table 4 and Table 5. In nQS, the decrease in error variance ranges from 3.07% to 4.49 % with an associated improvement of R^2 from R^2_{Red}, while the decrease oscillates between 2.95% up to 10% in the QS epoch. All the reported variables had significant improvement in the regression performance as indicated by the associated p-values.

The differences in maturational trends reported by Table 4 and Table 5 are investigated at each recording time by the two ways ANOVA test. Based on the FDR ranking in Table 4 and Table 5, we reported $CI(F_{P2})$ in nQS, $asym(\theta)$ in QS and $P(HF)$ in QS in Figure 4, 5 and 6.

In non-quiet sleep, we found a statistically significant interaction effect between measuring point and SBP group on EEG complexity index ($F(2,178) = 6.62, p \leq 0.01$). Figure 4 shows that the complexity index increases over time (main effect of measuring point: $F(2,178) = 42.17, p \leq 0.01$). Simple main effects analysis showed that preterm infants in the high SBP group have a lower complexity index than children in the low SBP group at the 5 days recording ($p \leq 0.01$). This difference is not statistically significant for the 34 weeks ($p = 0.59$) or PSG ($p = 1$) recording.

In quiet sleep, we found a statistically significant measuring point-by-SBP group interaction effect for $asym(\theta)$ ($F(2,208) = 8.52, p \leq 0.01$, Figure 5). As expected, rEEG asymmetry decreased over time (main effect of measuring point $F(2,208) = 101.71, p \leq 0.01$). Simple main effects analysis showed a higher rEEG asymmetry in preterm infants in the high SBP group compared to the low SBP group at the first measuring point at 5 days ($p \leq 0.01$). This difference was still marginally significant at the 34 weeks recording ($p = 0.05$). For the last recording (PSG), rEEG asymmetry did not statistically differ between the low and high SBP group ($p = 0.72$). Figure 6 shows that the HF oscillations increase over time (main effect of measuring point: $F(2,191) = 5.97, p \leq 0.01$), but statistically significant interaction effect between measuring point and SBP group is found ($F(2,191) = 4.56, p \leq 0.01$). The simple main effect analysis shows a higher $P(HF)$ in the high SBP group at the PSG recording time ($p \leq 0.01$), but there is no difference for the 5 days ($p = 0.43$) or 34w ($p = 1$) recording time.

The results for the patients with a GA below 29 weeks are reported in Table 6 only for QS. The variables in nQS did not pass the FDR test. Similarly to the entire dataset, the HF power and the asymmetry in the alpha and theta band in QS have a positive association with the SBP variable ($P(HF)$ has $B_{SBP} = 0.005$ with p<0.01 and asym(alpha) has $B_{SBP} = 0.064$ with $p \leq 0.05$). Unlike the entire dataset, the sympathetic tone P(LF) is also significantly associated with the SBP variable (P(LF) has B_{SBP}= 0.009 with p<0.05). The LLR test and F-statistics support the significant decrease in error variance and improvement in R^2. The change in error ranges from 6.38% to 13.2%.

Based on FDR ranking, we reported the $asym(\alpha)$ in QS and $P(HF)$ in QS in Figure 7 and 8 and we showed the results of simple main effect analysis based on the ANOVA test. In a subset analysis of infants with <29 weeks GA, we found a significant SBP-by-measuring point interaction on rEEG asymmetry in quiet sleep ($F(2,71) = 3.86, p = 0.03$). Asymmetry decreased over time (main effect of measuring point: : $F(2,71) = 61.61, p \leq 0.01$). At the 34 weeks recording, infants in the high SBP group showed a significantly higher rEEG asymmetry than the infants in the low SBP group (p =0.02). At the recording at 5 days and the PSG recording, this difference did not reach significance ((p =0.91 and p

=0.98, respectively). A significant SBP-by-measuring point interaction on P(HF) is found in quiet sleep ($F(2,67) = 3.49, p = 0.04$). HF oscillations also increase over time (main effect of measuring point: $F(2,67) = 6.49, p \leq 0.01$). Post-hoc analysis showed this difference in HF oscillations between the high and low SBP group is only significantly different at the last, PSG, recording (p =0.04).

Discussion

In this study, we confirmed our hypothesis that a high number of early skin breaking procedures in premature infants is associated with a dysmature EEG. We also found that a high amount of SBPs is associated with a higher heart rate variability.

Data were collected in a neonatal unit where a lot of attention is given to monitoring and minimizing pain and discomfort, and where individualized developmental care and family integrated care principles are fundamental to the unit's care philosophy. Nevertheless, this study confirms that preterm infants experience a high amount of skin breaking procedures during their NICU stay.

Developmental studies show that both EEG and HRV are expected to change with infant's development. If electrophysiological patterns in these signals keep the traits and grapho-elements which are typical of early gestational age, they are labelled as dysmature. The two main features of dysmature EEG, which are discontinuity and slow-wave persistence, are all expected to significantly decrease with development (Pavlidis et al., 2017b; Wallois, 2010). As demonstrated by [43,58], EEG complexity increases with increasing PMA, while range EEG asymmetry is higher in the first week of life and has a downward trend with development. For HRV, the band-power of the main HRV tones (VLF,LF and HF) are all expected to increase with infants' development [9,12,26].

To our knowledge, this is the first study that shows the effect of pain-related stress on the functional maturation of the brain and the autonomic nervous system in premature infants. Our results show that a high number of early skin breaking procedures is significantly associated to an EEG with lower EEG complexity and higher rEEG asymmetry, which can imply a dysmature EEG [32,34,43,58], and a higher HRV. Although the level of SBPs is strongly correlated with GA and PMA (see Table 2 and Table 3) as expected, the association between EEG and HRV variables and SBPs was not only confirmed after controlling for age at birth and age at recording, but was also supported by the decrease in prediction error when procedural pain was entered in the model. Simple main effect analyses shows at which recording time the functional variables statistically differ between high and low SBPs groups. Post hoc analyses confirm that EEG shows dysmature traits in the first weeks of life, while the vagal tone is higher at PSG in the infants that experience a high amount of SBPs. Similar results were obtained in the early-GA group in terms of an association between high SBPs, dysmature EEG and greater HRV. Interestingly, the results tend to be similar in the QS state (Table 5 and Table 6), while no significant differences were found in nQS for the early-GA group compared to the entire dataset.

Early pain might act on the infant's development through different mechanisms, mainly sensitization to pain of the central nervous system and lowering sensory threshold [20]. Early pain and injuries might developmentally regulate nociceptive pathways, such as hyperinnervation of the periphery and increasing receptive fields of the dorsal horn of neurons [49,53]. This peripheral sensitization might lead to the central sensitization, which can affect the central nociceptive pathways and thalamus. Consequently, the thalamocortical projections will be abnormally distributed since their topography and structural organization is activity-dependent [18]. In premature infants, any impact on the thalamus development and thalamo-cortical connections will have a direct impact on the cortical activity, since the high-amplitude delta bursts type of activity is a result of the predominance of the subcortical centers [30,46]. During the development of thalamocortical projections, the axons of the thalamus will contend the

activity on the cortex. If early pain disrupts the thalamo-cortical connections, the activity on the cortex will also be different [18].

Previous research showed that pain stimulation might induce higher delta activity and delta brushes, which are diffused over the entire cortex due to underdeveloped cortico-cortical connections, as also supported by fMRI studies [55]. This widespread diffused delta activity is present up to 35 weeks of GA, before it is replaced by a mature cortical response at full-term age [50]. We therefore speculated that neonatal pain might induce a different brain rhythmicity, especially in terms of δ band, and might lead to a greater discontinuous tracing on the cortex, as also shown in Figure 4, 5 and 6. Since pain-related stress and cumulated pain might ultimately induce a diffused delta-burst activity [19,27,50], pain can ultimately increase the discontinuity of the EEG and contribute to a more dysmature pattern. Therefore, the greater rEEG asymmetry and the lower EEG complexity are the result of a more dysmature tracing.

Clearly, other subtle factors or causes of this persistence EEG dysmaturity cannot be excluded. However, Doesburg et al. [17] also found that a different brain rhythmicity was associated with cumulated pain, which was associated to reduced visual-perceptual abilities, and Grunau et al. showed that pain-related stress is associated with a lower cognitive outcome [23]. In parallel, several authors have shown that a dysmature EEG in premature infants is associated with worse cognitive outcome [6,29,57]. Furthermore, early-life pain and the resulting disruption of thalamocortical pathways are also associated with a lower cognitive outcome [18]. Therefore, our results might provide the functional link which can discriminate infants at risk for developmental delay: a higher SBP load might induce a more dysmature EEG which is related to a lower development outcome. Currently, follow-up developmental testing is taking place in our patient sample so we will be able to link the current results with developmental outcome measures in the future.

Unlike EEG, the results related to HRV are somewhat counterintuitive. Normally, a lower heart-rate variability in premature infants is associated to a lower mental outcome [26] and the maturation of ANS is characterized by an increase in short and long-term HRV, which means an increase in HF and LF oscillations [12]. Based on the cortical findings, one would expect that a higher SBP would decrease the HRV power in different bands. However, both HF and LF oscillations seem to increase with increasing age and increasing SBP. The increase in short and long-term variations of the tachogram might be the consequence of a faster ANS development to modulate the noxious response. This might be a further consequence of central pain sensitization and the alteration of the stress response at ANS control level and the HPA axis [18,22,56]. However, this hypothesis requires further testing in future studies.

A notable difference regards the sleep states: QS substantially presents more significant associations between stress and functional features than nQS. Similarly to HRV, definitive conclusions cannot be drawn, but it is interesting to note that the greater number of associations are revealed in the calmest behavioral state with the most discontinuous EEG tracing [1]. This can be a further proof that early-life stress can induce a more discontinuous EEG, with a long-lasting effect to infant's physiology that goes beyond a simple sleep interruption or deprivation. However, QS is the latest state to mature and is typically characterized by a discontinuous tracing, which is one of the main traits of dysmaturity [1]. Therefore, the association between stress and dysmaturity might be easier to investigate in this stage than in nQS, which is normally a mix of active sleep and awake with a more continuous tracing.

Another crucial point regards the most vulnerable patients, who have GA ≤ 29 weeks. Duerden et al. found a stronger association between SBPs and the thalamic volume [18] in extremely preterm infants. One might expect that the association between SBPs and EEG dysmaturity is mainly driven by the young GA of the patients with high SBPs. We did, however, confirm the link between high SBPs, EEG dysmaturity and higher HRV in the GA ≤ 29 weeks subgroup. Therefore, the current results show similar EEG

dysmaturity and HRV behavior for both the entire dataset and the vulnerable patient group in case of high SBPs. Interestingly, this similarity is present only for the QS state, while the results were not confirmed during nQS in the early-GA group. This similarity in the calmest state of the sleep cycle might further support the long-lasting effect of stress on sleep architecture and physiology.

Conclusions

The current study aimed to quantify the association between early SBPs and EEG and HRV functional trends in preterm infants. We found a more discontinuous EEG and a larger HRV in infants that were exposed to high levels of early procedural pain. These dysmaturity patterns provide further evidence that central pain sensitization in premature babies might affect their future development and cognitive and behavioural outcome. Pain and stress assessment via functional monitoring might help clinicians to optimize their pain treatment at cot-side. Since the early-life experience in the first days of life is crucial for future development, the use of EEG and HRV might complement clinicians' guideline about analgesia in order to ameliorate the neurodevelopmental outcome of the patients.

Acknowledgements

The authors would like to thank all children and parents who participated in the study. They are also thankful to the research nurses Isabelle Hermans, Julie Messiaen, and student Elien De Saeger for the support in the SBPs collection and to technicians Katrien Lemmens and Jan Vervisch for the EEG measurements. Research supported by Bijzonder Onderzoeksfonds KU Leuven (BOF) : C24/15/036 ``The effect of perinatal stress on the later outcome in preterm babies", EU: H2020 MSCA-ITN-2018: 'INtegrating Functional Assessment measures for Neonatal Safeguard (INFANS)', funded by the European Commission under Grant Agreement #813483. This research received funding from the Flemish Government (AI Research Program). SVH and ML are affiliated to Leuven.AI - KU Leuven institute for AI, B-3000, Leuven, Belgium. Mario Lavanga is a SB Ph.D. fellow at Fonds voor Wetenschappelijk Onderzoek (FWO), Vlaanderen, supported by the Flemish government.

References

[1] André M, Lamblin MD, d'Allest AM, Curzi-Dascalova L, Moussalli-Salefranque F, Nguyen The Tich S, Vecchierini-Blineau MF, Wallois F, Walls-Esquivel E, Plouin P. Électroencéphalographie du nouveau-né prématuré et à terme. Aspects maturatifs et glossaire. Neurophysiol Clin 2010;40:59–124.

[2] Ansari AH, De Wel O, Lavanga M, Caicedo A, Dereymaeker A, Jansen K, Vervisch J, De Vos M, Naulaers G, Van Huffel S. Quiet sleep detection in preterm infants using deep convolutional neural networks. J Neural Eng 2018;15:066006. doi:10.1088/1741-2552/aadc1f.

[3] Bailón R, Laouini G, Grao C, Orini M, Laguna P, Meste O. The integral pulse frequency modulation model with time-varying threshold: Application to heart rate variability analysis during exercise stress testing. IEEE Trans Biomed Eng 2011;58:642–652.

[4] Barrett AB, Barnett L, Seth AK. Multivariate Granger causality and generalized variance. Phys Rev E 2010;81:041907. doi:10.1103/PhysRevE.81.041907.

[5] Bhutta AT, Cleves MA, Casey PH, Cradock MM, Anand KJSS, Children S, Cleves MA, Casey PH, Cradock MM, Anand KJSS. Cognitive and Behavioral Outcomes of School-Aged Children Who Were Born Preterm. J Am Med Assoc 2007;288:728–737.

[6] Le Bihannic A, Beauvais K, Busnel A, de Barace C, Furby A. Prognostic value of EEG in very premature newborns. Arch Dis Child Fetal Neonatal Ed 2012;97:F106-9. doi:10.1136/adc.2010.204735.

[7] Bosl W, Tierney A, Tager-Flusberg H, Nelson C. EEG complexity as a biomarker for autism spectrum disorder risk. BMC Med 2011;9:18. doi:10.1186/1741-7015-9-18.

[8] Brummelte S, Grunau RE, Chau V, Poskitt KJ, Brant R, Vinall J, Gover A, Synnes AR, Miller SP. Procedural pain and brain development in premature newborns. Ann Neurol 2012;71:385–396. doi:10.1002/ana.22267.

[9] Clairambault J, Curzi-dascalovab L, Kauffmann F, Mkdiguea C. Heart Rate Variability in Normal Sleeping and Preterm Neonates Full-Term. Early Hum Dev 1992;28:169–183.

[10] Cong X, Ludington-Hoe SM, McCain G, Fu P. Kangaroo Care modifies preterm infant heart rate variability in response to heel stick pain: pilot study. Early Hum Dev 2009;85:561–7. doi:10.1016/j.earlhumdev.2009.05.012.

[11] Costa M, Goldberger AL, Peng C-KK. Multiscale Entropy Analysis of Complex Physiologic Time Series. Phys Rev Lett 2002;89.

[12] Curzi-Dascalova L. Development of sleep and autonomic nervous system contorl in premature and full-term newborns. Arch Pediatr 1994;2:255–262.

[13] David M, Hirsch M, Karin J, Toledo E, Akselrod S. An estimate of fetal autonomic state by time-frequency analysis of fetal heart rate variability. J Appl Physiol 2007;102. Available: http://jap.physiology.org/content/102/3/1057.long. Accessed 11 Sep 2017.

[14] Dereymaeker A, Pillay K, Vervisch J, Van Huffel S, Naulaers G, Jansen K, De Vos M. An Automated Quiet Sleep Detection Approach in Preterm Infants as a Gateway to Assess Brain Maturation. Int J Neural Syst 2017:1750023.

[15] Dick OE. Multifractal analysis of the psychorelaxation efficiency for the healthy and pathological human brain. Chaotic Model Simul 2012;1:219–227.

[16] Doesburg SM, Chau CM, Cheung TPL, Moiseev A, Ribary U, Herdman AT, Miller SP, Cepeda IL, Synnes A, Grunau RE. Neonatal pain-related stress, functional cortical activity and visual-perceptual abilities in school-age children born at extremely low gestational age. Pain 2013;154:1946–1952.

[17] Doesburg SM, Chau CM, Cheung TPL, Moiseev A, Ribary U, Herdman AT, Miller SP, Cepeda IL, Synnes A, Grunau RE. Neonatal pain-related stress, functional cortical activity and visual-perceptual abilities in school-age children born at extremely low gestational age. Pain 2013;154:1946–1952. doi:10.1016/j.pain.2013.04.009.

[18] Duerden EG, Grunau RE, Guo T, Foong J, Pearson A, Au-Young S, Lavoie R, Chakravarty MM, Chau V, Synnes A, Miller SP. Early procedural pain is associated with regionally-specific alterations in thalamic development in preterm neonates. J Neurosci 2018;38:878–886.

[19] Fabrizi L, Slater R, Worley A, Meek J, Boyd S, Olhede S, Fitzgerald M. A shift in sensory processing that enables the developing human brain to discriminate touch from pain. Curr Biol 2011;21:1552–1558.

[20] Fitzgerald M. The development of nociceptive circuits. Nat Rev Neurosci 2005;6:507–520.

[21] Ghosh D, Chen W, Raghunathan T. The false discovery rate: a variable selection perspective. J Stat Plan Inference 2006;136:2668–2684.

[22] Grunau RE. Neonatal pain in very preterm infants: long-term effects on brain, neurodevelopment and pain reactivity. Rambam Maimonides Med J 2013;4:e0025. doi:10.5041/RMMJ.10132.

[23] Grunau RE, Whitfield MF, Petrie-Thomas J, Synnes AR, Cepeda IL, Keidar A, Rogers M, Mackay M, Hubber-Richard P, Johannesen D. Neonatal pain, parenting stress and interaction, in relation to cognitive and motor development at 8 and 18 months in preterm infants. Pain 2009;143:138–146.

[24] Hoyer D, Tetschke F, Jaekel S, Nowack S, Witte OW, Schleußner E, Schneider U. Fetal Functional Brain Age Assessed from Universal Developmental Indices Obtained from Neuro-Vegetative Activity Patterns. PLoS One 2013;8:1–8.

[25] Isler JR, Stark RI, Grieve PG, Welch MG, Myers MM. Integrated information in the EEG of preterm infants increases with family nurture intervention, age, and conscious state. PLoS One 2018;13:e0206237. doi:10.1371/journal.pone.0206237.

[26] Javorka K, Lehotska Z, Kozar M, Uhrikova Z, Kolarovszki B, Javorka M, Zibolen M. Heart Rate Variability in Newborns. Physiol Res 2017;66:203–214. doi:10.33549/physiolres.933676.

[27] Jones L, Fabrizi L, Laudiano-Dray M, Whitehead K, Meek J, Verriotis M, Fitzgerald M. Nociceptive Cortical Activity Is Dissociated from Nociceptive Behavior in Newborn Human Infants under Stress. Curr Biol 2017;27:3846-3851.e3. doi:10.1016/J.CUB.2017.10.063.

[28] Kim SB, Chen VCP, Park Y, Ziegler TR, Jones DP. Controlling the False Discovery Rate for Feature Selection in High-resolution NMR Spectra. Stat Anal Data Min 2008;1:57–66. doi:10.1002/sam.10005.

[29] Kong AHT, Lai MM, Finnigan S, Ware RS, Boyd RN, Colditz PB. Background EEG features and prediction of cognitive outcomes in very preterm infants: A systematic review. Early Hum Dev 2018;127:74–84. doi:10.1016/J.EARLHUMDEV.2018.09.015.

[30] Kostovic I, Judas M. The development of the subplate and thalamocortical connections in the human foetal brain. Acta Paediatr Int J Paediatr 2010;99:1119–1127. doi:10.1111/j.1651-2227.2010.01811.x.

[31] Lake DE, Richman JS, Griffin MP, Moorman JR. Sample entropy analysis of neonatal heart rate variability. Am J Physiol Integr Comp Physiol 2002;283:R789–R797. doi:10.1152/ajpregu.00069.2002.

[32] Lavanga M, De Wel O, Caicedo A, Heremans E, Jansen K, Dereymaeker A, Naulaers G, Van Huffel S. Automatic quiet sleep detection based on multifractality in preterm neonates: Effects of maturation. Proceedings of the 39th Annual International Conference of the IEEE Engineering in Medicine and Biology Society (EMBC). IEEE, 2017. pp. 2010–2013. doi:10.1109/EMBC.2017.8037246.

[33] Lavanga M, De Wel O, Caicedo A, Jansen K, Dereymaeker A, Naulaers G, Van Huffel S. A brain-age model for preterm infants based on functional connectivity. Physiol Meas 2018;39:044006. doi:10.1088/1361-6579/aabac4.

[34] Lavanga M, Wel O De, Caicedo A, Jansen K, Dereymaeker A, Naulaers G, Huffel S Van. A brain-age model for preterm infants based on functional connectivity. Physiol Meas 2018;39:044006.

[35] Linsell L, Johnson S, Wolke D, Morris J, Kurinczuk JJ, Marlow N. Trajectories of behavior, attention, social and emotional problems from childhood to early adulthood following extremely preterm birth: a prospective cohort study. Eur Child Adolesc Psychiatry 2019;28:531–542.

[36] Linsell L, Johnson S, Wolke D, O'Reilly H, Morris JK, Kurinczuk JJ, Marlow N. Cognitive trajectories from infancy to early adulthood following birth before 26 weeks of gestation: A prospective, population-based cohort study. Arch Dis Child 2018;103:363–370.

[37] Marret S, Ancel PY, Marpeau L, Marchand L, Pierrat V, Larroque B, Foix-L'Hélias L, Thiriez G, Fresson J, Alberge C, Rozé JC, Matis J, Bréart G, Kaminski M. Neonatal and 5-year outcomes after birth at 30-34 weeks of gestation. Obstet Gynecol 2007;110:72–80.

[38] Mento G, Bisiacchi PS. Neurocognitive development in preterm infants: Insights from different approaches. Neurosci Biobehav Rev 2012;36:536–555.

[39] Moeyersons J, Amoni M, Huffel S Van, Willems R, Varon C. R-DECO: An open-source Matlab based graphical user interface for the detection and correction of R-peaks. bioRxiv 2019:560706.

[40] O'Toole JM, Boylan GB. NEURAL: quantitative features for newborn EEG using Matlab. arXiv Prepr arXiv170405694 2017. Available: http://arxiv.org/abs/1704.05694. Accessed 27 Nov 2019.

[41] O'Toole JM, Boylan GB. Quantitative Preterm EEG Analysis: The Need for Caution in Using Modern Data Science Techniques. Front Pediatr 2019;7:174. doi:10.3389/fped.2019.00174.

[42] O'Toole JM, Boylan GB, Vanhatalo S, Stevenson NJ. Estimating functional brain maturity in very and extremely preterm neonates using automated analysis of the electroencephalogram. Clin Neurophysiol 2016;127:2910–2918.

[43] O'Toole JM, Pavlidis E, Korotchikova I, Boylan GB, Stevenson NJ. Temporal evolution of quantitative EEG within 3 days of birth in early preterm infants. Sci Rep 2019;9.

[44] Pavlidis E, Lloyd RO, Boylan GB. EEG-A Valuable Biomarker of Brain Injury in Preterm Infants. Developmental Neuroscience. S. Karger AG, 2017, Vol. 39. pp. 23–35.

[45] Pavlidis E, Lloyd RO, Mathieson S, Boylan GB. A review of important electroencephalogram features for the assessment of brain maturation in premature infants. Acta Paediatr Int J Paediatr 2017;106:1394–1408.

[46] Pavlidis E, Lloyd RO, Mathieson S, Boylan GB. A review of important electroencephalogram features for the assessment of brain maturation in premature infants. Acta Paediatr 2017;106:1394–1408. doi:10.1111/apa.13956.

[47] Popivanov D, Stomonyakov V, Minchev Z, Jivkova S, Dojnov P, Jivkov S, Christova E, Kosev S. Multifractality of decomposed EEG during imaginary and real visual-motor tracking. Biol Cybern 2006;94:149–156.

[48] Ranger M, Chau CMY, Garg A, Woodward TS, Beg MF, Bjornson B, Poskitt K, Fitzpatrick K, Synnes AR, Miller SP, Grunau RE. Neonatal Pain-Related Stress Predicts Cortical Thickness at Age 7 Years in Children Born Very Preterm. PLoS One 2013;8:e76702. doi:10.1371/journal.pone.0076702.

[49] Reynolds ML, Fitzgerald M. Long-term sensory hyperinnervation following neonatal skin wounds.

J Comp Neurol 1995;358:487–498. doi:10.1002/cne.903580403.

[50] Slater R, Fabrizi L, Worley A, Meek J, Boyd S, Fitzgerald M. Premature infants display increased noxious-evoked neuronal activity in the brain compared to healthy age-matched term-born infants. Neuroimage 2010;52:583–589.

[51] Smith GC, Gutovich J, Smyser C, Pineda R, Newnham C, Tjoeng TH, Vavasseur C, Wallendorf M, Neil J, Inder T. Neonatal intensive care unit stress is associated with brain development in preterm infants. Ann Neurol 2011;70:541–549. doi:10.1002/ana.22545.

[52] The International Neonatal Network. The CRIB (clinical risk index for babies) score: a tool for assessing initial neonatal risk and comparing performance of neonatal intensive care units. Lancet 1993;342:193–198.

[53] Torsney C, Fitzgerald M. Spinal Dorsal Horn Cell Receptive Field Size is Increased in Adult Rats Following Neonatal Hindpaw Skin Injury. J Physiol 2003;550:255–261. doi:10.1113/jphysiol.2003.043661.

[54] Valenza G, Citi L, Lanata A, Gentili C, Barbieri R, Scilingo EP. Applications of Heartbeat Complexity Analysis to Depression and Bipolar Disorder. Complexity and Nonlinearity in Cardiovascular Signals. Cham: Springer International Publishing, 2017. pp. 345–374. doi:10.1007/978-3-319-58709-7_13.

[55] Verriotis M, Chang P, Fitzgerald M, Fabrizi L. The development of the nociceptive brain. Neuroscience 2016;338:207–219. doi:10.1016/J.NEUROSCIENCE.2016.07.026.

[56] Vinall J, Grunau RE. Impact of repeated procedural pain-related stress in infants born very preterm. Pediatr Res 2014;75:584–587.

[57] Watanabe K, Hayakawa F, Okumura A. Neonatal EEG: A powerful tool in the assessment of brain damage in preterm infants. Brain Dev 1999;21:361–372.

[58] De Wel O, Lavanga M, Dorado A, Jansen K, Dereymaeker A, Naulaers G, Van Huffel S. Complexity Analysis of Neonatal EEG Using Multiscale Entropy: Applications in Brain Maturation and Sleep Stage Classification. Entropy 2017;19:516. doi:10.3390/e19100516.

[59] Zhang D, Ding HH, Liu Y, Zhou C, Ding HH, Ye D. Neurodevelopment in newborns: A sample entropy analysis of electroencephalogram. Physiol Meas 2009;30:491–504. doi:10.1088/0967-3334/30/5/006.

Figure Legends

Figure 1 - **An overview of all recordings in the dataset**



Figure 2 – **The average skin-breaking procedure during the NICU stay**



Figure 4 – **Complexity Index in non-quiet sleep**.



A



B

Figure 5 – **rEEG Asymmetry in QUIET sleep.**



A



B

Figure 6 – **HF Oscillations in QUIET sleep.**



A



B

Figure 7 – **rEEG Asymmetry in early-GA patients.**



A



B

Figure 8 – **HF Oscillations in early-GA patients.**



A



B

Title	**The effect of early procedural pain in preterm infants on the maturation of EEG and heart rate variability**
Authors	1. Mario Lavanga 2. Bieke Bollen 3. Alexander Caicedo 4. Anneleen Dereymaeker 5. Katrien Jansen 6. Els Ortibus 7. Sabine Van Huffel 8. Gunnar Naulaers
Corresponding author	Mario Lavanga mlavanga@esat.kuleuven.be
Summary	Stress exposure and early-pain procedure might increase the level of EEG and HRV dismaturity, which can ultimately impact the development outcome of the infant.

Figure

Figure 1 - **An overview of all recordings in the dataset**. The Gantt-Chart-like overview of all recordings for the different patients. The number of stacked bars represents the number of recordings and the color is associated for the recording time: blue for the first recording, red for the second recording at 34 w and the yellow is the recording at discharge (PSG). The length represents the cumulative amount of SBPs. In particular, the blue bar is the cumulated SBPs up to first recording, while the red and the yellow bars have the incremental values of cumulated SBPs with respect to the first recording.

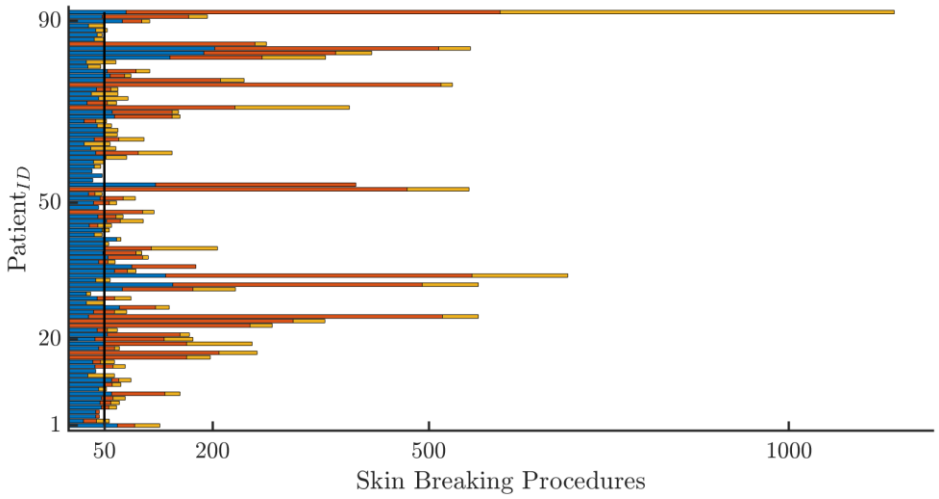


Figure 2 – **The average skin-breaking procedure during the NICU stay.** The chart of the skin breaking procedure is displayed as average over the different patients in the two groups, HIGH SBPs (SBPs >=50) in magenta and LOW SBPs (SBPs < 50) in green. The curves show the SBP dynamics during the neonatal intensive care unit stay in the first 100 days. The average chart is represented by the continuous thick line, while the upper bound and the lower bound represent the error margin. The curve has been defined as $\mu(t) \pm \frac{\sigma(t)}{\sqrt{N(t)}}$, where $\mu(t)$ is the mean of the patient distribution, $\sigma(t)$ is the standard deviation and $N(t)$ represents the number of patients. The variable t represents each postnatal day. The exponential decay highlights that most procedural pain is concentrated in the first days of life.

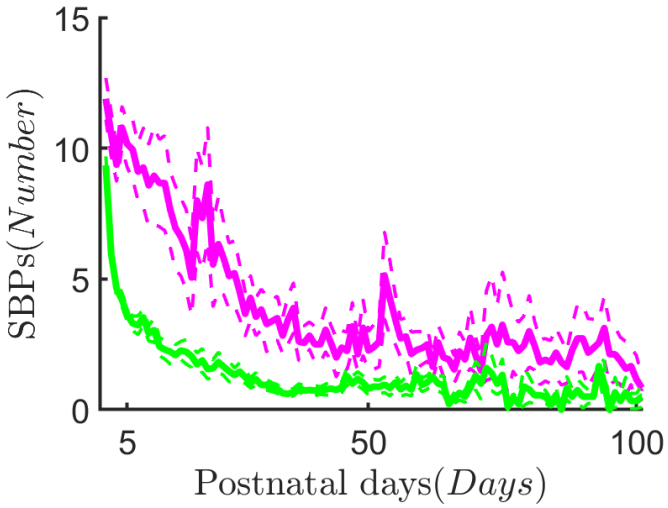


Figure 3 – **Distributions of SBP data at 5 days.** The histogram distributions for the cumulative amount of SBPs at 5 days from birth. The right panel shows the distribution for the entire dataset, while the second one depicts the distribution for the low gestational age dataset (GA <= 29 weeks). The black continuous line represents the median value of the distribution, the dashed line represents the mean and the dotted dashed line is 75% quantile of the investigated distribution.

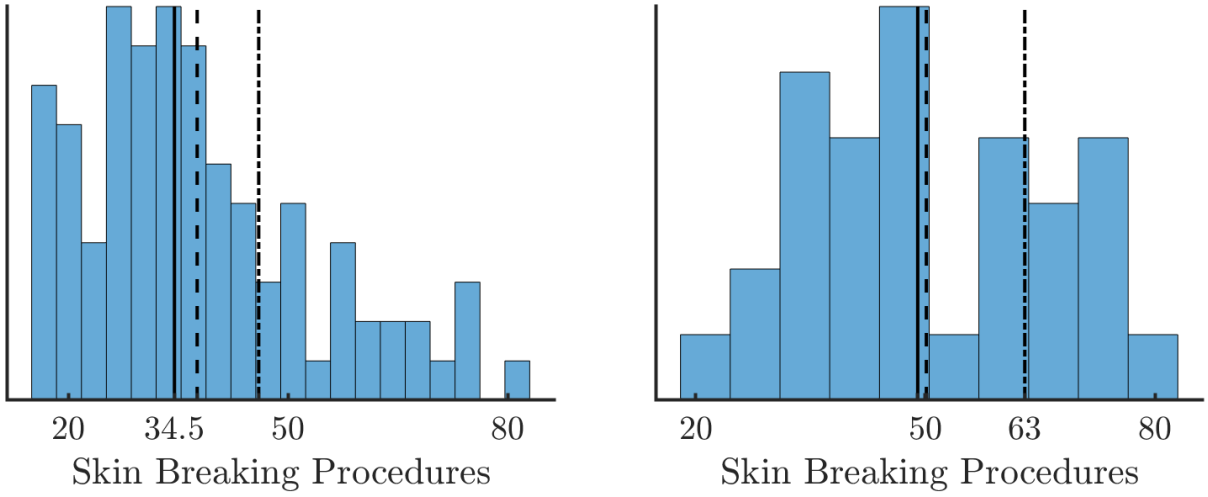


Figure 4 **– Complexity Index in non-quiet sleep**. The figure shows the association with complexity index (CI) and early skin-breaking procedure (SBPs). Data are reported for the entire dataset during non-quiet sleep (nQS). The left panel shows how the CI maturational trend differs in case of high SBPs (magenta curve, SBP ≥ 50) compared to low SBPs (green curve, SBP < 50). The blue/green triangles represent the patient with low SBPs (N = 73) and red/orange circles the high SBPs (N= 19). The right panel shows the boxplot trend as output of the two-ways ANOVA: the division between HIGH SBPs and LOW SBPs is reported for each recording time. The complexity index increases over time (main effect of measuring point: $F(2,178) = 42.17, p \leq 0.01$), but statistically significant interaction effect between measuring point and SBP group is found ($F(2,178) = 6.62, p \leq 0.01$). The simple main effect analysis shows a lower complexity in HIGH SBPs group at the 5 days recording ($p \leq 0.01$, indicated as ** in the figure), but there is no significant difference for the 34 weeks ($p = 0.59$) or PSG ($p = 1$) recording time.

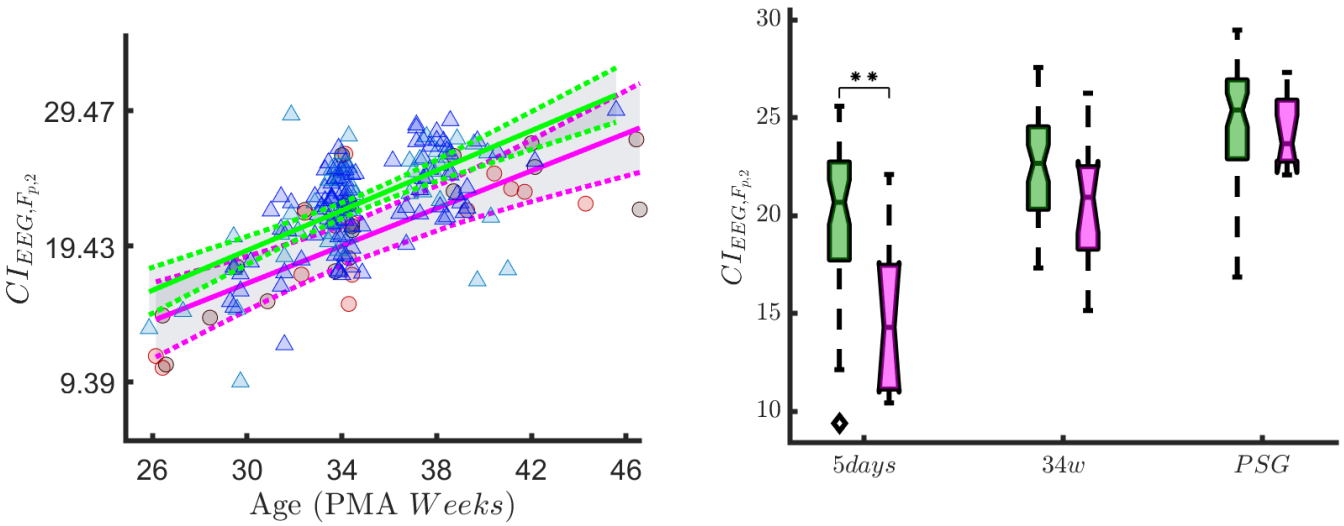


Figure 5 – **rEEG Asymmetry in QUIET sleep.** The figure shows the association between rEEG asymmetry in the theta band (asymm) and early skin-breaking procedures (SBPs) Data are reported for the entire dataset during QUIET sleep (QS). The left panel shows how the asymmetry maturational trend differs in case of high SBPs (magenta curve, SBP ≥ 50) compared to low SBPs (green curve, SBP < 50). SBPs seem to increase the level of asymm throughout the development HF oscillations. The right panel shows the boxplot trend as output of the two-ways ANOVA: the division between HIGH SBPs and LOW SBPs is reported for each recording time. The asymmetry decreases over time (main effect of measuring point: $F(2,208) = 101.71, p \leq 0.01$), but statistically significant interaction effect between measuring point and SBP group is found ($F(2,208) = 8.52, p \leq 0.01$). The simple main effect analysis shows a higher asymmetry in the HIGH SBPs group at the 5 days recording ($p \leq 0.01$, indicated as ** in the figure) and a marginal significant difference for the 34 weeks ($p = 0.05$, indicated as * in the figure). The rEEG asymmetry does not statistically differ between HIGH and LOW SBPs groups at PSG recording time ($p = 0.72$).

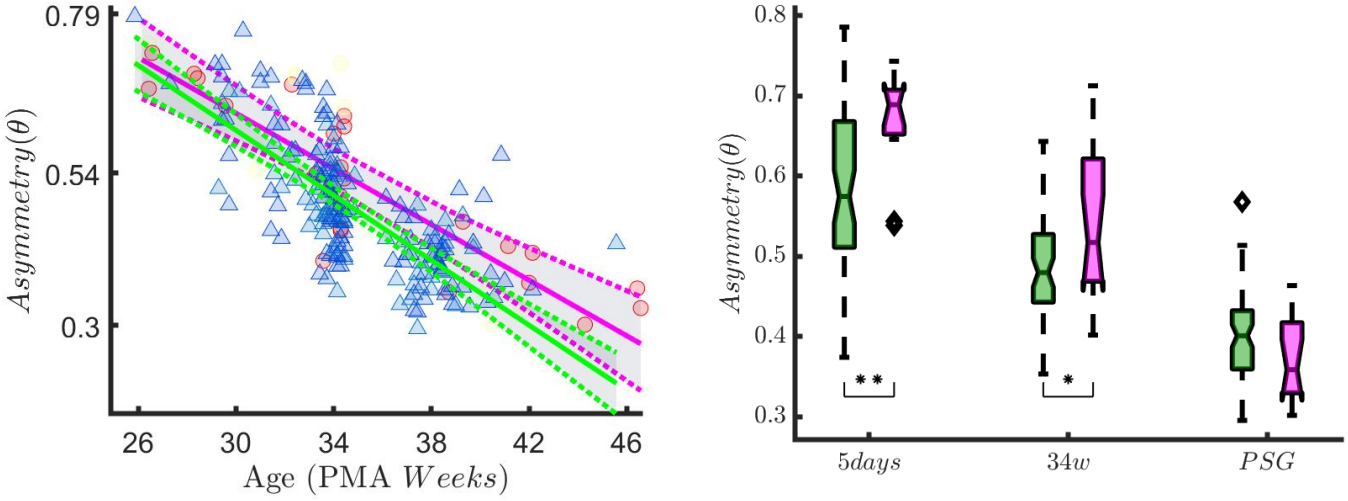


Figure 6 –**HF Oscillations in QUIET sleep.** The figure shows the association between HF oscillations of the tachogram P(HF) and early skin-breaking procedure (SBPs). Data are reported for the entire dataset during QUIET sleep (QS). The left panel show how P(HF) maturational trend differs in case of high SBPs (magenta curve, SBP ≥ 50) compared to low SBPs (green curve, SBP < 50). SBPs seem to increase the power of HF oscillations. The right panel shows the boxplot trend as output of the two-ways ANOVA: the division between HIGH SBPs and LOW SBPs is reported for each recording time. The HF oscillations increases over time (main effect of measuring point: $F(2,191) = 5.97, p \leq 0.01$), but statistically significant interaction effect between measuring point and SBP group is found ($F(2,191) = 4.56, p \leq 0.01$). The simple main effect analysis shows a higher $P(HF)$ in HIGH SBPs group at the PSG recording time ($p \leq 0.01$, indicated as ** in the figure), but there is no difference for the 5 days ($p = 0.43$) or 34w ($p = 1$) recording time.

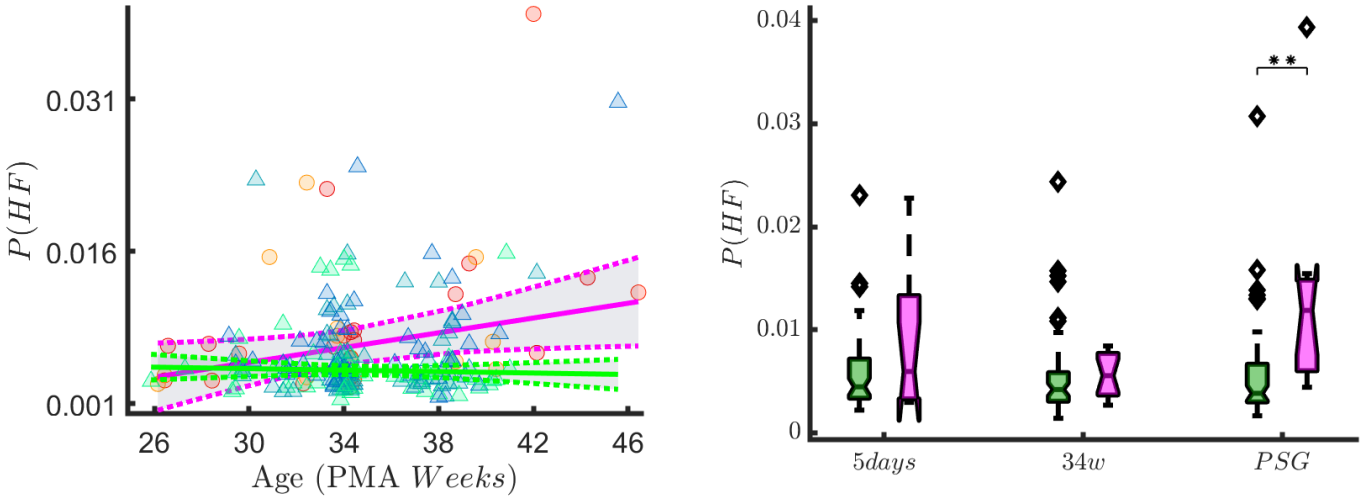


Figure 7 – **rEEG Asymmetry in early-GA patients.** The figure shows the association between the rEEG asymmetry in the alpha band (asymm, Left Panel A) and early skin-breaking procedures (SBPs). Data are reported for the patients with gestational age below 29 weeks during QUIET sleep (QS). The left panel shows how the asymm trend differs in case of high SBPs (magenta curve, SBP ≥ 50) compared to low SBPs (green curve, SBP < 50). SBPs seem to increase the level of asymm throughout the development. The right panel shows the boxplot trend as output of the two-ways ANOVA: the division between HIGH SBPs and LOW SBPs is reported for each recording time. A significant SBP-by-measuring point interaction on rEEG asymmetry is found in quiet sleep ($F(2,71) = 3.86, p = 0.03$). Asymmetry also decreases over time (main effect of measuring point: $F(2,71) = 61.61,\ p \leq 0.01$). At the 34 weeks recording, infants in the high SBP group showed a significantly higher rEEG asymmetry than the infants in the low SBP group (p =0.02, indicated as * in the figure). At the recording at 5 days and the PSG recording, this difference did not reach significance (p =0.91 and p =0.98, respectively).

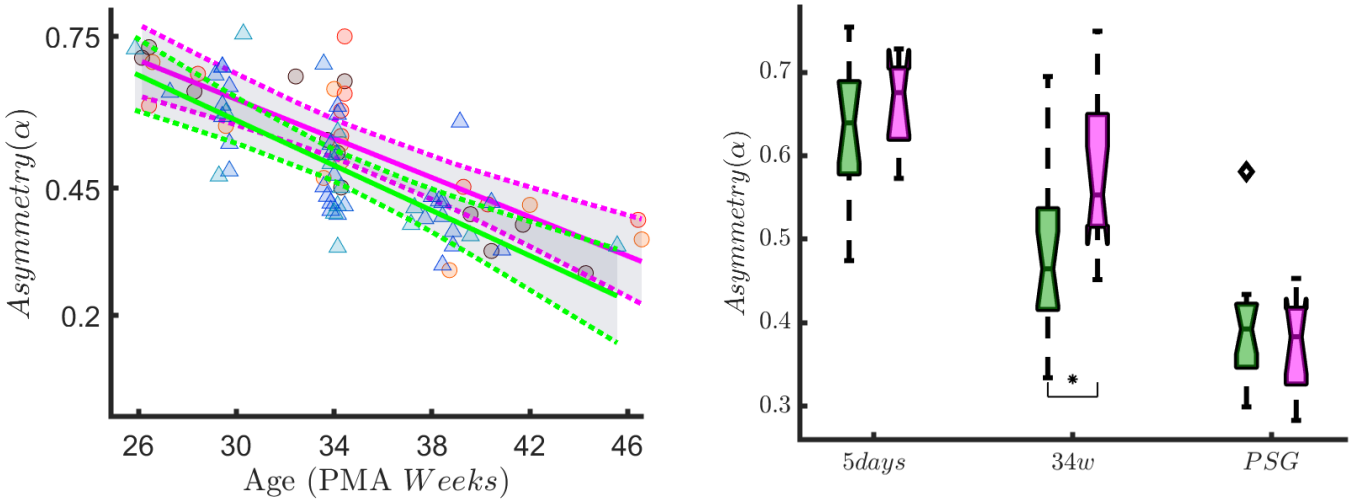
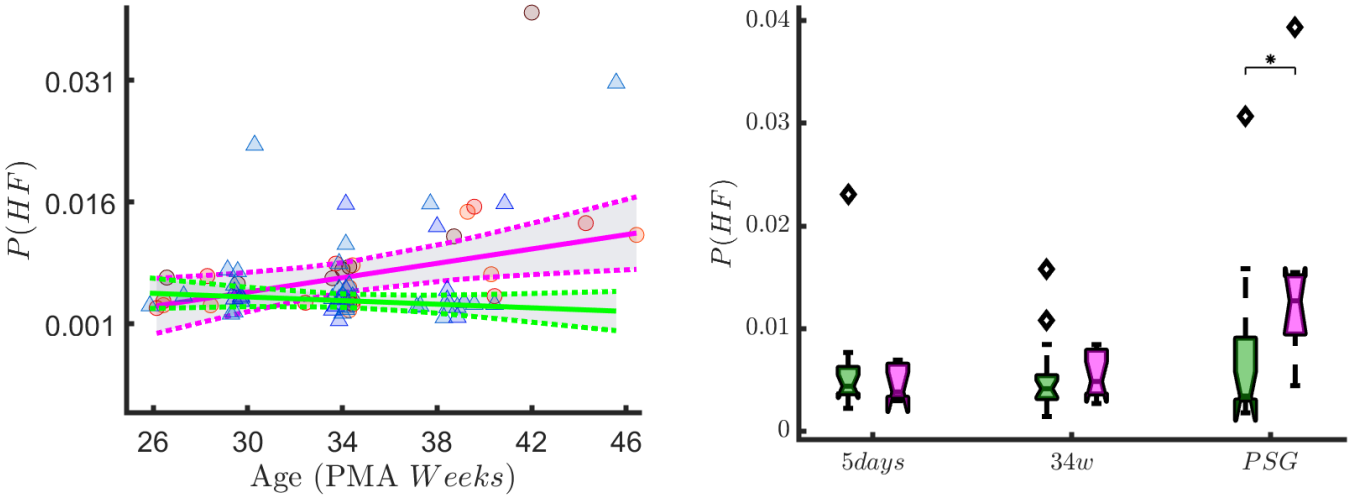


Figure 8 –**HF Oscillations in early-GA patients.** The figure shows the association with the vagal tone (P(HF)) and early skin-breaking procedures (SBPs). Data are reported for the patients with gestational age below 29 weeks (n=31) during QUIET sleep (QS). The left panel shows how the P(HF) maturational trend differs in case of high SBPs (magenta curve, SBP ≥ 50) compared to low SBPs (green curve, SBP < 50). SBPs seem to increase the power of HF oscillations. The right panel shows the boxplot trend as output of the two-ways ANOVA: the division between HIGH SBPs and LOW SBPs is reported for each recording time. The p-value associated to the ANOVA is reported on y-axis, while the output of the Tukey-Kramer multiple comparison test is reported below each boxplots group. A significant SBP-by-measuring point interaction on P(HF) is found in quiet sleep ($F(2,67) = 3.49, p = 0.04$). HF oscillations also increases over time (main effect of measuring point: $F(2,67) = 6.49$, $p \leq 0.01$). Post-hoc analysis showed this difference in HF oscillations between the HIGH and LOW SBP group is only significantly different at the last, PSG, recording (p =0.04, indicated as * in the figure).



Figure

Figure 1 - **An overview of all recordings in the dataset**. The Gantt-Chart-like overview of all recordings for the different patients. The number of stacked bars represents the number of recordings and the color is associated for the recording time: blue for the first recording, red for the second recording at 34 w and the yellow is the recording at discharge (PSG). The length represents the cumulative amount of SBPs. In particular, the blue bar is the cumulated SBPs up to first recording, while the red and the yellow bars have the incremental values of cumulated SBPs with respect to the first recording.

Figure 2 – **The average skin-breaking procedure during the NICU stay.** The chart of the skin breaking procedure is displayed as average over the different patients in the two groups, HIGH SBPs (SBPs >=50) in magenta and LOW SBPs (SBPs < 50) in green. The curves show the SBP dynamics during the neonatal intensive care unit stay in the first 100 days. The average chart is represented by the continuous thick line, while the upper bound and the lower bound represent the error margin. The curve has been defined as $\mu(t) \pm \frac{\sigma(t)}{\sqrt{N(t)}}$, where $\mu(t)$ is the mean of the patient distribution, $\sigma(t)$ is the standard deviation and $N(t)$ represents the number of patients. The variable t represents each postnatal day. The exponential decay highlights that most procedural pain is concentrated in the first days of life.

Figure 3 – **Distributions of SBP data at 5 days.** The histogram distributions for the cumulative amount of SBPs at 5 days from birth. The right panel shows the distribution for the entire dataset, while the second one depicts the distribution for the low gestational age dataset (GA <= 29 weeks). The black continuous line represents the median value of the distribution, the dashed line represents the mean and the dotted dashed line is 75% quantile of the investigated distribution.

Figure 4 **– Complexity Index in non-quiet sleep**. The figure shows the association with complexity index (CI) and early skin-breaking procedure (SBPs). Data are reported for the entire dataset during non-quiet sleep (nQS). The left panel shows how the CI maturational trend differs in case of high SBPs (magenta curve, SBP ≥ 50) compared to low SBPs (green curve, SBP < 50). The blue/green triangles represent the patient with low SBPs (N = 73) and red/orange circles the high SBPs (N= 19). The right panel shows the boxplot trend as output of the two-ways ANOVA: the division between HIGH SBPs and LOW SBPs is reported for each recording time. The complexity index increases over time (main effect of measuring point: $F(2,178) = 42.17, p \leq 0.01$), but statistically significant interaction effect between measuring point and SBP group is found ($F(2,178) = 6.62, p \leq 0.01$). The simple main effect analysis shows a lower complexity in HIGH SBPs group at the 5 days recording ($p \leq 0.01$, indicated as ** in the figure), but there is no significant difference for the 34 weeks ($p = 0.59$) or PSG ($p = 1$) recording time.

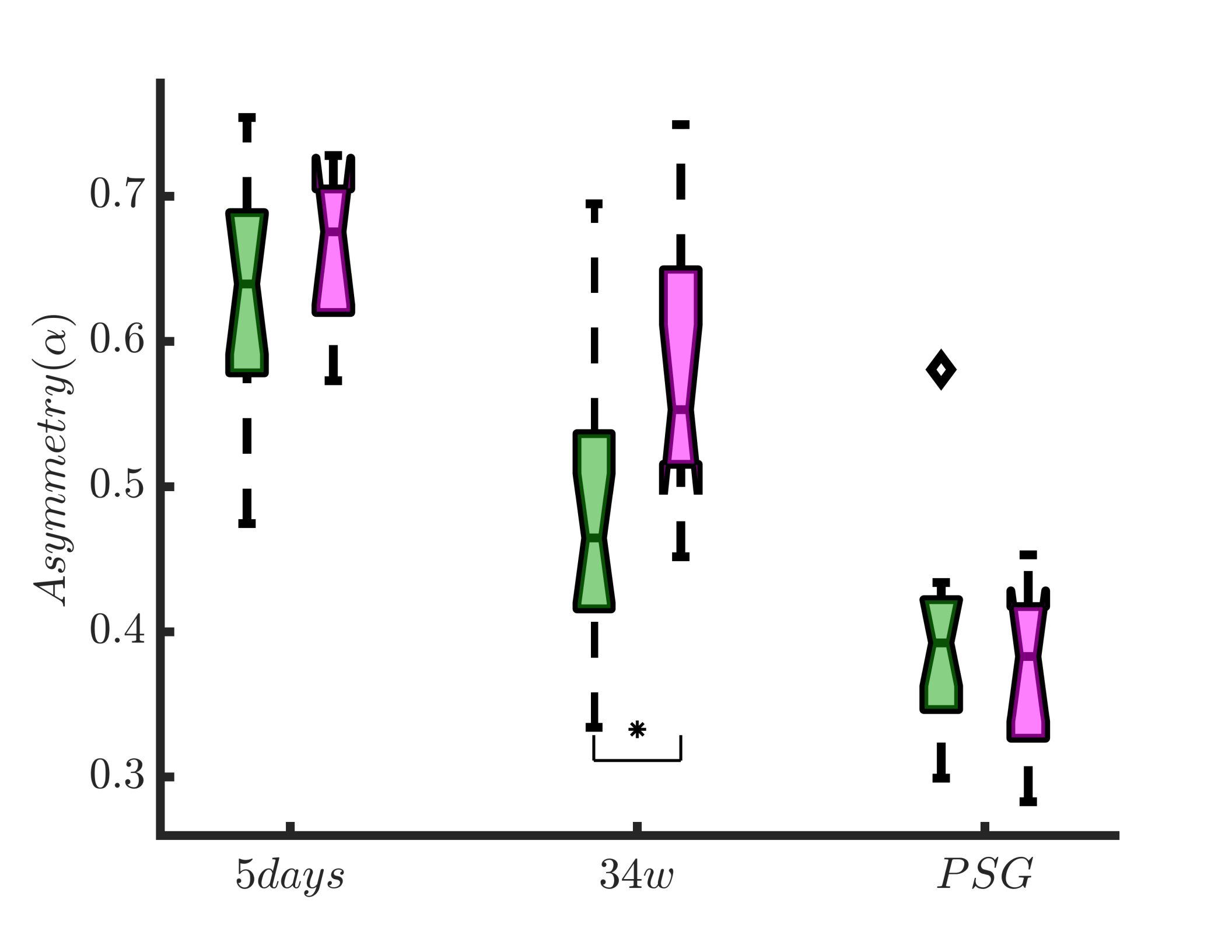
Figure 5 – **rEEG Asymmetry in QUIET sleep.** The figure shows the association between rEEG asymmetry in the theta band (asymm) and early skin-breaking procedures (SBPs) Data are reported for the entire dataset during QUIET sleep (QS). The left panel shows how the asymmetry maturational trend differs in case of high SBPs (magenta curve, SBP ≥ 50) compared to low SBPs (green curve, SBP < 50). SBPs seem to increase the level of asymm throughout the development HF oscillations. The right panel shows the boxplot trend as output of the two-ways ANOVA: the division between HIGH SBPs and LOW SBPs is reported for each recording time. The asymmetry decreases over time (main effect of measuring point: $F(2,208) = 101.71, p \leq 0.01$), but statistically significant interaction effect between measuring point and SBP group is found ($F(2,208) = 8.52, p \leq 0.01$). The simple main effect analysis shows a higher asymmetry in the HIGH SBPs group at the 5 days recording ($p \leq 0.01$, indicated as ** in the figure) and a marginal significant

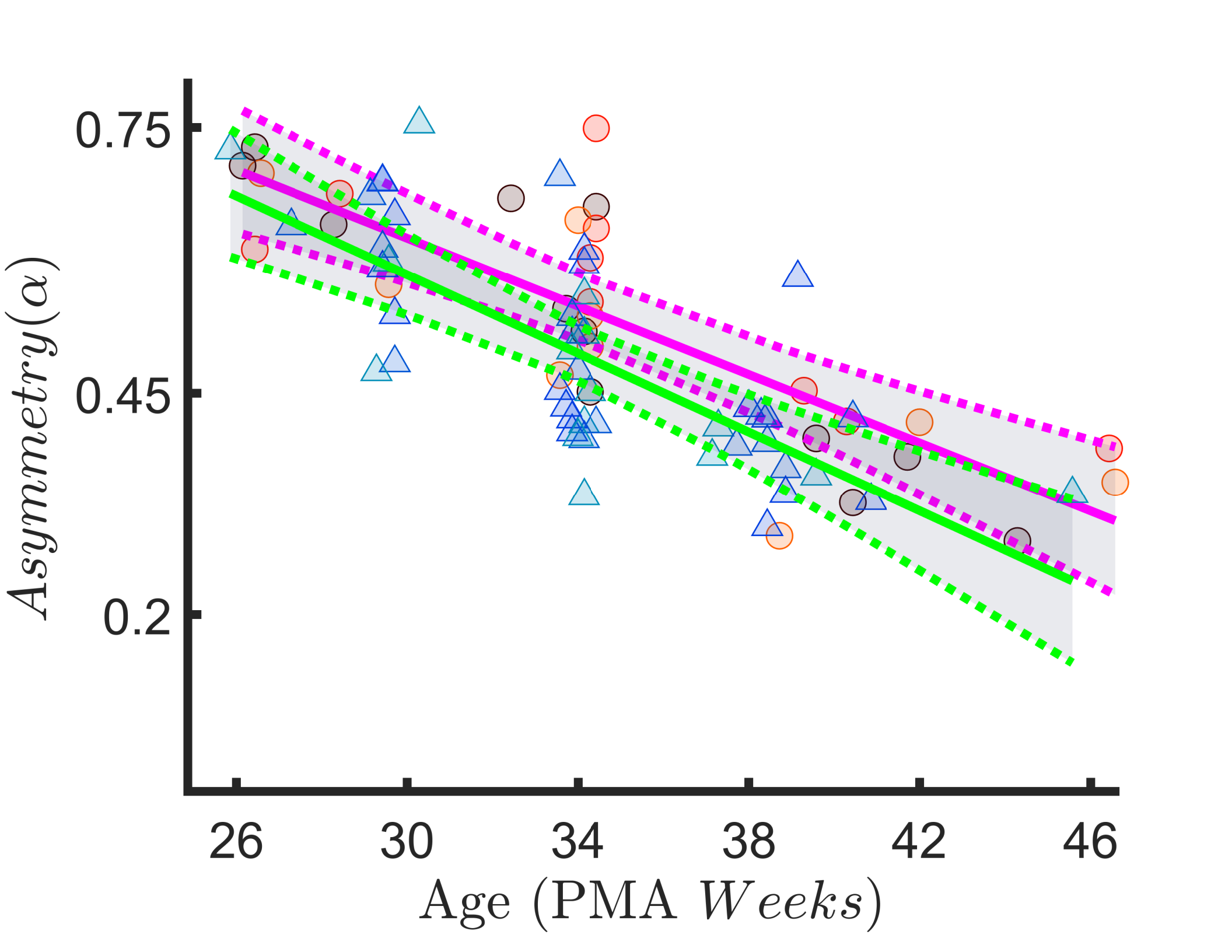
difference for the 34 weeks ($p = 0.05$, indicated as * in the figure). The rEEG asymmetry does not statistically differ between HIGH and LOW SBPs groups at PSG recording time ($p = 0.72$).

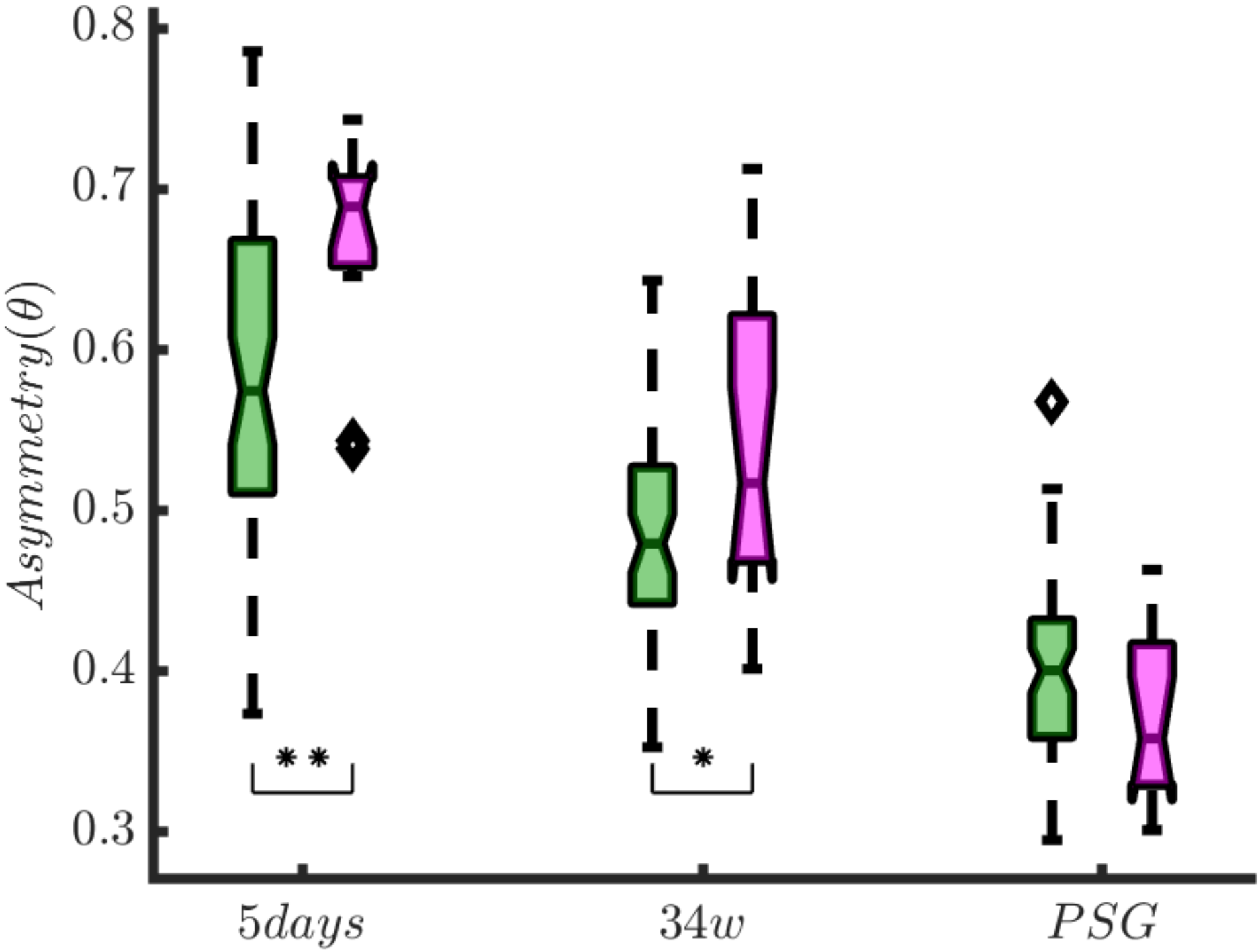
Figure 6 –**HF Oscillations in QUIET sleep.** The figure shows the association between HF oscillations of the tachogram P(HF) and early skin-breaking procedure (SBPs). Data are reported for the entire dataset during QUIET sleep (QS). The left panel show how P(HF) maturational trend differs in case of high SBPs (magenta curve, SBP ≥ 50) compared to low SBPs (green curve, SBP < 50). SBPs seem to increase the power of HF oscillations. The right panel shows the boxplot trend as output of the two-ways ANOVA: the division between HIGH SBPs and LOW SBPs is reported for each recording time. The HF oscillations increases over time (main effect of measuring point: $F(2,191) = 5.97, p \leq 0.01$), but statistically significant interaction effect between measuring point and SBP group is found ($F(2,191) = 4.56, p \leq 0.01$). The simple main effect analysis shows a higher $P(HF)$ in HIGH SBPs group at the PSG recording time ($p \leq 0.01$, indicated as ** in the figure), but there is no difference for the 5 days ($p = 0.43$) or 34w ($p = 1$) recording time.

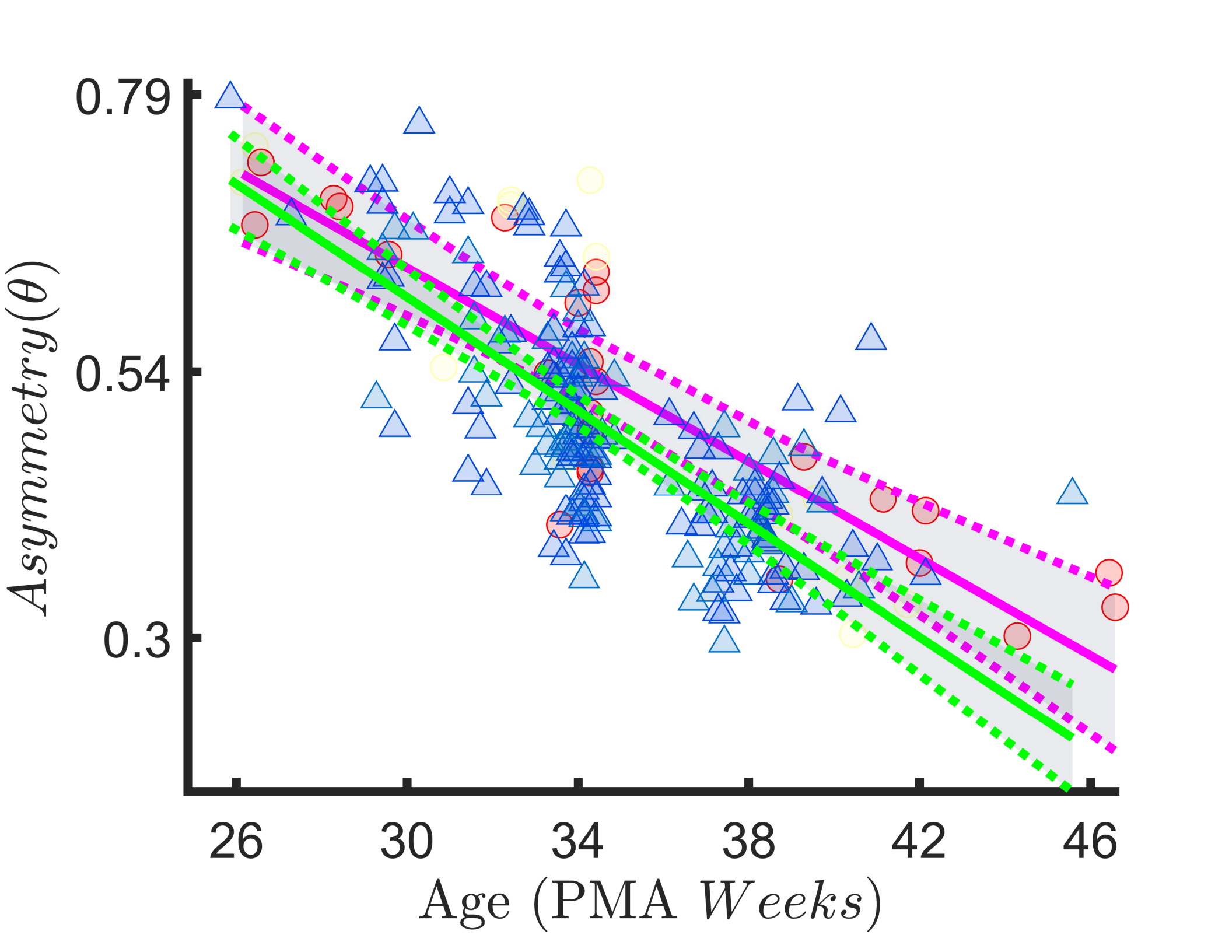
Figure 7 – **rEEG Asymmetry in early-GA patients.** The figure shows the association between the rEEG asymmetry in the alpha band (asymm, Left Panel A) and early skin-breaking procedures (SBPs). Data are reported for the patients with gestational age below 29 weeks during QUIET sleep (QS). The left panel shows how the asymm trend differs in case of high SBPs (magenta curve, SBP ≥ 50) compared to low SBPs (green curve, SBP < 50). SBPs seem to increase the level of asymm throughout the development. The right panel shows the boxplot trend as output of the two-ways ANOVA: the division between HIGH SBPs and LOW SBPs is reported for each recording time. A significant SBP-by-measuring point interaction on rEEG asymmetry is found in quiet sleep ($F(2,71) = 3.86, p = 0.03$). Asymmetry also decreases over time (main effect of measuring point: $F(2,71) = 61.61, p \leq 0.01$). At the 34 weeks recording, infants in the high SBP group showed a significantly higher rEEG asymmetry than the infants in the low SBP group (p =0.02, indicated as * in the figure). At the recording at 5 days and the PSG recording, this difference did not reach significance (p =0.91 and p =0.98, respectively).

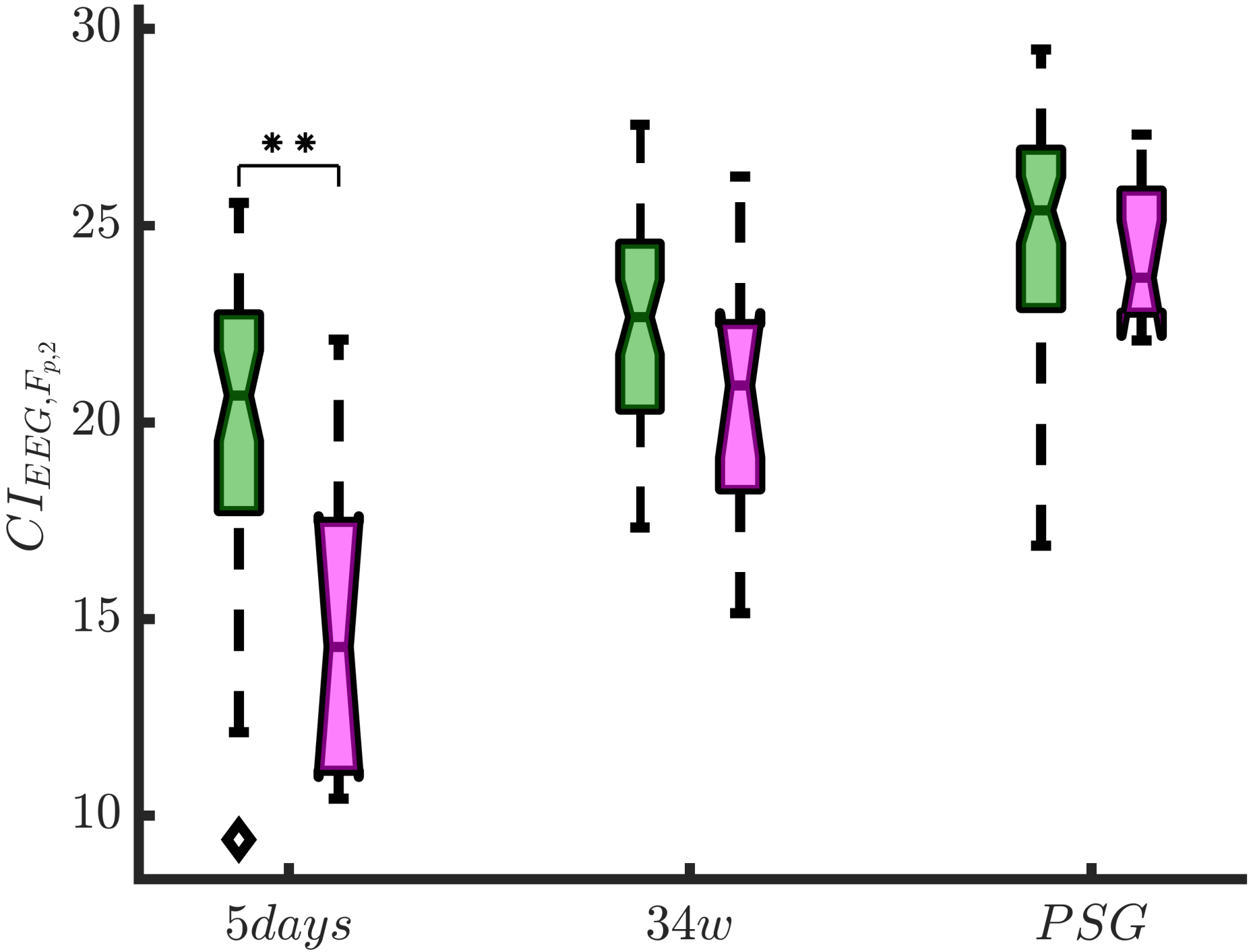
Figure 8 –**HF Oscillations in early-GA patients.** The figure shows the association with the vagal tone (P(HF)) and early skin-breaking procedures (SBPs). Data are reported for the patients with gestational age below 29 weeks (n=31) during QUIET sleep (QS). The left panel shows how the P(HF) maturational trend differs in case of high SBPs (magenta curve, SBP ≥ 50) compared to low SBPs (green curve, SBP < 50). SBPs seem to increase the power of HF oscillations. The right panel shows the boxplot trend as output of the two-ways ANOVA: the division between HIGH SBPs and LOW SBPs is reported for each recording time. The p-value associated to the ANOVA is reported on y-axis, while the output of the Tukey-Kramer multiple comparison test is reported below each boxplots group. A significant SBP-by-measuring point interaction on P(HF) is found in quiet sleep ($F(2,67) = 3.49, p = 0.04$). HF oscillations also increases over time (main effect of measuring point: $F(2,67) = 6.49$, $p \leq 0.01$). Post-hoc analysis showed this difference in HF oscillations between the HIGH and LOW SBP group is only significantly different at the last, PSG, recording (p =0.04, indicated as * in the figure).

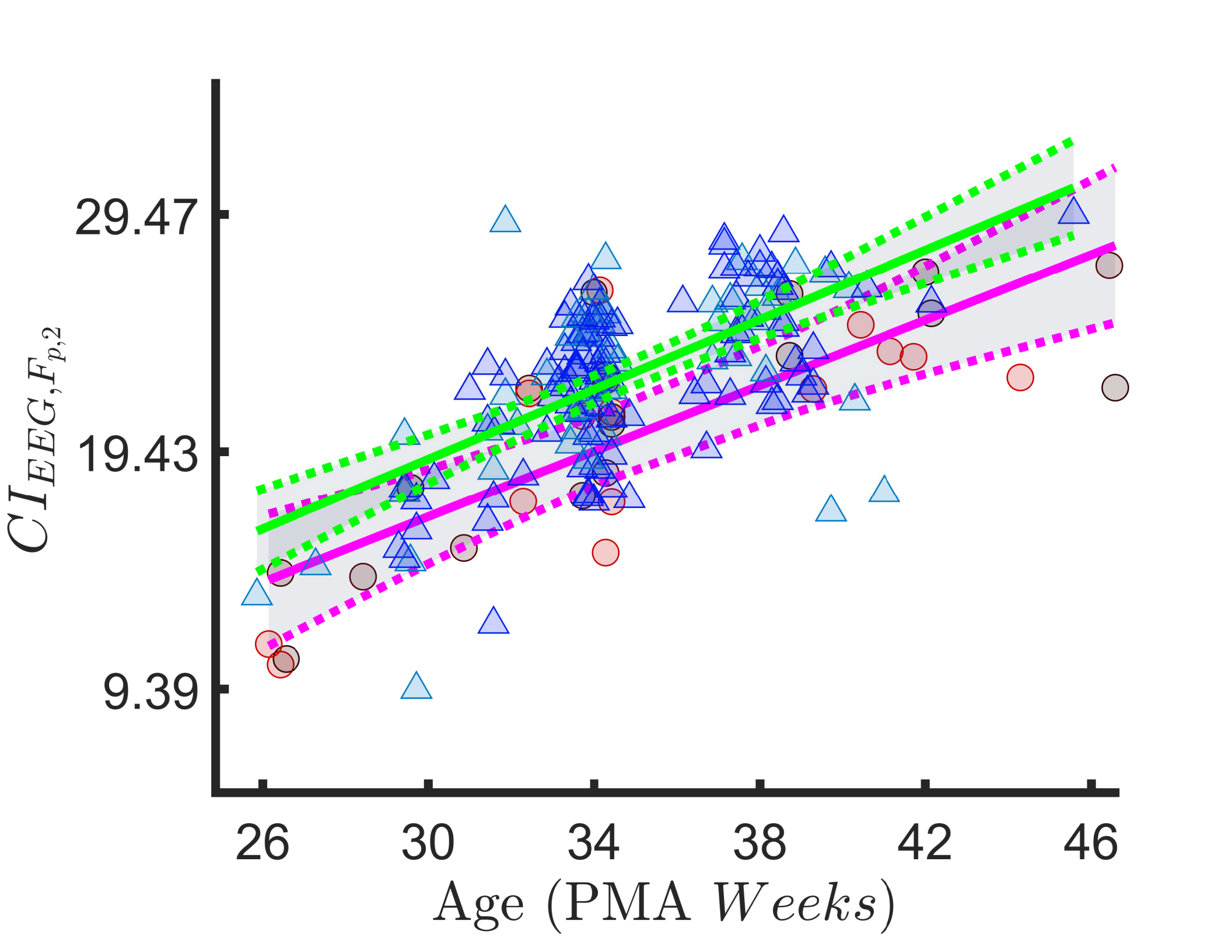

0.7
0.6
0.5
0.4
0.3
Asymmetry(α)
*
5days
34w
PSG

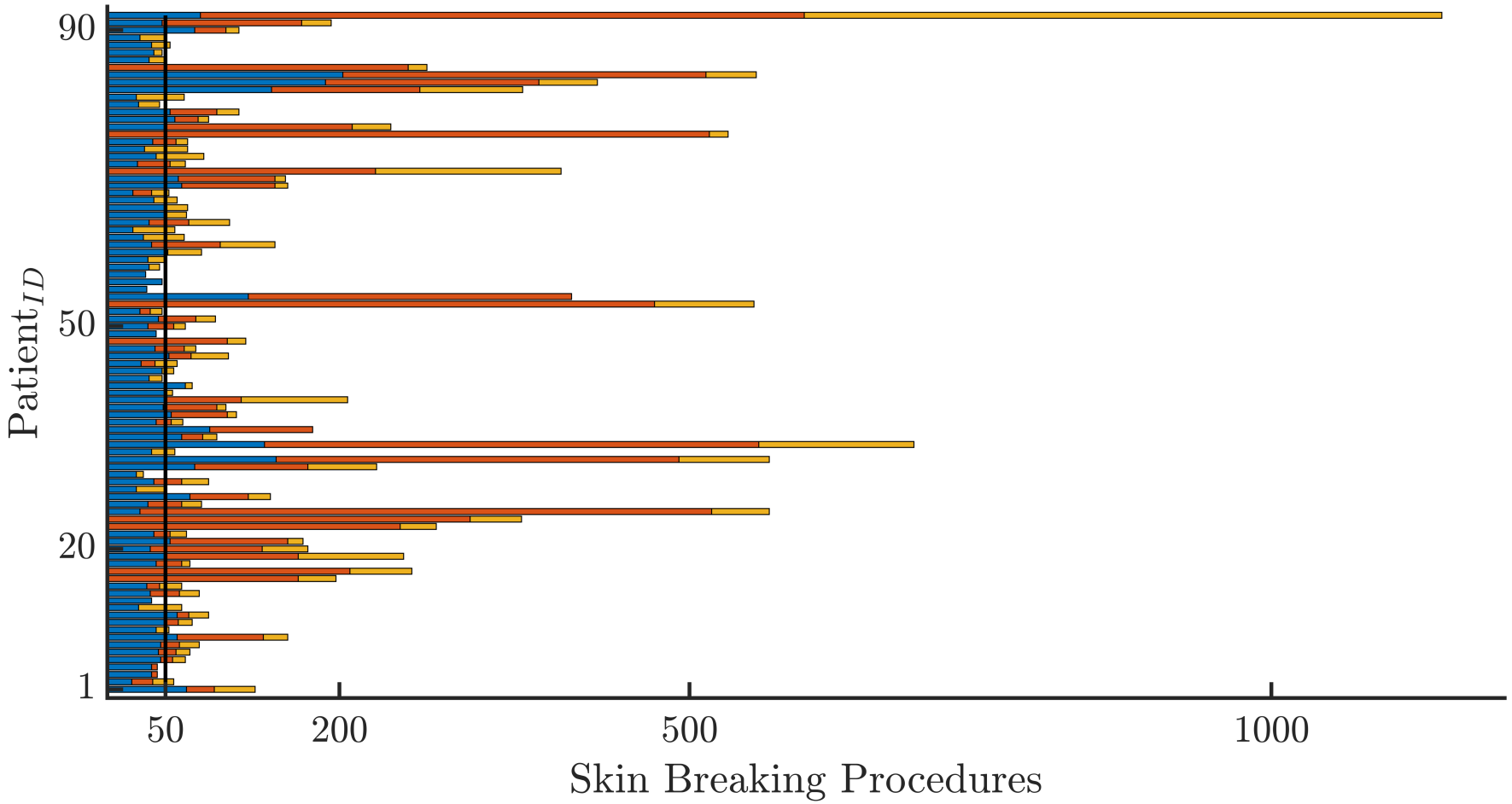

0.75
0.45
0.2
$Asymmetry(\alpha)$
26
30
34
38
42
46
Age (PMA $Weeks$)

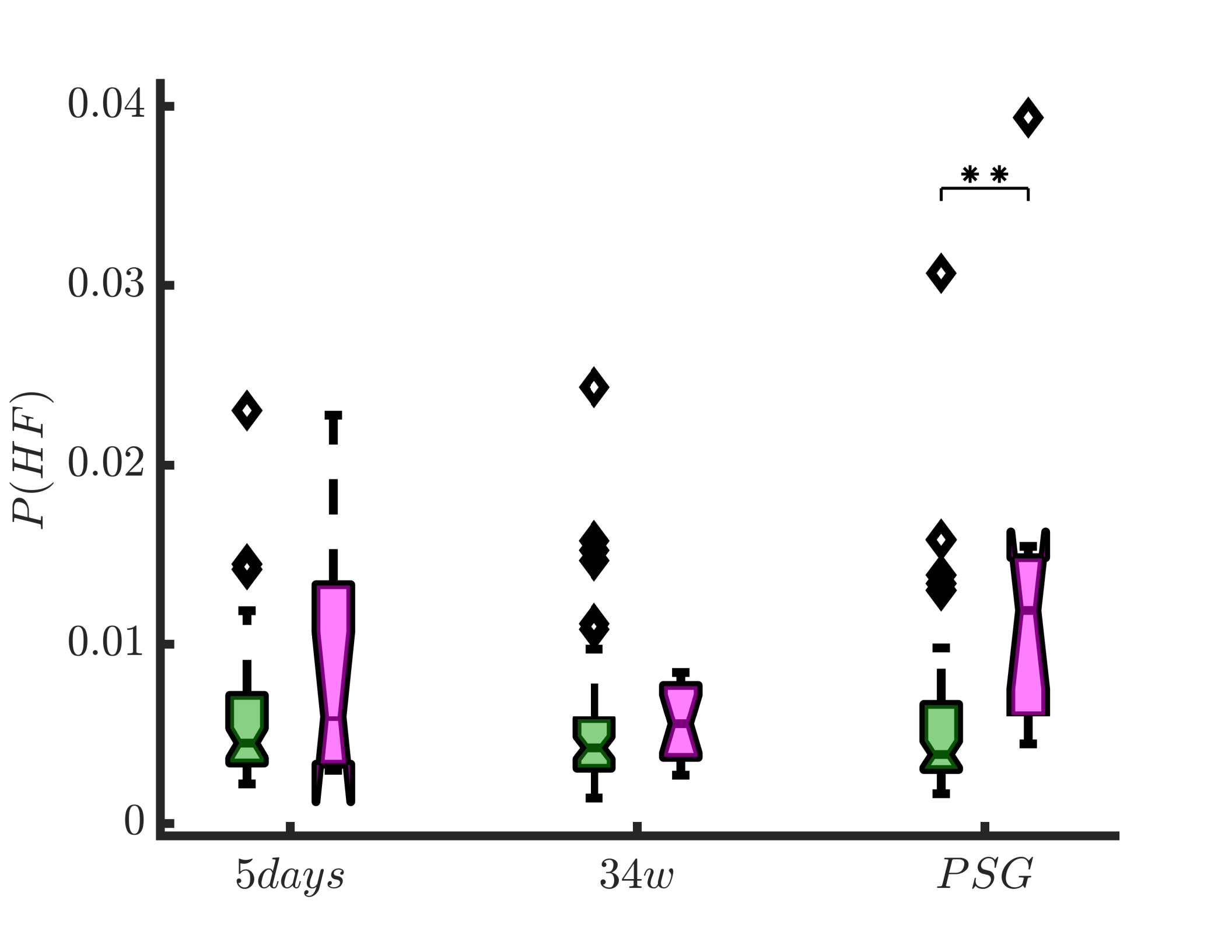

0.8
0.7
0.6
0.5
0.4
0.3
Asymmetry(θ)
**
*
5days
34w
PSG

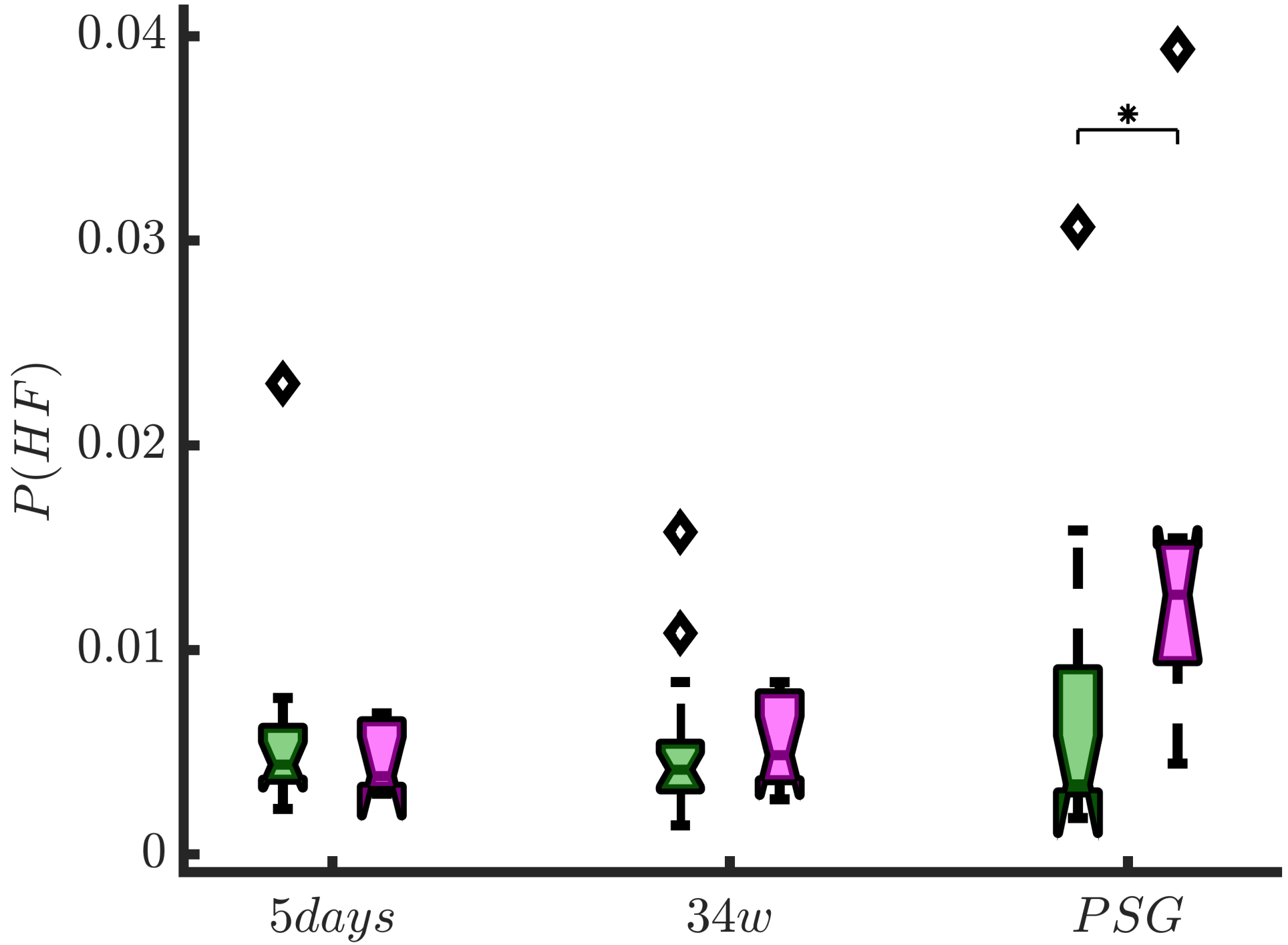

0.79
0.54
0.3
Asymmetry(θ)
26
30
34
38
42
46
Age (PMA Weeks)

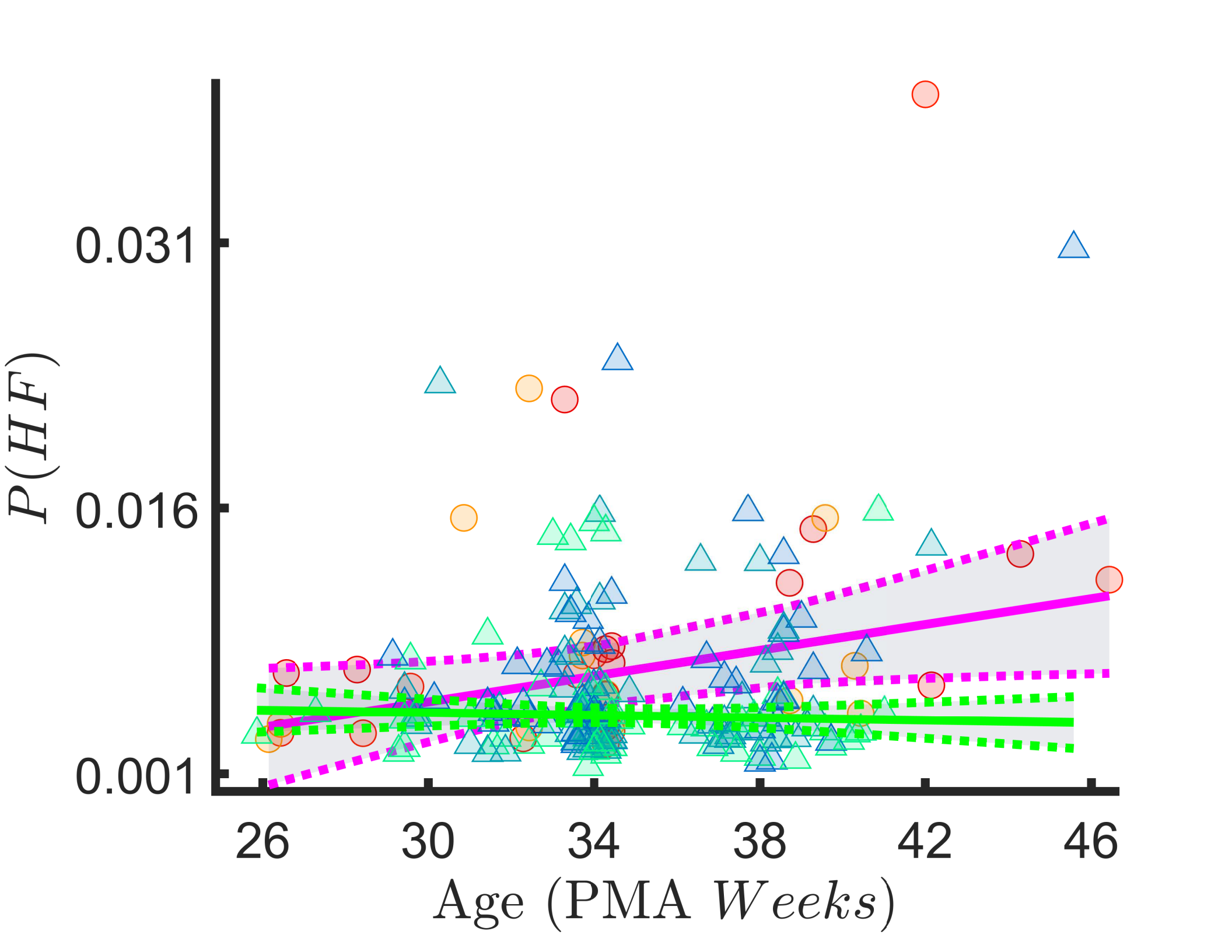

30
25
20
15
10
$CI_{EEG,F_{p,2}}$
* *
5days
34w
PSG

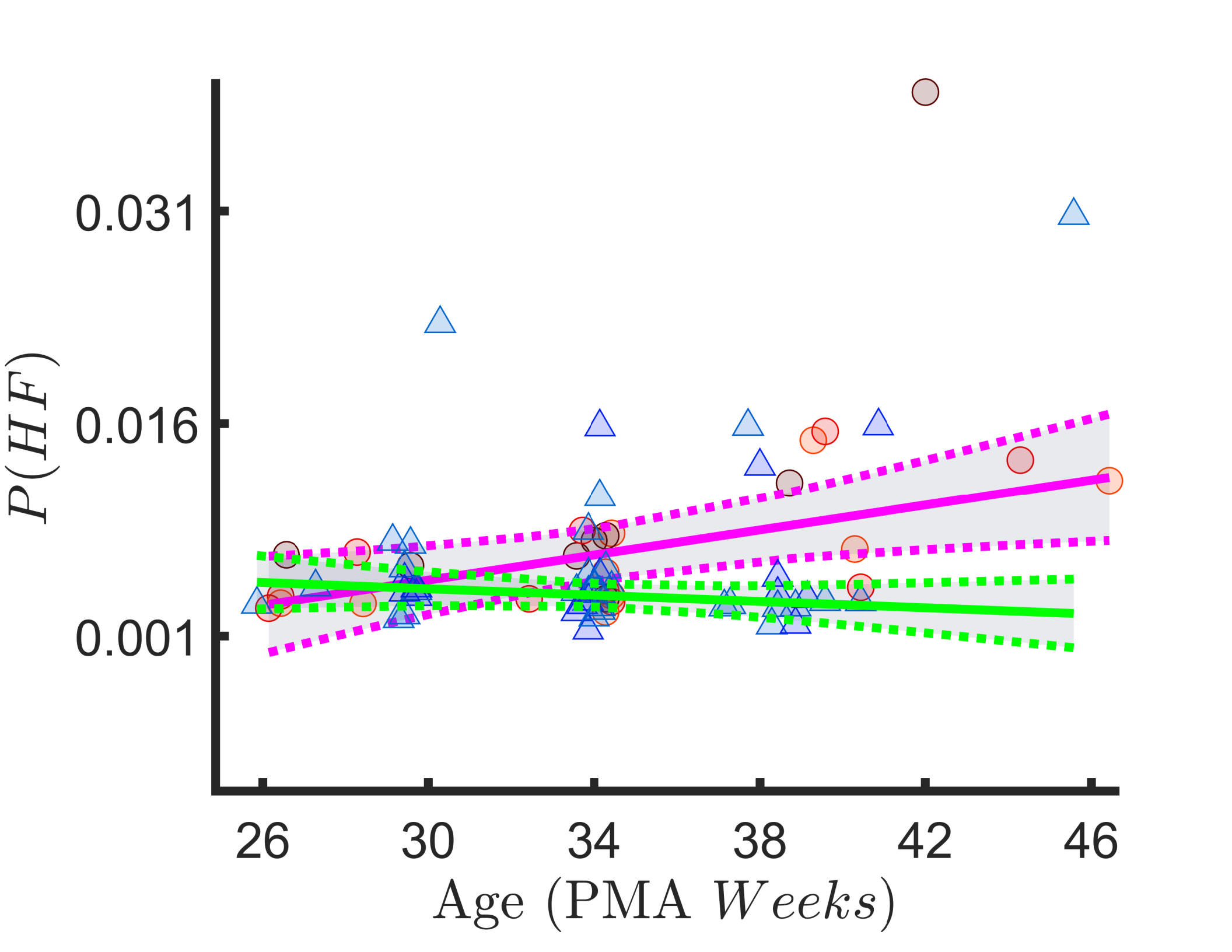

29.47
19.43
9.39
$CI_{EEG,F_{p,2}}$
26
30
34
38
42
46
Age (PMA $Weeks$)

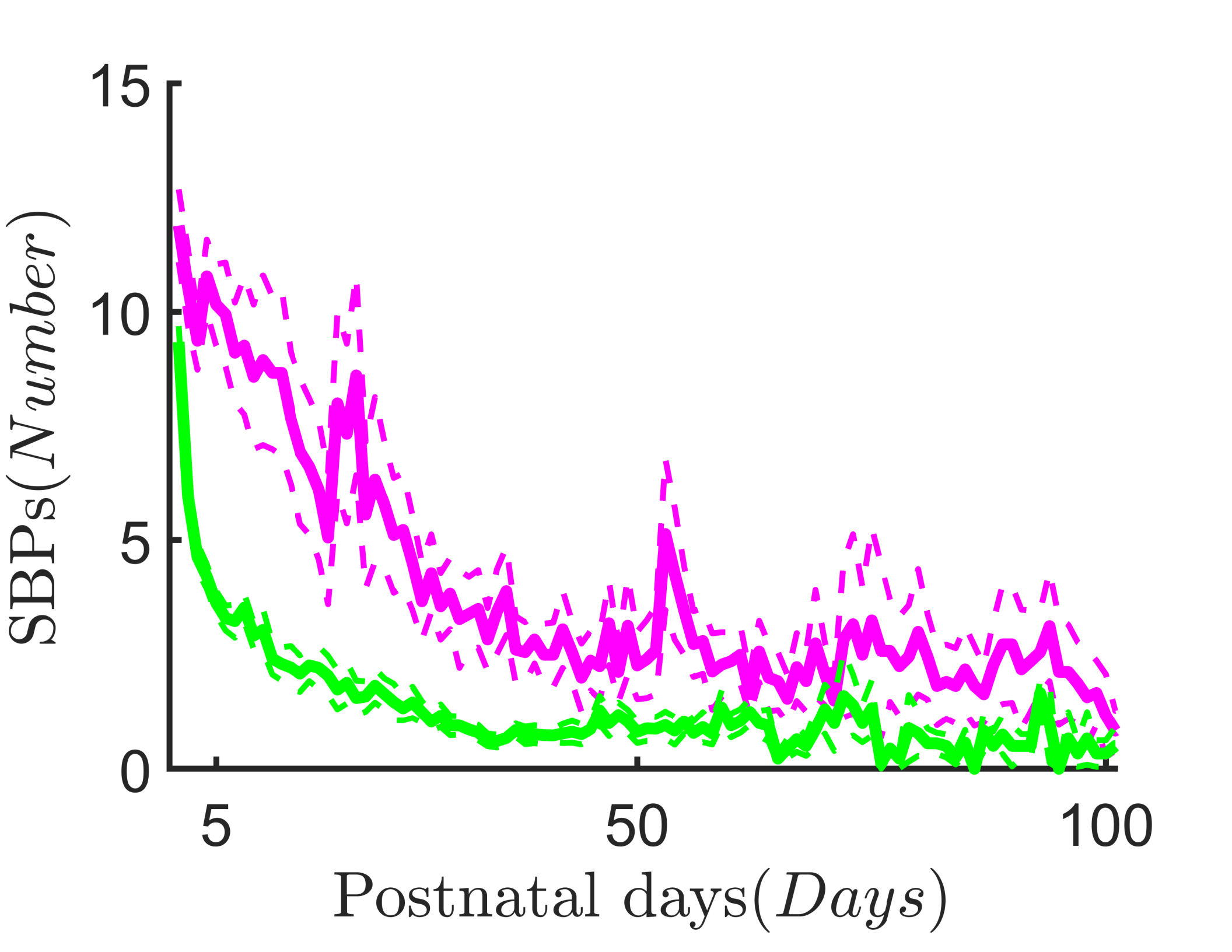

90
50
20
1
Patient$_{ID}$
50
200
500
1000
Skin Breaking Procedures

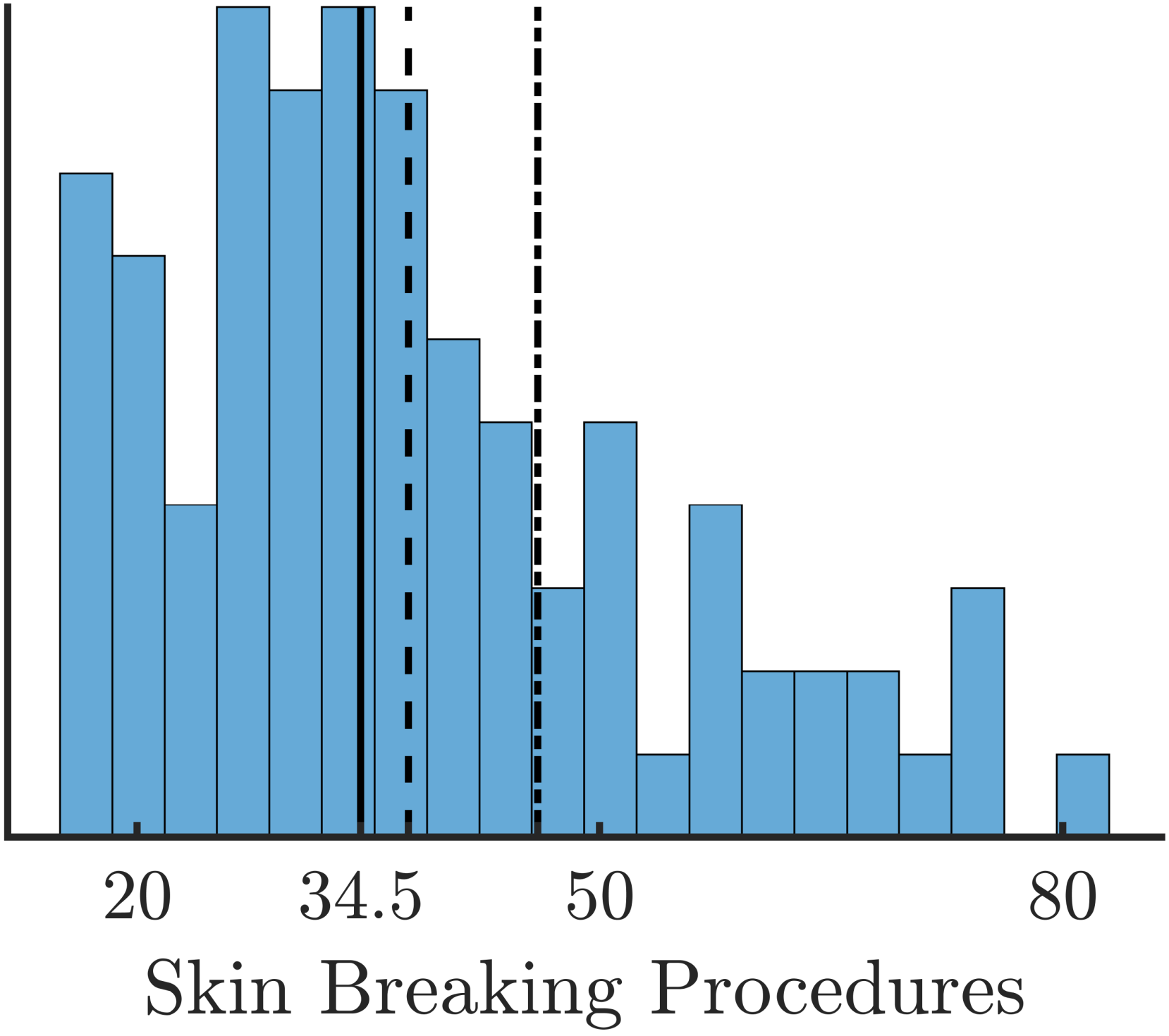

0.04
0.03
0.02
0.01
0
P(HF)
* *
5days
34w
PSG

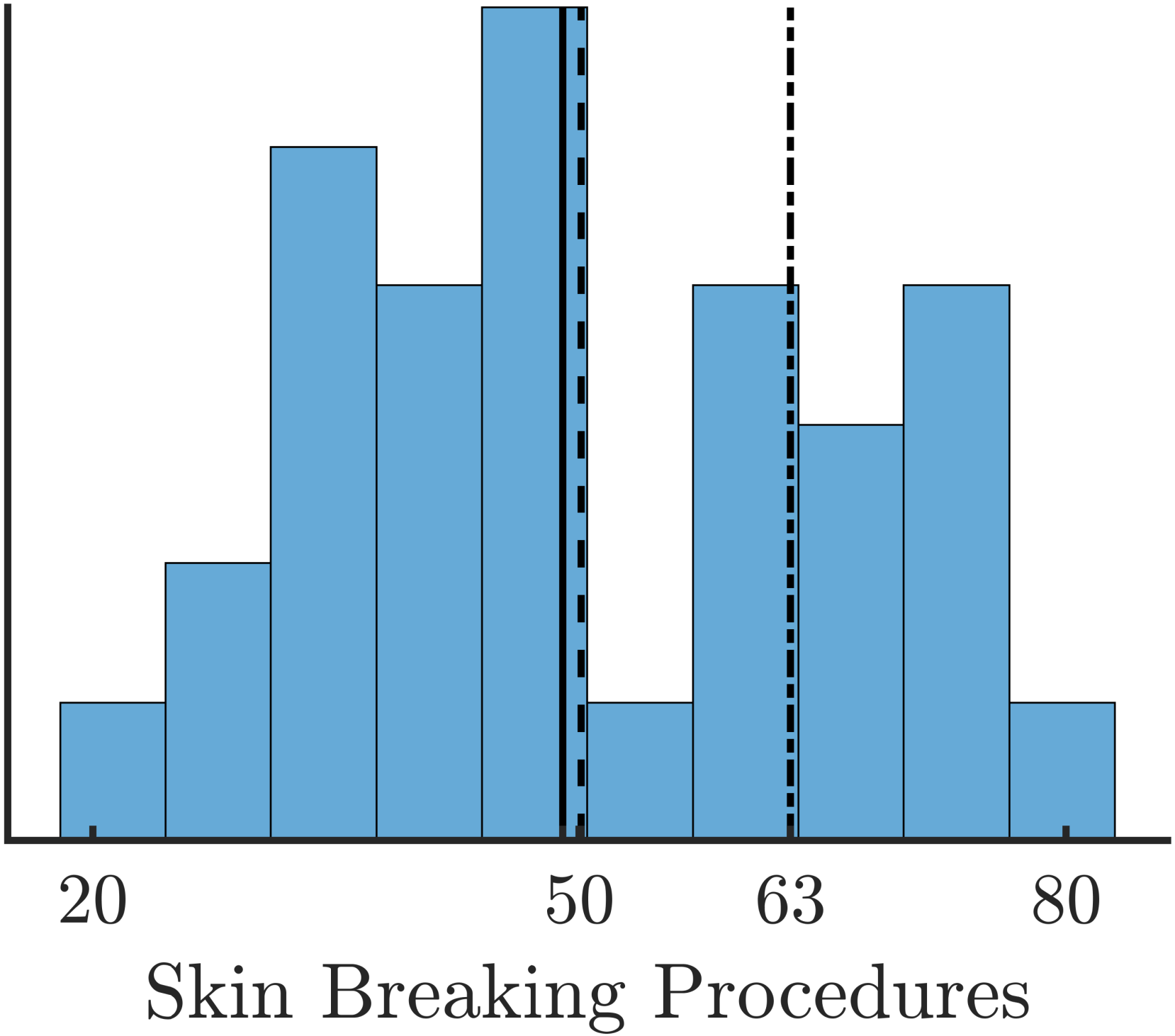

0.04
0.03
0.02
0.01
0
P(HF)
*
5days
34w
PSG


0.031
0.016
0.001
$P(HF)$
26
30
34
38
42
46
Age (PMA $Weeks$)


0.031
0.016
0.001
$P(HF)$
26
30
34
38
42
46
Age (PMA $Weeks$)


15
10
5
0
SBPs($Number$)
5
50
100
Postnatal days($Days$)


20
34.5
50
80
Skin Breaking Procedures


20
50
63
80
Skin Breaking Procedures

Table

Table 1. **Overview of all different SBP categories monitored in the study**. The first column is related to all puncture procedures, the second column relate to ventilation procedures and the last one is related to other painful procedures.

SBP categories: Punctures	SBP categories: Ventilation	SBP categories: Other
venous or arterial blood sample	Placing CPAP tube	Placing thorax drain
placing peripheral venous catheter	endotracheal aspiration	Care thorax drain
placing deep venous katheter	Aspiration mouth and nose	Placement gastro-intestinal tube
placing umbilical arterial and/or venous catheter		wound care
Lumbal Punction		Surgery
Intubation		Eye examination

Table 2. **Summary of patient data set at different time points**: SBP (Skin Breaking Procedure at 5 days), GA (gestational age in weeks), birth weight (in g), PMA (postmenstrual age in weeks) at different recording dates (5days, 34w, PSG), CRIB score, APGAR at 5 minutes from birth, the number of days in mechanical ventilation and CPAP and caffeine treatment (number of patients receiving treatment, standard dose 5mg/kg) at first and second EEG measurement and the ultrasound evaluation. Data are split in HIGH SBP (SBP >=50) and LOW SBP (SBP <50). Data are median [IQR] except for the caffeine treatment. Data were compared between the low and high SBP group using Mann-Whitney-U tests for continuous variables and χ^2 tests for categorical variables.

	HIGH SBP (n=19)	LOW SBP (n=73)	p-value
SBP	60 [56.25-69.5]	31 [24-37]	<= 0.01
GA (weeks)	26.57 [25.29-29.5]	32 [29.5-32.57]	<= 0.01
PMA at 5days (1st Rec)	28.57 [26.43-31.57]	32.86 [31-33.57]	<= 0.01
PMA at 34w (2nd Rec)	34.29 [33.71-34.29]	34.07 [33.86-34.29]	0.32
PMA at PSG (3rd Rec)	39.93 [38.71-42]	38.43 [37.36-39.21]	<= 0.01
Birth Weight (g)	950 [820-1137.5]	1540 [1230-1800]	<= 0.01
CRIB Score	2 [1-4.75]	0 [0-1]	<= 0.01
APGAR 5min	8 [6.25-9]	8 [6-8]	.14
Days of mechanical ventilation	2.5 [0-16.5]	0 [0-0]	<= 0.01
Days of CPAP	41.5 [7.75-55.5]	4 [2-28]	<= 0.01
Caffeine (at 5days)	17	63	.715
Caffeine (at 34w)	15	31	<= 0.05

Table 3. **Summary of most vulnerable patient data with GA $\leq$ 29 weeks** : SBP (Skin Breaking Procedure at 5 days), GA (gestational age in weeks), birth weight (in g), PMA (postmenstrual age in weeks) at different recording dates (5days, 34w, PSG), CRIB score, APGAR at 5 minutes from birth, the number of days in mechanical ventilation and CPAP, caffeine treatment (number of patients receiving treatment, standard dose 5mg/kg) at first and second EEG measurement and the ultrasound evaluation. Data are split in HIGH SBP (SBP >=50) and LOW SBP (SBP <50). Data are median [IQR] except for the caffeine treatment. Data were compared between the low and high SBP group using Mann-Whitney-U tests for continuous variables and χ^2 tests for categorical variables.

	HIGH SBP (n=14)	**LOW SBP (n=17)**	**p-value**
SBP	65.5 [58-73]	40 [32-44]	$\leq$ 0.01
GA	26.14 [25.14-26.86]	28.43 [26.71-28.71]	$\leq$ 0.01
PMA at 5days (1st Rec)	26.57 [26.21-28.64]	29.43 [27.54-29.68]	0.05
PMA at 34w (2nd Rec)	34.29 [34-34.29]	34 [33.86-34.14]	0.08
PMA at PSG (3rd Rec)	39.93 [39.29-42]	38.64 [38.14-40]	0.08
Birth Weight	890 [800-1050]	1090 [905.5-1203.25]	0.1
CRIB Score	2.5 [1-6]	2 [1-4.5]	0.64
APGAR 5min	8 [5.75-9]	8 [6-8.75]	0.95
Days of mechanical ventilation	9 [0-19]	1 [0-1.5]	0.20
Days of CPAP	44 [35-80.5]	44 [36-55]	0.71
Caffeine (at 5days)	12	14	0.80
Caffeine (at 34w)	12	16	0.43

Table 4. **Results of the linear mixed effect model for the non-quiet sleep (nQS) state in the ENTIRE dataset.** Only the features that have a significant association with early skin-breaking procedure are reported. The values B represent the fixed-effect coefficients for the SBP, GA and PMA variables with the associated significance level (p-value). For each feature, the following parameters are reported: the mean-absolute error (MSE), the coefficient of determination R^2, the coefficient of determination of the model with only GA and PMA (R^2_{Red}) , the log-likelihood ratio (LLR) F-statistics, the decrease of error variance $\Delta(\%)$ with SBP variable. The p-value is indicated with following symbols: + for p-value <= 0.0001, ** for p <= 0.01, * for p <=0.05 and (n) for not significant p-values. CI stands for complexity index and P(HF) stands for HF power in the tachogram.

$\boldsymbol{Feature}$	$\boldsymbol{B_{SBP}}$	$\boldsymbol{B_{GA}}$	$\boldsymbol{B_{PMA}}$	$\boldsymbol{MSE}$	$\boldsymbol{R^2}$	$\boldsymbol{R^2_{Red}}$	$\boldsymbol{F_{LLR}}$	$\Delta(\%)$
$CI(Fp2)$	-1.585^{*}	0.241^{*}	0.669^{+}	8.04	0.48	0.46	6.93^{*}	3.23
$P(HF)$	0.003^{*}	0.00008^{n}	0.00046^{+}	0.00002	0.21	0.09	9.7^{**}	4.49
$CI(T4)$	-1.333^{*}	0.266^{**}	0.541^{+}	7.11	0.42	0.4	6.58^{*}	3.07
$CI(O2)$	-1.229^{*}	0.214^{*}	0.691^{+}	6.578	0.53	0.51	6.84^{*}	3.19

Table 5. **Results of the linear mixed effect model for the QUIET sleep (QS) state in the ENTIRE dataset.** Only the features that have a significant association with early skin-breaking procedure are reported. The values B represent the fixed-effect coefficients for the SBP, GA and PMA variables with the associated significance level (p-value). For each feature, the following parameters are reported: the mean-absolute error (MSE), the coefficient of determination R^2, the coefficient of determination of the model with only GA and PMA (R^2_{Red}) , the log-likelihood ratio (LLR) F-statistics, the decrease of error variance $\Delta(\%)$ with SBP variable and and the two-ways ANOVA p-value associated to the SBP main effect. The p-value is indicated with following symbols: + for p-value <= 0.0001, ** for p <= 0.01, * for p <=0.05 and (n) for not significant p-values. CI stands for complexity index, P(HF) stands for HF power in the tachogram and asymmetry is the asymmetry of rEEG in the different frequency bands.

$\boldsymbol{Feature}$	$\boldsymbol{B_{SBP}}$	$\boldsymbol{B_{GA}}$	$\boldsymbol{B_{PMA}}$	$\boldsymbol{MSE}$	$\boldsymbol{R^2}$	$\boldsymbol{R^2_{Red}}$	$\boldsymbol{F_{LLR}}$	$\Delta(\%)$
$Asym(\theta)$	0.051^{**}	0.002^{n}	-0.023^{+}	0.005	0.62	0.56	12.72^{**}	5.85
$CI(C3)$	-2.223^{**}	-0.182^{n}	1.077^{+}	9.739	0.62	0.59	11.68^{**}	5.39
$P(HF)$	0.003^{**}	0.00015^{n}	0.0003^{**}	0.00002	0.13	0.01	22.41^{**}	10.1
$Asym(\delta)$	0.048^{**}	0.004^{n}	-0.021^{+}	0.005	0.55	0.49	11.02^{**}	5.09
$Asym(\alpha)$	0.056^{**}	0.006^{*}	-0.022^{+}	0.006	0.56	0.45	9.65^{**}	4.47
$CI(Fp2)$	-1.759^{**}	-0.211^{*}	1.05^{+}	7.93	0.65	0.63	8.78^{*}	4.08
$CI(O1)$	-2.137^{**}	-0.176^{n}	1.041^{+}	8.828	0.63	0.59	10.53^{**}	4.87
$CI(O2)$	-1.705^{*}	-0.143^{n}	1.031^{+}	7.468	0.67	0.61	9.03^{*}	4.19
$CI(Fp1)$	-1.628^{*}	-0.256^{*}	1.058^{+}	8.096	0.65	0.63	7.03^{*}	3.28
$CI(T3)$	-1.771^{*}	-0.099^{n}	1.027^{+}	6.186	0.73	0.64	9.23^{*}	4.28
$Asym(\beta)$	0.047^{*}	0.005^{n}	-0.02^{+}	0.005	0.53	0.41	7.29^{*}	3.4
$CI(T4)$	-1.626^{*}	-0.133^{n}	1.017^{+}	6.83	0.72	0.6	6.33^{*}	2.95

Table 6. **Results of the linear mixed effect model for the quiet sleep (QS) state in the patients with a GA below 29 weeks**. Only the features that have a significant association with early skin-breaking procedure are reported. The values B represent the fixed-effect coefficients for the SBP, GA and PMA variables with the associated significance level (p-value). For each feature, the following parameters are reported: the mean-absolute error (MSE), the coefficient of determination R^2, the coefficient of determination of the model with only GA and PMA (R^2_{Red}) , the log-likelihood ratio (LLR) F-statistics, the decrease of error variance $\Delta(\%)$ with SBP variable and the two-ways ANOVA p-value associated to the SBP main effect. The p-value is indicated with following symbols: + for p-value <= 0.0001, ** for p <= 0.01, * for p <=0.05 and (n) for not significant p-values. P(HF) and P(LF) stand for HF and LF power in the tachogram, while asymmetry is the asymmetry of rEEG in the different frequency bands.

$\boldsymbol{Feature}$	$\boldsymbol{B_{SBP}}$	$\boldsymbol{B_{GA}}$	$\boldsymbol{B_{PMA}}$	$\boldsymbol{MSE}$	$\boldsymbol{R^2}$	$\boldsymbol{R^2_{Red}}$	$\boldsymbol{F_{LLR}}$	$\Delta(\%)$
$P(HF)$	0.005^{**}	0.002^{**}	0.00057^{+}	0.00003	0.27	0.16	10.48^{**}	13.2
$Asym(\alpha)$	0.064^{*}	0.006^{n}	-0.021^{+}	0.005	0.7	0.58	6.52^{*}	8.43
$P(LF)$	0.009^{*}	0.002^{n}	0.001^{+}	0.00014	0.31	0.18	7.9^{*}	10.1
$Asym(\theta)$	0.05^{*}	0.005^{n}	-0.024^{+}	0.005	0.74	0.66	4.88^{n}	6.38

Click here to access/download
Files for Review Purposes Only [Not for Publication]
new_authorship_NAULAERS.pdf

Click here to access/download
Files for Review Purposes Only [Not for Publication]
new_authorship_LAVANGA.pdf

Click here to access/download
Files for Review Purposes Only [Not for Publication]
new_authorship_DORADO.pdf

Click here to access/download
Files for Review Purposes Only [Not for Publication]
new_authorship_JANSEN.pdf

Click here to access/download
Files for Review Purposes Only [Not for Publication]
new_authorship_VAN_HUFFEL.pdf

Click here to access/download
Files for Review Purposes Only [Not for Publication]
new_authorship_ORTIBUS.pdf

Click here to access/download
Files for Review Purposes Only [Not for Publication]
new_authorship_BOLLEN.pdf

Click here to access/download
Copyright Transfer Agreement--REQUIRED from ALL authors of submission at revision stage
PAIN_eCopyright_Transfer_Form__BOLLEN.pdf

Click here to access/download
Copyright Transfer Agreement--REQUIRED from ALL authors of submission at revision stage
PAIN_eCopyright_Transfer_Form_ORTIBUS.pdf

Click here to access/download
Copyright Transfer Agreement--REQUIRED from ALL authors of submission at revision stage
PAIN_eCopyright_Transfer_Form_LAVANGA.pdf

Click here to access/download
Copyright Transfer Agreement--REQUIRED from ALL authors of submission at revision stage
PAIN_eCopyright_Transfer_Form_JANSEN.pdf

Click here to access/download
Copyright Transfer Agreement--REQUIRED from ALL authors of submission at revision stage
PAIN_eCopyright_Transfer_Form_DEREYMAEKER.pdf

Click here to access/download
Copyright Transfer Agreement--REQUIRED from ALL authors of submission at revision stage
PAIN_eCopyright_Transfer_Form_NAULEARS.pdf

Click here to access/download
Copyright Transfer Agreement--REQUIRED from ALL authors of submission at revision stage
PAIN_eCopyright_Transfer_Form_VAN_HUFFEL.pdf

Click here to access/download
Copyright Transfer Agreement--REQUIRED from ALL authors of submission at revision stage
PAIN_eCopyright_Transfer_Form_CAICEDO.pdf

Click here to access/download
ICMJE Conflict of Interest Form--REQUIRED from ALL authors of submission at revision stage
coi_disclosure_BOLLEN.pdf

Click here to access/download
ICMJE Conflict of Interest Form--REQUIRED from ALL authors of submission at revision stage
coi_disclosure_CAICEDO.pdf

Click here to access/download
ICMJE Conflict of Interest Form--REQUIRED from ALL authors of submission at revision stage
coi_disclosure_Dereymaeker.pdf

Click here to access/download
ICMJE Conflict of Interest Form--REQUIRED from ALL authors of submission at revision stage
coi_disclosure_JANSEN.pdf

Click here to access/download
ICMJE Conflict of Interest Form--REQUIRED from ALL authors of submission at revision stage
coi_disclosure_LAVANGA.pdf

Click here to access/download
ICMJE Conflict of Interest Form--REQUIRED from ALL authors of submission at revision stage
coi_disclosure_NAULAERS.pdf

Click here to access/download
ICMJE Conflict of Interest Form--REQUIRED from ALL authors of submission at revision stage
coi_disclosure_ORTIBUS.pdf

Click here to access/download
ICMJE Conflict of Interest Form--REQUIRED from ALL authors of submission at revision stage
coi_disclosure_VAN_HUFFEL.pdf